SCUOLA DI DOTTORATO
UNIVERSITÀ DEGLI STUDI DI MILANO-BICOCCA

School of Medicine and Surgery

PhD program in NEUROSCIENCE Cycle XXXII

Curriculum in EXPERIMENTAL NEUROSCIENCE

OXALIPLATIN-INDUCED PERIPHERAL NEUROTOXICITY IN MOUSE MODELS: DIFFERENT TREATMENT SCHEDULES AND FOCUS ON OXIDATIVE STRESS

Candidate: Dr. POZZI ELEONORA

Registration number: 739312

Tutor: Prof. PAOLA MARMIROLI

Coordinator: Prof. GUIDO CAVALETTI

ACADEMIC YEAR 2018/2019

INDEX

SUMMARY **1**

INTRODUCTION **3**

1. CHEMOTHERAPY-INDUCED PERIPHERAL NEUROTOXICITY 3

2. ROLE OF MITOCHONDRIAL DYSFUNCTIONS AND OXIDATIVE STRESS.. 7

3. PLATINUM-BASED COMPOUNDS 8

3.1 OXALIPLATIN 9

4. OXALIPLATIN-INDUCED PERIPHERAL NEUROTOXICITY (OIPN) 10

4.1 CLINICAL FEATURES OF OXALIPLATIN-INDUCED PERIPHERAL NEUROTOXICITY 10

4.2 MECHANISMS OF OXALIPLATIN-INDUCED PERIPHERAL NEUROTOXICITY 11

4.3 ROLE OF MITOCHONDRIAL DYSFUNCTIONS AND OXIDATIVE STRESS IN OXALIPLATIN-INDUCED PERIPHERAL NEUROTOXICITY 12

5. ROLE OF MITOCHONDRIAL DYSFUNCTIONS AND OXIDATIVE STRESS IN PERIPHERAL NEUROTOXICITES 14

6. ANIMAL MODELS OF OXALIPLATIN-INDUCED PERIPHERAL NEUROTOXICITY 16

6.1 "ACUTE" MODELS OF OXALIPLATIN-INDUCED PERIPHERAL NEUROTOXICITY 16

6.2 "CHRONIC" MODELS OF OXALIPLATIN-INDUCED PERIPHERAL NEUROTOXICITY 17

6.3 OIPN MOUSE MODELS TAKEN INTO CONSIDERATION FOR THE STUDY 18

AIMS OF THE STUDY **21**

METHODS **22**

A. OXALIPLATIN-INDUCED PERIPHERAL NEUROTOXICITY CHARACTERIZATION: *IN VIVO* STUDY 22

1. ANIMAL HUSBANDRY AND TREATMENT 22

2. EXPERIMENTAL DESIGN 23

2.1 Study 1 23

2.2 Study 2 24

2.3 Study 3 24

2.4 Study 4 25

3. CLINICAL MONITORING AND BODY WEIGHT 25

4. ASSESSMENT OF OXALIPLATIN-INDUCED NEUROPATHIC PAIN 25

4.1 Behavioural Testing - Dynamic Test 25

4.2 Behavioural Testing - Cold Plate test 26

5. ASSESSMENT OF OXALIPLATIN-INDUCED PERIPHERAL NEUROTOXICITY 26

5.1 Neurophysiological examination 26

5.2 Morphological and morphometric analyses 27
5.2.1 DRG 27
5.2.2 Peripheral nerves 27
5.2.3 IENF 28
B. OXIDATIVE STRESS EVALUATION 28
1. THIOBARBITURIC ACID REACTIVE SUBSTANCE ASSAY 28
2. WESTERN BLOT ANALYSIS 29
STATISTICAL ANALYSIS 29
RESULTS 30
STUDY 1 30
A. *IN VIVO* STUDY AND OXALIPLATIN-INDUCED PERIPHERAL NEUROTOXICITY CHARACTERIZATION 30
1. CLINICAL MONITORING AND BODY WEIGHT 30
2. ASSESSMENT OF OXALIPLATIN-INDUCED PERIPHERAL NEUROTOXICITY 30
2.1 Behavioural Testing - Dynamic Test 31
2.2 Behavioural Testing - Cold Plate test 31
2.3 Neurophysiological examination 32
2.4 Morphological and morphometric analyses 32
2.4.1 DRG 33
2.4.2 Peripheral nerves 34
2.4.3 IENF 37
B. OXIDATIVE STRESS EVALUATION 38
1. THIOBARBITURIC ACID REACTIVE SUBSTANCE ASSAY 38
STUDY 2 39
A. *IN VIVO* STUDY AND OXALIPLATIN-INDUCED PERIPHERAL NEUROTOXICITY CHARACTERIZATION 39
1. CLINICAL MONITORING AND BODY WEIGHT 39
2. ASSESSMENT OF OXALIPLATIN-INDUCED PERIPHERAL NEUROTOXICITY 39
2.1 Behavioral Testing - Dynamic Test 39
2.2 Behavioural Testing - Cold Plate test 40
2.3 Neurophysiological examination 41
2.4 Morphological and morphometric analyses 41
2.4.1 DRG 41
2.4.2 Peripheral nerves 42
2.4.3 IENF 43
B. OXIDATIVE STRESS EVALUATION 44
1. THIOBARBITURIC ACID REACTIVE SUBSTANCE ASSAY 44

STUDY 3 45

A. *IN VIVO* STUDY AND OXALIPLATIN-INDUCED PERIPHERAL NEUROTOXICITY CHARACTERIZATION 45

1. CLINICAL MONITORING AND BODY WEIGHT 45

2. ASSESSMENT OF OXALIPLATIN-INDUCED PERIPHERAL NEUROTOXICITY 45

2.1 Behavioral Testing - Dynamic Test 46

2.2 Behavioral Testing - Cold Plate test 46

2.3 Neurophysiological examination 47

2.4 Morphological and morphometric analyses 47

2.4.1 DRG 47

2.4.2 Peripheral nerves 48

2.4.3 IENF 50

B. OXIDATIVE STRESS EVALUATION 51

1. THIOBARBITURIC ACID REACTIVE SUBSTANCE ASSAY 51

STUDY 4 52

A. *IN VIVO* STUDY AND OXALIPLATIN-INDUCED PERIPHERAL NEUROTOXICITY CHARACTERIZATION 52

1. CLINICAL MONITORING AND BODY WEIGHT 52

2. ASSESSMENT OF OXALIPLATIN-INDUCED PERIPHERAL NEUROTOXICITY 52

2.1 Behavioral Testing - Dynamic Test 53

2.2 Behavioral Testing - Cold Plate test 54

2.3 Neurophysiological examination 54

2.4 Morphological and morphometric analyses 55

2.4.1 DRG 56

2.4.2 Peripheral nerves 57

2.4.3 IENF 59

B. OXIDATIVE STRESS EVALUATION 60

1. THIOBARBITURIC ACID REACTIVE SUBSTANCE ASSAY 60

2. WESTERN BLOT ANALYSIS 60

DISCUSSION AND CONCLUSIONS 63

ABBREVIATIONS 75

REFERENCES 76

SUMMARY

The toxicity of anticancer drugs represents one of the major limitations in their clinical use, due to severe and long-term damage, leading to impairment of patient's quality of life. Among the side effects of chemotherapy, peripheral neurotoxicity is one of the most disabling for cancer patients.

Oxaliplatin (OHP) is one of the most neurotoxic antineoplastic drugs. It is a platinum-based agent widely used for the treatment of metastatic colorectal cancer. Patients undergoing OHP-regimen can experience two clinically distinct forms of peripheral neuropathy: an acute cold-enhanced form and a chronic distal sensory neuropathy.

Due to the lack of effective pharmacological therapies in preventing and/or alleviating neuropathic symptoms, OHP dose reduction or interruption is often mandatory. Despite extensive investigation, the pathogenesis of OHP-induced peripheral neurotoxicity (OIPN) is still largely unknown.

In literature several preclinical *in vivo* studies, different from each other in schedules of OHP treatment, are described. Some of these studies demonstrated the development of mechanical and cold allodynia after OHP treatment but the characterization of peripheral neurotoxicity was limited. In fact, to verify the OINP onset, in addition to the evaluation of neuropathic pain, neurophysiological and histopathological analyses (dorsal root ganglia [DRG] and nerves examination, evaluation of intraepidermal nerve fiber [IENF] density) should be assessed. Over the last years, several workgroups have explored various putative mechanisms possibly involved in the onset and development of chemotherapy-induced peripheral neurotoxicity and among them mitochondrial dysfunction has recently been suggested. Mitochondrial dysfunction and associated oxidative stress may result in chronic neuronal energy impairment leading to neuropathic symptoms.

The first aim of this work was to compare OIPN mouse models reported in three published studies with OIPN mouse model currently used in our laboratory, using a multimodal assessment. Moreover, given the potential role of oxidative stress in the pathogenesis of peripheral neurotoxiity, the possibility that OHP treatment could induce oxidative stress and eventually mitochondrial dysfunctions has also been analysed.

Taken together, the results of this study indicate that a single dose of OHP 5 mg/kg administrated in tail vein is able to reproduce the clinical features of acute OIPN. In fact, cold-induced hyperalgesia was observed at 24 hours after the first OHP administration. On the other hand, to reproduce the clinical features of chronic OIPN, prolonged OHP treatment

is required. In fact, alterations in caudal and digital nerves amplitudes and mechanical allodynia together with a reduction in IENF density were observed only after 4 weeks of OHP 5 mg/kg administrated intravenously twice a week, the schedule currently used in our laboratory. Changes in DRG morphometry were instead more commonly observed also in the other OHP schedules reproduced in this study. As a whole, these results suggested that our laboratory OHP model is the one which better mimic the OIPN features.

Regarding the pathogenic aspect, this study is far from clarifying the role of mitochondrial dysfunction and oxidative stress in the onset of OIPN, even if some results have been obtained. In general, oxidative stress levels measured with TBARS assay did not increase considerably in DRG and caudal nerves following OHP treatment with any schedule used, whereas sciatic nerves showed an increase in TBARS level at 2 weeks after a cumulative dose at 20 mg/kg (intravenous administration) and at 4 weeks after 30 mg/kg (intraperitoneal administration). Furthermore, a significant increase in protein expression levels of respiratory chain complex I in DRG collected from the animals treated for 4 weeks with our OHP schedule was detected. In the same samples, a decrease in phosphoryled form of DRP1 was observed closely approximating significance after 2 weeks of OHP treatment, indicating reduced mitochondrial fission process.

In conclusion, a reliable animal model should be able to evaluate acute and chronic neurotoxicity in order to study the mechanism underlying OIPN. Setting a standard method of evaluation would be useful to obtain consistent results among different workgroups. Moreover, mitochondrial dysfunction and oxidative stress may be implicated in the onset of OIPN but further investigations are required.

INTRODUCTION

1. CHEMOTHERAPY-INDUCED PERIPHERAL NEUROTOXICITY

Peripheral neuropathy refers to disease or damage to peripheral nerves that carry signals to and from the central nervous system.

Peripheral nerve diseases could be classified according to their time course, distribution of nerves primarily affected, etiology and clinic-pathological features. On the basis of the type of nerves involved and of the patient's symptoms, neuropathies can be divided in motor, sensory, autonomic or mixed. Overall, inherited or acquired forms of peripheral neuropathy are recognized.

Among acquired neuropathies, drug-induced peripheral neuropathy (DIPN) consists in damage to nerves caused by a chemical substance used in the treatment or prevention of a disease, e.g. antibiotics, antivirals, immunosuppressants and antitumor agents (Vilholm et al., 2014). Therefore, chemotherapy-induced peripheral neuropathy (CIPN) may be considered a subclass of DIPN. CIPN is one of the most frequent side effects caused by some commonly used antineoplastic agents:

- Vinca alkaloids (i.e. vincristine [VCR], vinblastine, vindesine, vinorelbine, and vinflunine) are widely used in the treatment of hematologic and lymphatic malignancies and solid tumors,
- Taxanes (i.e. paclitaxel [PTX] and docetaxel) are used to treat several types of solid tumors (breast, ovary and non-small cell lung cancers),
- Epothilones (i.e. ixabepilone) are used in the treatment of advanced breast cancer, prostate cancer and other solid tumors, useful in treating taxane-resistant cancers,
- Platinum-based compounds (i.e. cisplatin [CDDP], carboplatin [CRB] and oxaliplatin [OHP]) are commonly used in the treatment of different types of solid tumors (ovarian, testicular, small cell lung cancers and advanced colorectal cancer),
- Proteasome inhibitors (i.e. bortezomib [BTZ], carfilzomib) and thalidomide are used to treat multiple myeloma,
- Arsenic compounds (i.e. arsenic trioxides) are used in acute promyelocytic leukaemia treatment,

(Vilholm et al., 2014; Zajaczkowska et al., 2019; **Tab. 1**).

The mechanism of action of these antineoplastic agents is fairly known, but the mechanisms underlying peripheral neurotoxicity remain often unclear.

Microtubule inhibitors including vinca alkaloids, taxanes, and epothilones exert antineoplastic effect by impairing microtubule dynamics, and this may lead to axonal degeneration and decrease of axonal transport.

Platinum-based compounds exert antineoplastic effect by creating platinum adducts to nuclear or mitochondrial DNA. Accumulation of platinum in dorsal root ganglia (DRG) is likely to be involved in the development of peripheral neurotoxicity, but it can hardly be the only cause of damage.

The mechanisms of anticancer activity of the proteasome inhibitor BTZ have not yet been stably related to the pathogenesis of CIPN (Grisold et al., 2012).

In general, the susceptibility of peripheral nervous system (PNS) to chemotherapeutic agents seems to be associated to the lack of an efficient vascular barrier that allows exposure to drug molecules and toxins. In fact, DRG are not protected whereas nerves are protected by blood-nerve barrier, which is less efficient than blood brain barrier (Areti et al., 2014).

CIPN is more often a predominantly sensory neuropathy which affects 19-85% of cancer patients, depending on the dose and the class of chemotherapeutic drugs that they receive (Zajaczkowska et al., 2019; **Tab. 2**).

In most cases sensory symptoms develop symmetrically in the distal segments of the limbs, particularly in the legs, with a typical “glove and stocking" distribution and include paresthesias (i.e. tingling and numbness), dysesthesias, loss of sensory perception and neuropathic pain. In rare cases, also motor symptoms may occur. Patients may complain of CIPN symptoms even weeks or months after cessation of the therapy, and with platinum drugs this occurrence may even be characterized by clinical worsening (“coasting” phenomenon).

The severity of symptoms may sometimes require a reduction in drug dosage or discontinuation of the treatment and/or significantly impair quality life of patients. For these reasons, the onset of CIPN represents the most common limiting factor of antineoplastic treatment (Grisold et al., 2012; Cavaletti et al., 2015; Boyette-Davis et al., 2018; Kim et al., 2018; Malacrida et al., 2019; Marmiroli et al., 2019; Zajaczkowska et al., 2019; **Tab. 2**).

The development and severity of neuropathic symptoms could be evaluated using clinical scales, among which National Cancer Institute-Common Terminology Criteria (NCI-CTC) is one of the most frequently used. Moreover, large sensory and motor fibers could be assessed with nerve conduction studies by using standard methods which include the measurement of sensory and motor nerve conduction velocity (NCV), sensory nerve action

potential (SNAP) and compound muscle action potential (CMAP) associated to electromyography. On the other hand, skin biopsy allows evaluation of the involvement of small sensory fibers (Grisold et al., 2012; Velasco et al., 2017).

Drug	**Type of cancer treated**	**Mechanism of drug action in treating cancer**
Vinca alkaloids	Hematologic and lymphatic malignancies and solid tumors	Inhibition microtubule polymerization, mitotic arrest
Taxanes	Several types of solid tumors (breast, ovary and non-small cell lung cancers)	Inhibition microtubule depolymerization, mitotic arrest
Epothilones	Advanced breast cancer, prostate cancer and other solid tumors. Useful in treating taxanes-resistant cancers	Inhibition microtubule depolymerization
Platinum-based compounds	Different types of solid tumors (ovarian, testicular, small cell lung cancers and advanced colorectal cancer)	DNA cross-linking, cell cycle arrest, apoptosis
Proteasome inhibitors	Multiple myeloma	Inhibition proteasome degradation, cell cycle arrest
Arsenic compounds	Acute promyelocytic leukaemia	Inhibition of glycolysis and mitochondrial respiration

Table 1. Common antineoplastic drugs known to induce neuropathy.
(Velasco et al., 2017; Zajaczkowska et al., 2019)

Drug	Typical neuropathic symptoms
Vinca alkaloids	Sensorimotor neuropathy. Paresthesias, numbness, impairment of all sensory modalities in a stocking-and-glove distribution; neuropathic pain; muscle cramps, distal weakness, autonomic symptoms. VCR most neurotoxic
Taxanes	Sensorimotor neuropathy. PTX: paresthesias, numbness, impairment of all sensory modalities in a stocking-and-glove distribution; neuropathic pain; occasionally perioral and tongue paresthesias; myalgia, myopathy, distal weakness. Docetaxel: similar to PTX but more severe
Epothilones	Sensorimotor neuropathy. Similar to taxanes but less neuropathic pain
Platinum-based compounds	Sensory neuropathy. CDDP: paresthesias, numbness, impairment of all sensory modalities in a stocking-and-glove distribution OHP: cold-induced transient paresthesias in perioral and pharyngolaryngeal and limb extremities, cramps/muscle spasm in throat muscle, jaw spasm (acute form); similar to CDDP (chronic form). CRB: similar but milder than CDDP
Proteaseome inhibitors	Sensory (motor) neuropathy. Neuropathic pain, paresthesias and impairment of all sensory modalities in distal extremities of limbs
Arsenic compounds	Subacute and progressive sensorimotor neuropathy. Paresthesias, numbness and/or neuropathic pain in a stocking-and-glove; motor weakness

Table 2. Typical clinical features of CIPN associated with commonly used antineoplastic drug.

VCR: vincristine, PTX: paclitaxel, CDDP: cisplatin, OHP: oxaliplatin, CRB: carboplatin (Velasco et al., 2017; Zajaczkowska et al., 2019)

Among antineoplastic drugs, platinum-based compounds will be discussed with focus on OHP, which is the chemotherapeutic agent used in this study.

2. ROLE OF MITOCHONDRIAL DYSFUNCTIONS AND OXIDATIVE STRESS

Mitochondria are organelles involved in several cellular activities including cellular metabolism, homeostasis and stress response. Their inner membrane presents an electron transport chain (ETC) which is implicated in cellular energy production. ETC is constituted by five transmembrane protein complexes (I-V) that transfer electrons between donors and acceptors, generating an electrochemical proton gradient which lead to the synthesis of adenosine triphosphate (ATP), an essential molecule for cellular energy metabolism. Physiologically, the electrons flow through Complex I (NADH-ubiquinone oxidoreductase), Complex II (succinate dehydrogenase), Complex III (ubiquinol-cytochrome c reductase), Complex IV (Cytochrome c Oxidase) and finally reach the Complex V (ATP synthase) to produce ATP. Although this process is very efficient, about 0.2-2% of the electrons escape from the ETC and reduce oxygen to form the highly reactive free radical superoxide anions and hydrogen peroxide. Under normal conditions, the free radical amount is compensated by antioxidant systems. However, in some conditions (i.e. after administration of particular drugs) the antioxidant mechanisms are not able to deal with an excessive reactive oxygen species (ROS) production, leading to cell damage and finally cell death (Conklin et al., 2004; Zhao et al., 2019).

Moreover, in order to ensure the mitochondrial function, a correct mitochondrial dynamics is necessary. The balance between two opposite events, fission and fusion, is important to determine not only the mitochondrial morphology but also the subcellular location and function of mitochondria, which are associated with physiological and physio-pathological conditions. It is known that defects in either fusion or fission processes limit mitochondrial motility, decrease energy production and cell death. In particular, mitochondrial fission is characterized by the division of one mitochondrion into two daughter mitochondria whereas mitochondrial fusion is the union of two mitochondria resulting in one mitochondrion. In mammalian cells, these two processes are finely regulated by fission protein 1 (FIS1) and dynamin-related protein 1 (DRP1) and by the mitochondrial fusion proteins mitofusin 1 and 2 (MFN1 and MFN2, respectively) and optic atrophy 1 (OPA1). In particular, it is known that phosphorylation of DRP1 at serine 616 represents one of the key regulators of

mitochondrial fission DRP1. DRP1 phosphorylated induces its translocation from the cytosol to the outer membrane of mitochondrion where assembles and, forming a contractile ring drives mitochondrial fragmentation through a guanosine-5'-triphosphate (GTP)-dependent mechanism (Qi et al., 2013; Hu et al., 2017; Smith and Gallo, 2018; Tilokani et al., 2018).

Mitochondrial dysfunction has a critical role in several disorders including metabolic and cancer diseases and also in CIPN. In the last years, the suggestion that mitochondrial impairment in primary sensory neurons may be a possible mechanism underlying the CIPN onset (known as "myotoxicity hypothesis") has risen (Waseem et al., 2018).

3. PLATINUM-BASED COMPOUNDS

CDDP, CRB and OHP represent some of the main chemotherapeutic agents currently used for the treatment of different types of solid tumors.

Among platinum-based compounds, CDDP was the first antineoplastic drug approved by the Food and Drug Administration (FDA) in 1978 to treat metastatic testicular or ovarian cancer and also for treating bladder cancer. About ten years later, a second-platinum derivative with fewer side effects, CRB, was also approved for the treatment of advanced ovarian cancer, non-small cell lung and refractory testicular cancers. Later, in 2002, OHP was approved as third-generation platinum compound for use in the treatment of patients with metastatic colorectal cancer.

The activity of platinum as antitumor agent was discovered accidentally by Rosenberg and colleagues in 1965. Their study, investigating the role of electric currents on cellular divisions, consisted in using two platinum electrodes in ammonium chloride buffer containing Escherichia coli (*E. coli*). For this purpose, Rosemberg chose specifically platinum electrodes since platinum was considered an inert metal. However, he observed that *E. Coli* cells stopped cell division and discovered this phenomenon was caused not by the electric current but by chemical compounds that were released into the solution from the platinum electrodes. Among them, CDDP (cisdiamminedichloroplatinum(II)), showed antitumor efficacy against sarcoma 180 and leukaemia L1210 in mice (Rosemberg et al., 1965; Rosemberg et al., 1969; Rajapakse et al., 2017).

CDDP was hence the first platinum-based drug to be tested and actually used in the clinical practice alone or in combination therapy for several solid tumors.

Over the years, platinum compounds of second- (CRB) and third-generation (OHP) were developed in order to improve antitumor activity and reduce toxicity.

CDDP treatment is accompanied by several side effects including ototoxicity, myelotoxicity, nephrotoxicity and neurotoxicity. CRB is less neurotoxic than CDDP, however is characterized by myelotoxicity and possible mild sensory neurotoxicity. OHP is associated with acute and chronic neurotoxicity.

Thus, platinum compounds share peripheral neurotoxicity as dose-liming toxicity although different severity (CDDP and OHP >> CRB) and, among anticancer drugs, show the highest occurrence of neuropathy (up to 70-100%) (Mcwhinney et al., 2009; Grisold et al., 2012; Zajaczkowska et al., 2019).

The anticancer activity of platinum derivatives is due to the formation of platinum adducts with nuclear and mitochondrial DNA which result in altering cell cycle, mitochondrial activity and cell death by apoptosis. Hence, these mechanisms could partly be also responsible for damaging sensory neurons, but further investigation of the pathogenesis of neurotoxicity is necessary to identify suitable targets for neuroprotective pharmacological strategies (Grisold et al., 2012; Cavaletti et al., 2015).

3.1 OXALIPLATIN

OHP (cis-[oxalato]trans-1,2-diaminocyclohexane platinum(II)) was discovered in 1976 and then developed for treatment of patients with colorectal cancer and other digestive tract tumors. In 2002, the FDA approved OHP (Eloxatin®) to treat patients with metastatic colorectal cancer and two years later for use in combination with 5-fluorouracil (5-FU) and folinic acid (Leucovorin) as first line therapy for the treatment of metastatic colorectal cancer and solid tumors resistant to other platinum compounds. In fact, the substitution of ammine groups of CDDP with the diaminocyclohexane (DACH) group allowed to develop a less toxic compound and more effective alternative to CDDP and to overcome resistance against CDDP and CRB (Graham et al., 2004; Mcwhinney et al., 2009).

OHP is an organoplatinum complex in which the platinum atom is complexed with DACH and with an oxalate ligand as “leaving group”. Once in the plasma, OHP undergoes rapidly non-enzymatic biotransformation to active derivatives via displacement of the labile oxalate ligand. After displacement of the oxalate group, several transient reactive species are formed including monoaquo and diaquo DACH platinum, which covalently bind (alkylation) macromolecules, creating both inter- and intra-strand platinum-DNA crosslinks. The

formation of platinum adducts results in inhibition of DNA replication and transcription and cell-cycle nonspecific cytotoxicity.

Like other platinum-based compounds, the main mechanism by which OHP exerts its cytotoxicity is DNA damage. In particular, when dichloro (DACH) platinum derivatives enter into the cell nucleus, they form DNA mono-adducts especially on N7 site of an adjacent guanine and di-adducts, although with lower rate than CDDP. The apoptotic process is not triggered only by nuclear DNA damage but also by inhibition of mitochondrial DNA replication and transcription, RNA synthesis and by the activation of immunological reactions that lead to release of pro-inflammatory cytokines and then apoptosis (Alcindor et al., 2011; Mehmood 2014; Fong, 2016; Zajaczkowska et al., 2019).

4. OXALIPLATIN-INDUCED PERIPHERAL NEUROTOXICITY (OIPN)

4.1 CLINICAL FEATURES OF OXALIPLATIN-INDUCED PERIPHERAL NEUROTOXICITY

OHP can cause adverse effects to gastrointestinal (nausea and vomiting, or diarrhea) and hematopoietic (neutropenia and thrombocytopenia) systems, although with a mild severity compared to CDDP (Schmoll and Cassidy, 2001; Lee et al., 2014 a). However, the dose-limiting toxicity of OHP is peripheral neurotoxicity. In particular, OHP treatment induces two different forms of peripheral neurotoxicity: an acute cold-triggered and transient syndrome and a chronic form that develops after repeated administrations and it is often persistent. Acute neurotoxicity is a peculiar condition due to OHP treatment that develops in about 65-98% of patients during or shortly after infusion and may continue for one week. The symptoms of acute syndrome include cold-induced paresthesias of the extremities, dysesthesia of the perioral or laryngeal regions, jaw spasms, fasciculations and muscle cramps. The chronic form occurs in about 50-70% of patients as a sensory, axonal neuropathy with typical “glove and stocking" distribution, not always completely reversible (Mcwhinney et al., 2009; Zajaczkowska et al., 2019).

The onset of peripheral neurotoxicity seems to be time- and dose-dependent. Moreover, several studies demonstrated that the severity of acute symptoms is one of the risk factors associated with the development of high grade chronic OIPN.

4.2 MECHANISMS OF OXALIPLATIN-INDUCED PERIPHERAL NEUROTOXICITY

The exact molecular mechanisms underlying OIPN are not completely elucidated. However, it seems that the antitumor activity mechanisms of OHP could be responsible for its neurotoxic effect and some hypotheses have been proposed.

The acute symptoms described above seem to be related to a peripheral nerve hyperexcitability phenomena that consists in a transient OHP-induced channelopathy. In fact, oxalate ligand, a metabolite of OHP derived from its biotransformation, seems to interfere with the functionality of ion channels located in the cellular membrane such as voltage-gated sodium (Na^+), potassium (K^+) and transient receptor potential (TRP) channels. Some studies reported that oxalate is able to induce a slow inactivation of voltage-gated Na^+ channels and reduction in Na^+ current, causing an increase in duration of the relative refractory period of DRG sensory neurons. Moreover, the oxalate detachment can also induce a chelation of calcium (Ca^{2+}) and magnesium (Mg^{2+}) ions, affecting the Na^+ channels indirectly (oxalate is known as a chelator of these ions) (Gamelin et al., 2002; Park et al., 2011; Kanat et al., 2017; Oun et al., 2018).

Acute neurotoxicity is peculiar of OHP treatment, while the chronic form of OIPN is common to all platinum-based compounds. Over the years, several mechanisms involved in the pathogenesis of platinum-based compounds induced neurotoxicity have been proposed:

- Nuclear DNA damage in DRG

Similar to other platinum-based chemotherapeutic agents, chronic treatment with OHP causes a cumulative and dose dependent neurotoxicity, which result from platinum accumulation in DRG, the main site of PNS damage. As reported above, the lack of blood-brain barrier and the presence of fenestrated capillaries in DRG allow platinum derivatives to accumulate in DRG and in sensory neurons accordingly. Moreover, it is known that in DRG the OHP uptake is controlled by copper transporter 1 (CTR1) and by organic cation transporters 1-3 (OCT1-3).

Like CDDP, OHP derivatives once in the nucleus of the cells, bind DNA creating platinum adducts, although with a lesser extent than CDDP. In particular, an *in vitro* study evidenced that in DRG sensory neurons the platinum adducts amount induced by OHP is about three time less than those produced by equimolar doses of CDDP. In addition, it was observed that OHP induced cell death and inhibition of neurite outgrowth in DRG neurons in a dose-dependent manner, although with minor neurotoxic effect than CDDP (Ta et al., 2006).

Hence, the inhibition of DNA replication, RNA transcription and apoptotic pathway activation occur leading to neuronal atrophy.

- Glial cells and inflammatory mediators activation

DRG consist of sensory neurons and satellite glial cells, which are important for their structural role and supply nutriments to adjacent neurons. Recent studies suggested a possible link between glial cells activation and OHP-dependent neuropathic pain. In particular, it was observed that activation of glial cells promotes the pro-inflammatory cytokine release including IL-1β, IL-6 and TNF-α, which can contribute to the development of pain by activating the Toll-like receptor (TLR) family. Other than cytokines, also chemokines seem to be involved in the pathogenesis of OIPN. In fact, these inflammatory mediators induce recruitment and infiltration of immune cells like macrophages leading to neuroinflammation process onset and related pain. However, all these observations are still not consistent.

- Impairment of mitochondrial function and oxidative stress

Recent evidence suggest that also mitochondrial dysfunctions and related oxidative stress can be responsible for the pathogenesis of platinum-based compounds. The mechanisms are detailed in the following paragraph.

(Carozzi et al., 2015; Kanat et al., 2017; Zajaczkowska et al., 2019).

4.3 ROLE OF MITOCHONDRIAL DYSFUNCTIONS AND OXIDATIVE STRESS IN OXALIPLATIN-INDUCED PERIPHERAL NEUROTOXICITY

Regarding platinum-based compounds, platinum metabolites interfering with ETC can cause a considerable free radical (reactive oxygen species, ROS) generation followed by lipid peroxidation (cellular lipids are the primary targets of free radicals), protein and nucleic acid oxidation and reduction in plasma levels of antioxidants. The resulting oxidative stress can induce apoptosis and interfere with cellular metabolism in both cancer and healthy cells, which could be responsible, in turn, of drug toxicity, including neurotoxicity.

In preclinical studies, among platinum-derived anticancer drugs, CDDP was the first and most widely used drug to investigate the role of oxidative stress in the pathogenesis of its toxicity. Several *in vitro* and *in vivo* studies demonstrated that CDDP is able to induce oxidative damage in several cell types and tissues. In particular, it was reported an increase in superoxide anions levels, lipid peroxidation and in the expression of apoptotic signals as well as a reduction in antioxidant defence including superoxide dismutase, catalase,

glutathione peroxidase and glutathione reductase activities after CDDP exposure, especially in kidney and in cell lines of kidney. Moreover, it was demonstrated that high levels of platinum DNA adduct accumulate in DRG neurons, covalently binding mitochondrial DNA with similar rate as nuclear DNA. However, unlike nuclear DNA, mitochondria do not have any DNA repair system (Base Excision Repair, BER, and Nucleotide Excision Repair pathway, NER). The creation of adducts in DRG neurons leads to inhibition of mitochondrial DNA replication and transcription, followed by cellular apoptosis and changes in mitochondrial morphology including vacuolization. Thus, these processes can result in energy failure of neuronal cells. Taken together, these observations support the hypothesis that mitochondrial damage may play an important role in CDDP-induced peripheral neurotoxicity (Conklin et al., 2004; Canta et al., 2010; Carozzi et al., 2010; Podratz et al., 2010; Fong, 2016; Waseem et al., 2018).

Regarding OHP, the role of mitochondrial damage activity in OIPN onset has not been fully investigated.

Once in the cells OHP, like CDDP, binds nuclear DNA as well as mitochondrial DNA, forming DNA-platinum adducts. An *in vitro* study showed that the exposure of DRG neuronal cultures to high concentrations (largely higher than CDDP) of OHP was able to reduce cell viability and increase mitochondrial ROS production. Moreover, the authors investigated if ROS production following platinum compounds (CDDP, CRB and OHP) exposure was specifically generated in mitochondria by superoxide anion. They noticed that total ROS levels were increased after the treatments but only OHP increased the production of mitochondrial ROS in sensory neuronal cultures (Kelley et al., 2014).

In 2011, it was observed for the first time a significant deficit in ATP production and an increase in swollen and vacuolated mitochondria of rat sciatic and saphenous nerves after a cumulative dose of OHP 10 mg/kg, supporting the mitotoxicity hypothesis in the peripheral neurotoxicity onset. In addition, mitochondrial complexes of isolated sciatic nerves were examined, showing a reduction in respiration rate in ETC with minimal rate of ATP production following OHP treatment (Zheng et al., 2011; Xiao et al., 2012; Waseem et al., 2018). After that, an Italian workgroup proposed a rat model of OIPN (cumulative dose of 36 mg/kg) which showed that OHP induced a significant increase in lipid peroxidation and carbonylated proteins in plasma. In addition, OHP increased lipid peroxidation and DNA oxidation in sciatic nerves (Di Cesare Mannelli et al., 2012).

In another study, after cumulative dose of OHP 45 mg/kg a significant increase in ROS and reactive nitrogen species (RNS) levels was detected in DRG collected from treated mice (Toyama et al., 2014). Furthermore, it is known that OHP is able to induce mitochondrial apoptosis. This evidence emerged from some studies about culture of colorectal cancer cell lines, which confirmed that OHP is able to induce an increase in activation of caspase 3, and Bax/Bak pro-apoptotic proteins. These observations confirmed the ability of OHP to induce apoptotic process via the mitochondrial pathway, independently to nuclear DNA damage (Arango et al., 2004; Gourdier et al., 2004; Sorensen et al. 2017).

5. ROLE OF MITOCHONDRIAL DYSFUNCTIONS AND OXIDATIVE STRESS IN PERIPHERAL NEUROTOXICITES

Over the last years, several studies have shown that mitochondria dysfunction and related oxidative stress may be an etiological factor in many PNS diseases. In fact, mitochondrial injuries can impair the cellular energy metabolism, affecting several organs and cells, including neurons, and this process can lead to cell death. Mitochondrial dysfunction has been observed not only in models of CIPN but also in diabetic neuropathy, Charcot-Marie-Tooth (CMT) disease and in HIV-associated sensory neuropathy (Bennet et al., 2014; Lim et al., 2015).

Among CIPN, in addition to platinum-induced neurotoxicity, PTX-induced neurotoxicity has been investigated. *In vitro* and *in vivo* studies suggested the role of mitochondrial damage as key event in the onset of PTX-induced neurotoxicity. In particular, it is known that PTX binds to β-tubulin of axonal microtubules, interfering with axonal transport of mitochondria. Morphological alterations including swelling and vacuolation was first noted in peripheral nerve sensory axons and in lumbar DRG collected from rats with PTX-induced painful peripheral neurotoxicity, which may results in a chronic axonal energy deficit (Flatters et al., 2006; Zheng et al., 2011; Barriére et al., 2012; Xiao et al., 2012; Bobylev et al., 2015). Same evidence was subsequently observed in peripheral nerves of rats with painful neurotoxicity induced by VCR, BTZ and also OHP (Siau et al., 2006; Zheng et al., 2012; Bennet et al., 2014). Moreover, sciatic nerve axons collected from rats with peripheral neurotoxicity induced by PTX, BTZ and OHP showed significant deficits in mitochondrial respiration associated to Complex I and II and relating ATP production deficits (Zheng et al., 2011; Zheng et al., 2012).

Regarding diabetic neuropathy, first evidence suggested the increase in electron flux within the ETC followed by high level of ROS production in cultured endothelial cells exposed to high concentrations of glucose. In addition, *in vivo* studies observed an increase in ROS production, lipid peroxidation and decrease in antioxidant activities in both sensory neurons and peripheral nerves of animal models of type 1 and 2 diabetes. Moreover, DRG collected from streptozotocin-induced diabetic rats showed a reduction in activity of ETC. In particular, a significant reduction in expression of mitochondrial Complex I and IV components and a significant increase in the expression of activated form of DRP1 (a key mediator of mitochondrial fission) were reported (Chowdhury et al., 2010; Fernyhough, 2010; Akute et al., 2011; Pasaresi et al., 2018).

CMT disease is an inherited sensorimotor polyneuropathy. At least thirty genes seem to be associated with different forms of the disorder and four of these encoded for mitochondrial proteins. A recent clinical study demonstrated an increase in oxidative stress and mitochondrial dysfunction in erythrocytes and plasma of CMT1 patients. In particular, an overproduction in superoxide anion, a significant increase of lipid peroxidation in parallel with a reduction of the antioxidant activities were found in the blood of patients compared to healthy subjects. Moreover, it is known that mutations in MFN2, OPA1 and GDAP1 genes involved in mitochondrial dynamics have a role in the pathogenesis of CMT diseases. In addition, significant mitochondrial transport impairment in cultured DRG neurons expressing disease-mutated forms of MFN2 was observed. Thus, oxidative stress and mitochondrial dysfunction seem to be involved in CMT group of PNS diseases (Baloh et al., 2006; Palau et al., 2009; Chahbouni et al., 2017; Hameren et al., 2018).

Human immunodeficiency virus type-1 (HIV-1) infection can also be characterized by the occurrence of sensory peripheral neuropathy. Preclinical studies showed an enhanced ROS production in mitochondria followed by apoptotic process in HIV-infected cell cultures. It was also observed that the incidence of swollen and vacuolated mitochondria in axons and in Schwann cells was greater in patients with HIV than in uninfected controls. Moreover, there is evidence about augmented ROS levels in monocytes as well an increase in DNA oxidation, lipid peroxidation and a reduction of antioxidant defence activities in plasma of HIV-infected individuals (Banki et al., 1998; Dalakas et al., 2001; Wanchu et al., 2009; Ivanov et al., 2016; Niemann et al., 2014).

6. ANIMAL MODELS OF OXALIPLATIN-INDUCED PERIPHERAL NEUROTOXICITY

The use of animals as experimental models for human diseases is indispensable in order to investigate the pathogenesis of diseases and develop treatment strategies.

Over the last years, several mouse and rat models of CIPN including OIPN have been developed in order to reproduce and mimic, in the most faithful possible way, the clinical characteristics of the pathology and to better understand the pathogenesis of peripheral neurotoxicity.

Since OHP can cause acute and chronic forms of neuropathy, both "acute" and "chronic" models of OIPN have been developed, depending on the clinical aspect to be investigated. In the first case, mechanical allodynia and cold sensitivity are usually assessed, since they are early phenomena that can occur already after one dose of OHP. On the other hand, repeated administrations are required in order to induce chronic damage, that can be evidenced with neurophysiological, behavioural, morphological and morphometric analyses. Most of the studies reported in literature examine neurophysiological, behavioural and pathological aspects of OIPN using rat models, often after only a single administration of OHP. Therefore, these models are not representative for the chronic form of OIPN. Moreover, although models of OIPN in rats allow understanding some characteristics of neurotoxicity induced by OHP, only a very limited number of cancer cell lines can be implanted in immunocompetent rats. Thus, rat models have some limitations in evaluating both antineoplastic activity and neurotoxic effects of the anticancer compounds. For this reason, several models of immunocompetent and immunocompromised mouse models of OIPN have been recently developed.

6.1 "ACUTE" MODELS OF OXALIPLATIN-INDUCED PERIPHERAL NEUROTOXICITY

The first animal model useful to study the acute form of OIPN was developed in 2007. Rats were treated with a single intraperitoneal injection of OHP at three different doses (3, 6 or 12 mg/kg) and mechanical allodynia as well as thermal hyperalgesia were assessed daily for ten days after the administration. This study showed that a single OHP injection is able to induce hypersensitivity to cold and mechanical allodynia with a rapid onset, reproducing the neurotoxic profile of acute OIPN (Ling et al., 2007 a). These observations were confirmed by several subsequent studies performed by different workgroups (Aoki et al., 2014; Choi et

al., 2019; Lee et al., 2014 b; Yamamoto et al., 2016), including a study in which OHP was administered intravenously at the dose of 2 mg/kg (Joseph and Levine, 2009).

In 2017 a mouse model of acute form of OIPN was performed, treating with a single intraperitoneal injection of OHP 6 mg/kg. From 3 to 7 days after OHP administration mechanical allodynia was observed, while cold allodynia developed at day 3 and persist until day 5 (Kim et al., 2016).

6.2 "CHRONIC" MODELS OF OXALIPLATIN-INDUCED PERIPHERAL NEUROTOXICITY

In literature, there are different rat models developed to study chronic form of OIPN. Among them, one of the first models was developed in 2001. In this study, rats were treated intraperitoneally for repeated days with four different schedules of OHP using two cumulative doses (36 and 48 mg/kg). At the end of the treatments, a significant reduction in NCV and atrophy of DRG neurons in all the treated mice compared to control group were evidenced. After a follow-up period of 5 weeks, recovery of the pathological changes in the DRG occurred in OHP treated animals, together with improving in sensory NCV (Cavaletti et al., 2001). Some years later other rat models of chronic OIPN were described. One of them consisted in the administration of OHP intravenously at three different doses (1, 2 or 4 mg/kg), twice a week for 4.5 weeks. Mechanical allodynia was observed after the 4th injection and maintained until the end of experiment for all groups while cold hyperalgesia was observed after 2nd injection for the 2 mg/kg group and after injection 4 for the 1 and 4 mg/kg groups (Ling et al., 2007 b). In another study, rats treated with OHP 2.4 mg/kg intraperitoneally for five consecutive days for 3 weeks developed mechanical allodynia after the 3rd week of administration (Norcini et al., 2009). Mechanical allodynia and cold hyperalgesia were also observed in rats treated with intraperitoneal OHP 4 mg/kg, twice a week for 4 weeks. At the end of the treatment OHP caused degeneration and decrease in the density of myelinated fibers in sciatic nerve (Kawashiri et al., 2011).

In addition to rat models of chronic form of OIPN, several mouse models were developed in order to investigate the characteristic of chronic form of OIPN. In 2011, chronic OHP neurotoxicity was evaluated for the first time through a multimodal assessment in a mouse model. For this purpose, mice were treated with OHP 3.5 mg/kg twice a week for 4 weeks. After the OHP treatment, the animals showed not only mechanical allodynia and cold hyperalgesia but also a reduction in NCV of caudal and digital nerves associated with a

decrease in caudal action potential amplitudes as well as atrophy of DRG neurons. Moreover, DRG neurons appeared multinucleolated and with eccentric nucleoli while sciatic nerves presented mild signs of axonopathy (Renn et al., 2011).

Over the following years, due to the importance of mouse models in translational cancer research, several mouse models of OIPN were developed. Among them Coriat and collaborators treated mice with OHP 10 mg/kg once a week for 8 weeks, observing mechanical hypersensitivity and cold hypoesthesia from 4 to 8 days after OHP administration (Coriat et al., 2014). Mechanical hypersensitivity was also detected from days 8 to 27 in mice injected on alternate days with a cumulative dose of OHP 20 mg/kg (Makker et al., 2017); on the contrary, cold hypersensitivity was observed at day 2 until 7 in mice treated with OHP 15 mg/kg weekly for 3 weeks (Toyama et al., 2014).

6.3 OIPN MOUSE MODELS TAKEN INTO CONSIDERATION FOR THE STUDY

As reported in literature and in the paragraph above, several schedules of OHP are used to study the features of OIPN which differ from each other in route of administration, number and frequency of injections, duration of treatment and cumulative dose. Many of these schedules are generally unable to induce all the typical features of chronic OIPN, although they reproduce some aspects of the OIPN, such as neuropathic pain. To verify all the features of OINP onset, a multimodal assessment is highly advisable, therefore neurophysiological, behavioural examination and histopathological analysis should be performed and evaluated (Marmiroli et al., 2017).

Among scientific publications in this field, three mouse models obtained with different OHP schedules have been taken into consideration for this study. In particular, we chose studies in which OHP schedules are very different from each other in cumulative dose and duration of treatment. Thus, we selected two short-term OHP treatment characterized by high or low cumulative doses (20 and 3 mg/kg, respectively) and a longer schedule with a cumulative dose of 30 mg/kg.

The three published studies we selected are listed below:

*Study 1_* Schedule OHP 10 mg/kg, two doses on alternate days.

To investigate the mechanisms underlying neuropathic pain onset, Jiang and collaborators treated adult male C57BL/6 mice intraperitoneally with two doses of OHP 10 mg/kg at day0

and day2, respectively. The mechanical sensitivity using Von Frey filaments and cold sensitivity by tail immersion in a water bath set at 4°C were assessed.

Authors observed that OHP induced a significant decrease in mechanical withdrawal threshold (mechanical hypersensitivity) and tail withdrawal threshold (cold hypersensitivity) at 24 hours from the second administration, which persisted for the entire period of observation (days 6, 9, 12 and 15)(Jiang et al., 2016; **Fig. 1**).

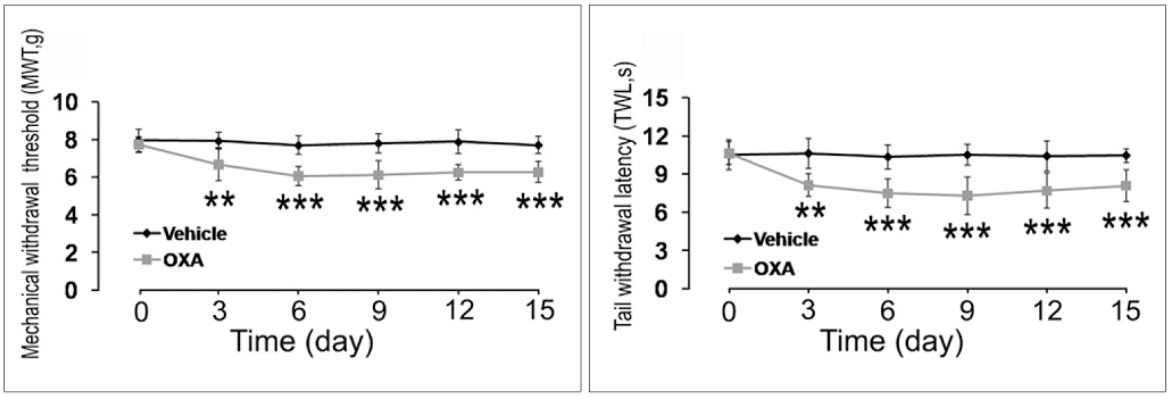

Figure 1. Assessment of mechanical-induced allodynia and cold-induced hyperalgesia.
(Jiang et al., 2016)

*Study 2_* Schedule OHP 3 mg/kg single dose.

To investigate the mechanisms underlying OIPN, Nassini and collaborators treated adult male C57BL/6 mice with a single intraperitoneal administration of OHP 3 mg/kg. The mechanical sensitivity using Von Frey filaments and cold sensitivity by tail immersion in a water bath set at 10°C were assessed.

They observed a time-dependent reduction in mechanical withdrawal threshold at days 3, 6, 10, 15 and 20. Moreover, OHP induced a time-dependent cold allodynia at days 3, 6 and 10 (Nassini et al., 2011; **Fig. 2**).

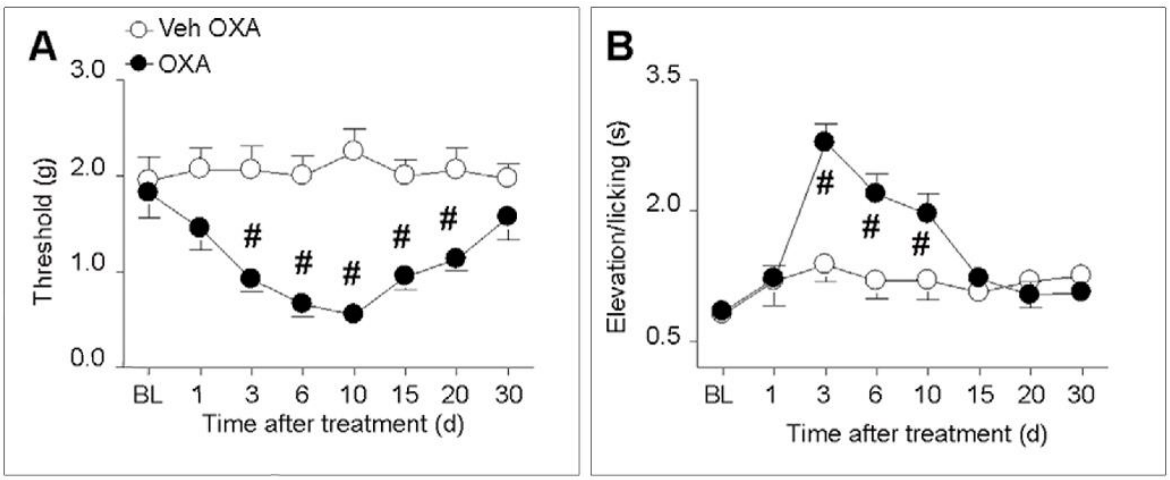

Figure 2. Assessment of mechanical-induced allodynia and cold-induced hyperalgesia.
(Nassini et al., 2011)

*Study 3*_ Schedule OHP 3 mg/kg, daily for five days for two cycle with five days of rest.

To establish a mouse model of OHP-induced painful neuropathy, Ta and collaborators treated adult male C57BL/6 mice with daily intraperitoneal injections for five days, followed by five days of rest, for two cycles. The mechanical sensitivity using Von Frey filaments and cold sensitivity by cold plate test with a temperature set at -4.2°C were assessed.

They observed a significant decrease in mechanical withdrawal threshold in treated mice compared to control group at the end of the second cycle. Moreover, OHP induced cold hypersensitivity at the end of both first and second cycles, which persisted until 6 weeks (Ta et al., 2009; **Fig. 3**).

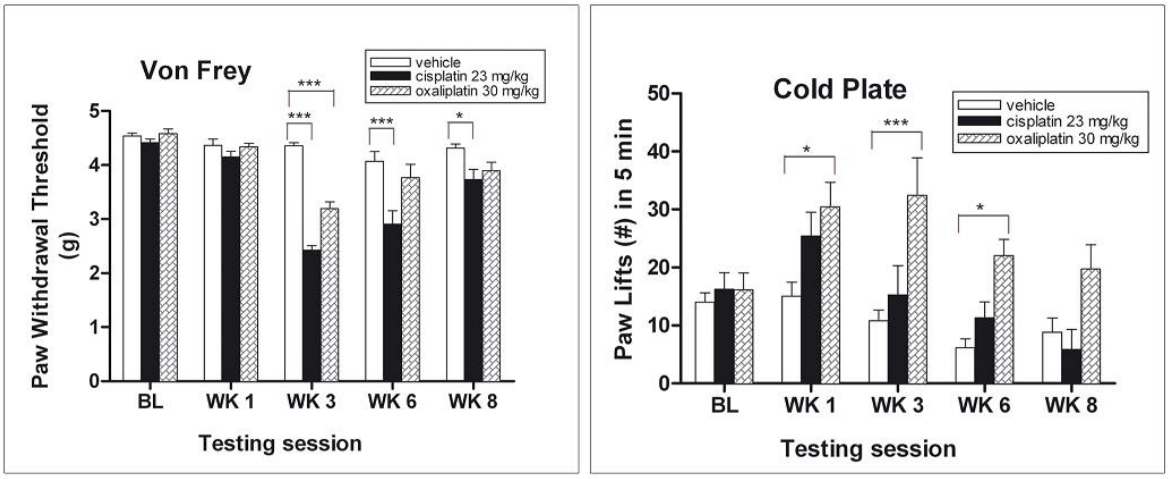

Figure 3. Assessment of mechanical-induced allodynia and cold-induced hyperalgesia.
(Ta et al., 2009)

AIMS OF THE STUDY

The aims of this study are:

1. **To compare OIPN mouse models reported in three different published studies with OIPN mouse model currently used in our laboratory through a multimodal approach.**

   Male mice were treated with four different schedules of OHP reported in literature to evaluate the onset of neurotoxicity through the multimodal assessment currently used in our laboratory: evaluation of general toxicity, behavioural tests, neurophysiological study, morphological and morphometric analyses were performed.

   This work is very important to ascertain which kind of OHP schedule could be more reliable for of acute and chronic OIPN animal models, useful for evaluating of pathogenic mechanisms underlying the onset of OIPN and neuroprotective strategies. Moreover, the establishment of a multimodal assessment would be important to try to standardise, or at least to reduce the difference among laboratories, in approaching CIPN studies.

2. **To evaluate one of the possible pathogenic mechanism underlying OIPN onset: the role of mitochondrial dysfunction and oxidative stress.**

   DRG and peripheral nerves, main sites of OHP damage, collected from animals treated with all the different schedules of OHP were analysed to evaluate the oxidative stress level following OHP treatment. Mitochondrial respiratory chain function and dynamics were examined in DRG following the long-term OHP treatment.

   It is important to note that mitochondrial function and oxidative stress have not been investigated before either in our OIPN mouse model nor in the OIPN mouse models taken into consideration.

METHODS

A. OXALIPLATIN-INDUCED PERIPHERAL NEUROTOXICITY CHARACTERIZATION: *IN VIVO* STUDY

1. ANIMAL HUSBANDRY AND TREATMENT

Ten-week-old male C57BL/6 and BALB/c mice (Envigo, San Pietro al Natisone, Italy) were employed for this study.

The care and husbandry of animals were compliant with national (D. L.vo 26/2014, Gazzetta Ufficiale della Repubblica Italiana, n.61, March 14th 2014) and international laws and policies (European Union directive 2010/63/UE; Guide for the Care and Use of Laboratory Animals, U.S. National Research Council, 1996).

Animals were maintained under standard animal housing conditions with a 12 h light–dark cycle, room temperature and relative humidity were set at 20 ± 2°C and 55 ± 10%, respectively. Treated and untreated mice were housed separately and with free access to water and food. The general condition of the animals was assessed daily.

OHP 5 mg/ml concentrate for solution for infusion (Accord Healthcare Limited, UK) was diluted in 5% glucose solution to give the desired concentration immediately before each administration.

Mice were treated with three different schedules of OHP reported in the literature and with the OHP schedule currently used in our laboratory. The four studies were performed to assess acute and chronic OHP neurotoxicity. Using injection volume of 10 ml/kg, mice were treated intraperitoneally (i.p.) or intravenously (i.v.) with oxaliplatin (OHP groups) or 5% glucose as vehicle (CTRL groups) as follows:

Study 1
- CTRL group, vehicle, d1 and d3, i.p., C57BL/6
- OHP group, oxaliplatin 10 mg/Kg, d1 and d3, i.p., C57BL/6

(Jiang et al., 2016)

Study 2
- CTRL group, vehicle, single i.p., C57BL/6
- OHP group, oxaliplatin 3 mg/Kg, single i.p., C57BL/6

(Nassini et al., 2011)

Study 3
- CTRL group, vehicle, q1dx5, 2 cycles with 5 days rest, i.p., C57BL/6
- OHP group, oxaliplatin 3 mg/Kg, q1dx5, 2 cycles with 5 days rest, i.p., C57BL/6

(Ta et al., 2009)

Study 4 - CTRL group, vehicle, 2qwx4, i.v., BALB/c

- OHP group, oxaliplatin 5 mg/Kg, 2qwx4, i.v., BALB/c

(Renn et al., 2011; Marmiroli et al., 2017, with dosage adjustment to 5 mg/kg)

2. EXPERIMENTAL DESIGN

Mice were randomly divided into two groups with 13 mice in each group/time point: a vehicle group injected with 5% glucose (CTRL group) and an OHP-treatment group (OHP group) treated with 4 different schedules of OHP (*Studies 1-4*).

At each time point, 13 animals of each group were employed for behavioural tests, dynamic test (D) and cold plate test (C), and neurophysiological determinations (N). After *in vivo* evaluations, mice were sacrified (S) under deep anaesthesia with isoflurane for biological sampling: skin biopsy was processed for the evaluation of IENF density while DRG, caudal and sciatic nerves were collected for morphological and morphometric analyses and oxidative stress evaluations (TBARS assay and Western Blot analysis).

2.1 Study 1

According to OIPN mouse models developed by Jiang and collaborators, C57BL/6 male mice were injected intraperitoneally with two doses of OHP 10 mg/kg (day1 and day3).

The evaluation time points were 24 hours after the second OHP injection, 1 and 2 weeks from the first dose of OHP.

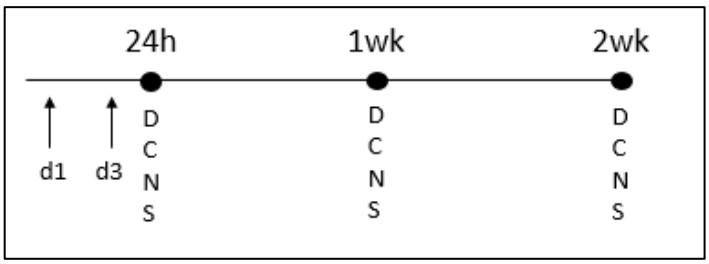

Figure 1. Experimental design *Study 1*.

2.2 Study 2

According to OIPN mouse models developed by Nassini and collaborators, C57BL/6 male mice were treated with a single intraperitoneal injection of OHP 3 mg/kg.

The evaluation time points were 24 hours, 1 and 2 weeks from the OHP injection.

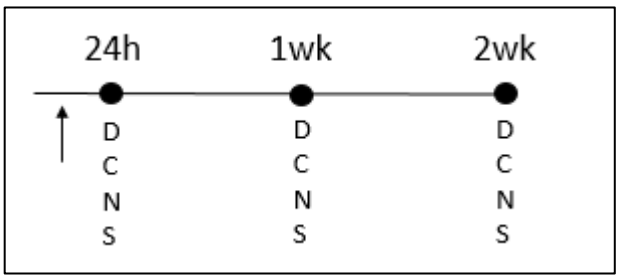

Figure 2. Experimental design *Study 2*.

2.3 Study 3

According to OIPN mouse models developed by Ta and collaborators, C57BL/6 male mice were treated with daily intraperitoneal injection of OHP 3 mg/kg for 5 days, followed by 5 days of rest, for two cycles.

The evaluation time points were 1, 2 and 4 weeks from the first OHP injection. In particular, 1 and 2 weeks coincided with the end of the first and second OHP treatment cycle respectively, while 4 weeks corresponded to 2 weeks of follow-up period.

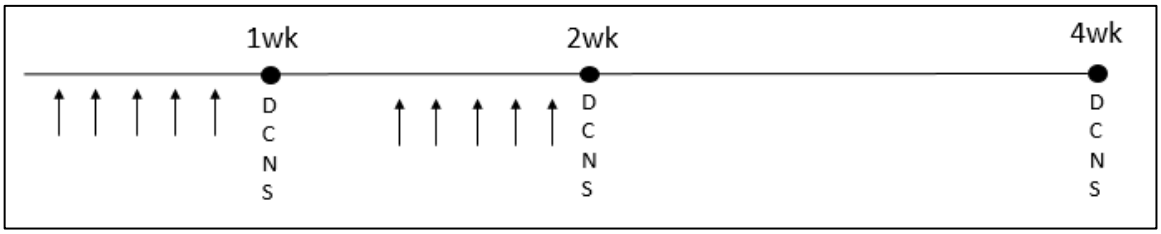

Figure 3. Experimental design *Study 3*.

2.4 Study 4

BALB/c male mice were treated intravenously by tail vein injection with OHP 5 mg/kg, twice weekly for 4 weeks, according to the standard OHP schedule employed in our laboratory, published by Renn and Marmiroli's workgroups. Since for this study we used OHP commonly used in the clinical practice with a different formulation than the previous one, we performed a preliminary *in vivo* dose-finding study (data not shown). As a result, a dose adjustment to 5 mg/kg, compared with published dosage (3.5 mg/kg), was required.
The evaluation time points were 24 hours, 1, 2, 4 and 6 weeks from the first OHP injection. In particular, 6 weeks corresponded to 2 weeks of follow-up period.

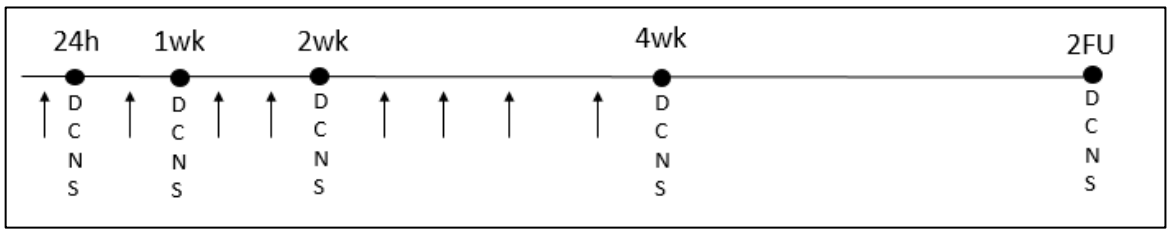

Figure 4. Experimental design *Study 4.*

3. CLINICAL MONITORING AND BODY WEIGHT

The mortality and general condition of the animals were evaluated and assessed daily. Body weight was recorded before each OHP injection for general toxicity assessment and eventually for drug dose adjustment and weekly during follow-up period to monitor animal health.

4. ASSESSMENT OF OXALIPLATIN-INDUCED NEUROPATHIC PAIN

For evaluating neuropathic pain, withdrawal pain threshold was determined by Dynamic test and Cold plate test.

4.1 Behavioural Testing - Dynamic Test

The mechanical threshold was assessed using Dynamic Aesthesiometer apparatus (model 37450 - Dynamic Plantar Aesthesiometer, Ugo Basile Biological Instruments, Comerio, Italy). Before testing, animals were placed in a Plexiglas chamber in the Dynamic Aesthesiometer for a 2 hours acclimatization period. A pointed metallic filament with 0.5

mm diameter was applied to the plantar surface of the hind paw, which exerted a progressively increasing pressure, reaching up to 15 grams within 15 seconds.
Paw withdrawal latencies are recorded three times for each hind and from the average of the values the mechanical threshold was obtained. These results represent the maximal pressure (expressed in grams) tolerated by the animals. The cut-off was set at 30 sec, after which the mechanical stimulus was automatically stopped.

4.2 Behavioural Testing - Cold Plate test

The cold nociceptive threshold was assessed using the Cold Plate (model 35100 - Hot/Cold Plate, Ugo Basile Biological Instruments, Comerio, Italy). This device was composed by a Plexiglass cylinder and a thermostatic plate set at 4°C.
During the test, each mouse was placed in the Plexiglass holding cage, free to move and walk and observed for 5 minutes. The number of pain signs/suffering (hind paws lifts, flicking/licking and jumpings) were recorded by a blind examiner in a trial of 5 minutes.
The trial was prematurely suspended if the mouse showed a strong intolerance to temperature (evident anxiety and vocalization).

5. ASSESSMENT OF OXALIPLATIN-INDUCED PERIPHERAL NEUROTOXICITY

5.1 Neurophysiological examination

To evaluate the onset of OIPN, neurophysiological evaluation was performed in the caudal and the digital nerves using an electromyography apparatus (Myto2 ABN Neuro, Firenze, Italy). Nerve Conduction Velocity (NCV) and Sensory Nerve Action Potential (SNAP), were measured by placing a couple of needle recording electrodes (cathode and anode) at the base of the tail (for caudal recordings) or at the ankle bone (for digital recordings) and a couple of stimulating electrodes 3.5 cm far from the recording points (for caudal recordings) or close to the fourth toe (for digital recordings).
Latencies were measured from stimulus onset and peak-to-peak amplitudes were calculated. The NCV was calculated by taking the measured distance between the recording and the stimulating points the stimulator and dividing by the onset latency. The onset latency is the time from the stimulus artefact to the onset of the first peak of the elicited action potential.

Intensity, duration and frequency of stimulation were set up in order to obtain optimal results.

During all the neurophysiological determinations, the body temperature of the animals was monitored with a rectal probe in a temperature-controlled room and the mice were under deep isoflurane anaesthesia.

5.2 Morphological and morphometric analyses

To detect alterations in the main target of platinum drug (DRG) and damages of the peripheral nerves and of small unmyelinated nerve fibers (nerves and skin), at each time point 3 animals for each group were sacrificed and L4-L5 DRG, caudal and digital nerves and hind paw skin biopsies were collected.

5.2.1 DRG

DRG were immediately fixed in 2% glutaraldehyde/4% paraformaldehyde in 0.12 M phosphate buffer solutions pH 7.4. Samples were then post-fixed in OsO_4 and embedded in epoxy resin. Serial 1.5-µm sections were prepared, stained with toluidine blue and examined with a Nikon Eclipse E200 light microscope (Leica Microsystems GmbH, Wetzlar, Germany) for morphological observations. Images were captured with a light microscope-incorporated camera at a magnification of 20x by *QWin* software (Leica DFC 280 Wetzlar, Germany) to perform morphometric analysis. The somatic, nuclear and nucleolar size areas of at least 200 DRG neurons/animal were manually measured with image analyser (*Image J* software, US National Institutes of Health). The same blinded operator performed all the morphometric measurements.

5.2.2 Peripheral nerves

Caudal and sciatic nerves were dissected out without stretching and immediately fixed in 3% glutaraldehyde in 0.12 M phosphate buffer solutions pH 7.4. Samples were then post-fixed in OsO_4 and embedded in epoxy resin. As for DRG analysis, 1.5-µm-thick semithin sections were stained with toluidine blue and examined with a Nikon Eclipse E200 light microscope (Leica Microsystems GmbH, Wetzlar, Germany) for morphological observations. Three images of one nerve section for 3 animals/group were captured with a light microscope-incorporated camera at a magnification of 60x by *QWin* software (Leica DFC 280 Wetzlar, Germany) and underwent morphometric analysis using an automatic

image analyser (*Image-Pro Plus* compiled by Immagini e Computer SNC, Milan, Italy). The mean diameter, frequency distribution and density of myelinated fibers were calculated.

5.2.3 IENF

Three-mm glabrous skin punch biopsies from the plantar hind paw were immediately fixed in 2% PGP (paraformaldehyde-lysine-periodate) fixative for 24 h at 4°C, cryoprotected and stored at -20°C until cryostat sectioning. Twenty-µm-thick sections were immunostained with rabbit polyclonal anti-protein gene product 9.5 (PGP 9.5; GeneTex, Irvine, CA, USA) using a free-floating protocol. The same blinded observer counted the total number of PGP 9.5-positive IENF crossing the dermal-epidermal junction under a light microscope at 40x magnification (Nikon Eclipse E200 light microscope, Leica Microsystems GmbH, Wetzlar, Germany). Images of skin biopsies were capture and length in mm of the interface between the derma and epidermal was manually measured with image analyser (*Image J* software, US National Institutes of Health). The IENF density was expressed as number of IENF/mm.

B. OXIDATIVE STRESS EVALUATION

1. THIOBARBITURIC ACID REACTIVE SUBSTANCE ASSAY

Since lipid peroxidation is a biochemical marker for oxidative stress, its levels in DRG, caudal and sciatic nerves were evaluated by quantification of thiobarbituric acid reactive substance (TBARS).

Briefly, frozen DRG pool, caudal and sciatic nerves from each mouse were homogenized in lysis buffer (Tris HCl 0.1 M pH 7.4, EDTA, glutathione) with a TissueLyser II (Qiagen, Milan, Italy) instrument, according to Ha and collaborator (Ha and Endou, 1992). 100 µl of homogenate was added in a solution containing 50 µl SDS 8.1%, 600 µl of phosphoric acid 1% and 200 µl of thiobarbituric acid 0.6% (TBA). Samples were then incubated at 95 °C for 45 minutes. After incubation samples were cooled to room temperature, extracted with 1 ml of n-butanol and then centrifuged at 3000 rpm for 20 minutes. The supernatant was measured fluorometrically at excitation wavelength of 532 nm and emission wavelength of 520 nm. Quantification was done using the standard curve with malondialdehyde (MDA) following similar conditions. Protein concentration to normalize samples was determined using a Bradford protein assay. The oxidative stress levels in the samples were expressed as nmol of MDA per µg of protein.

2. WESTERN BLOT ANALYSIS

Frozen DRG pool from each mouse was homogenized in lysis buffer (PBS pH 7.4, EDTA 0.5M pH 8, Igepal) supplemented with protease and phosphatase inhibitor cocktails (Cell Signaling Technology, Danvers, Massachusetts, USA) with a TissueLyser II (Qiagen, Milan, Italy) instrument. The resulting homogenate was centrifuged at 2000 rpm at 4°C for 5 minutes.

Equal amounts of protein extracts, determined using a Bradford protein assay, were separated on SDS-PAGE precast gel (4-15% gradient gel, Bio-Rad, Milan, Italy) and Western blot was performed. Incubation with primary antibody such as Total OXPHOS Rodent WB antibody cocktail (Abcam, Cambridge, UK), DRP1-Ser616 (Signalway Antibody, College Park, Maryland, USA), DRP1 (Cell Signaling Technology, Danvers, Massachusetts, USA) was performed overnight ad 4°C. After washing for 1 hour in PBS containing 0.1% Tween20, the membranes were incubated with the proper secondary antibody for 2 hours and detected using enhanced chemiluminescence (ECL) method (Bio-Rad, Milan, Italy).

ECL signals were acquired with a ChemiDoc™ XRS+ system (Bio-Rad, Milan, Italy) and the digital quantification of bands was performed with *ImageJ* software (US National Institutes of Health). The concentration of each target protein was normalized versus β-actin and also VDAC (data not shown).

The mean control value within a single experiment was set to 100 and all the other values were expressed as percentage.

STATISTICAL ANALYSIS

The differences between two groups (OHP-treated mice vs CTRL) were statistically evaluated using the analysis of Mann-Whitney nonparametric test or Unpaired t test (*GraphPad Prism* software, version 4.0, San Diego, CA, USA) and the differences were considered significant if $p<0.05$.

For Mann-Whitney analysis, the data were depicted with box-and-whiskers plots and represented as median (midline of the box), 25^{th} (bottom line of the box), 75^{th} percentile (top line of the box) and minimum and maximum (end of the whiskers). Otherwise, for Unpaired t test analysis, the data were depicted with column bars and represented as mean ± standard error of the mean (SEM).

RESULTS

STUDY 1

A. *IN VIVO* STUDY AND OXALIPLATIN-INDUCED PERIPHERAL NEUROTOXICITY CHARACTERIZATION

1. CLINICAL MONITORING AND BODY WEIGHT

All mice injected intraperitoneally with two doses of OHP 10 mg/kg (at day1 and day3) survived until the end of the study and a good general health status of the animals was observed. The body weight of OHP-injected animals was reduced after the 1st administration and during the entire period of observation, significantly ($p<0.01$) after the 2nd administration as shown in **Fig. 5**.

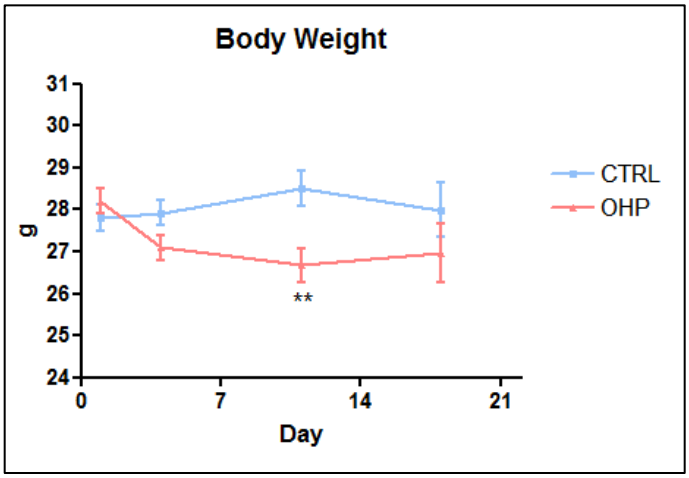

Figure 5. Body weight changes of mice injected intraperitoneally with OHP 10 mg/kg at day1 and day3 compared to vehicle-injected mice (CTRL).
OHP treatment caused a significant body weight loss after the 2nd dose.
Values of body weight expressed in grams (g) are shown as mean ± SEM, **p<0.01 vs CTRL, Unpaired t-test.

2. ASSESSMENT OF OXALIPLATIN-INDUCED PERIPHERAL NEUROTOXICITY

Withdrawal threshold of pain was assessed by Dynamic test and Cold plate test 24 hours after the 2nd OHP injection, 1 and 2 weeks from the 1st dose of OHP. The Dynamic test was used for mechanical allodynia or hypoesthesia testing. On the other hand, the Cold plate test was used to detect the presence of cold hyperalgesia or hypoalgesia.

At the same evaluation time points neurophysiological analyses were performed in the caudal and digital nerves to evaluate myelinated fibers function. In particular, SNAP and NCV were measured, which record mainly the largest nerve fibers.

Evaluation time points of morphological and morphometric analysis are reported in the specific paragraph.

2.1 Behavioural Testing - Dynamic Test

OHP treatment did not induced mechanical allodynia or hypoesthesia in mice during the entire period of observation (**Fig. 6**).

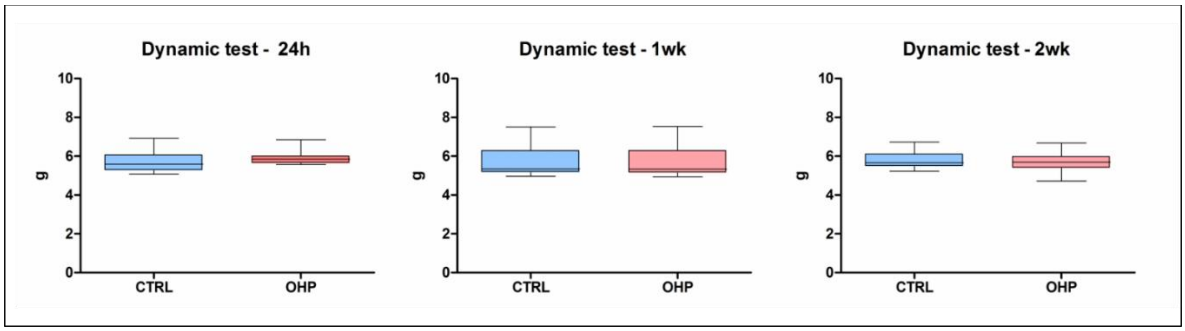

Figure 6. Assessment of mechanical withdrawal threshold.
There was no significant difference between OHP and CTRL groups following treatment at each evaluation time point.
The maximal pressure tolerated by the animals related to mechanical stimuli expressed in grams (g) is shown as median (n=13 per group).

2.2 Behavioural Testing - Cold Plate test

As reported in **Fig. 7**, at 24 hours after the 2nd OHP administration no significant differences in the response to cold stimulus were observed. OHP treatment induced cold hyperalgesia at 1 week ($p<0.01$) and 2 weeks ($p<0.05$) after the 1st OHP administration.

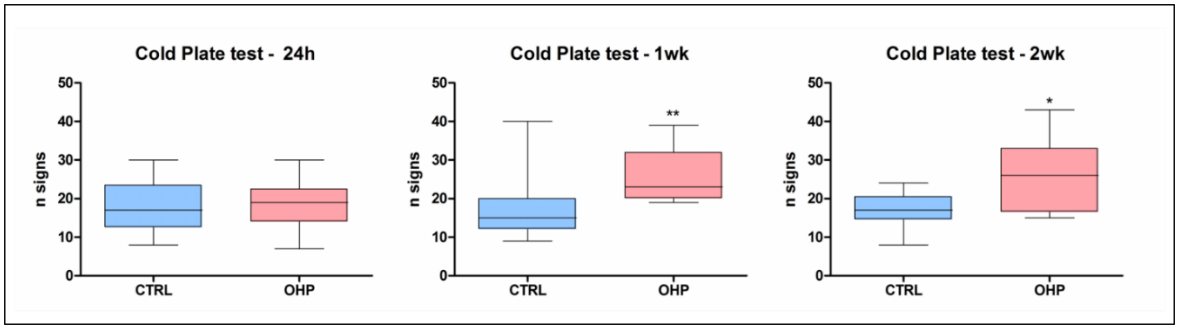

Figure 7. Assessment of cold nociceptive threshold.
At 24-hour evaluation time point there was no significant difference between OHP and CTRL group. OHP-treated group exhibited a significant increase in the number of pain signs (hind paws lifts, flicking/licking and jumpings) compared to CTRL group at 1 and 2 weeks after the start of treatment. The number of pain signs is shown as median (n=13 per group), *$p<0.05$, **$p<0.01$ vs CTRL, Mann-Whitney test.

2.3 Neurophysiological examination

The OHP-treated mice did not show any significant difference in SNAP and NCV measured in caudal and digital nerves, compared to CTRL mice during the entire period of observation (**Fig. 8**).

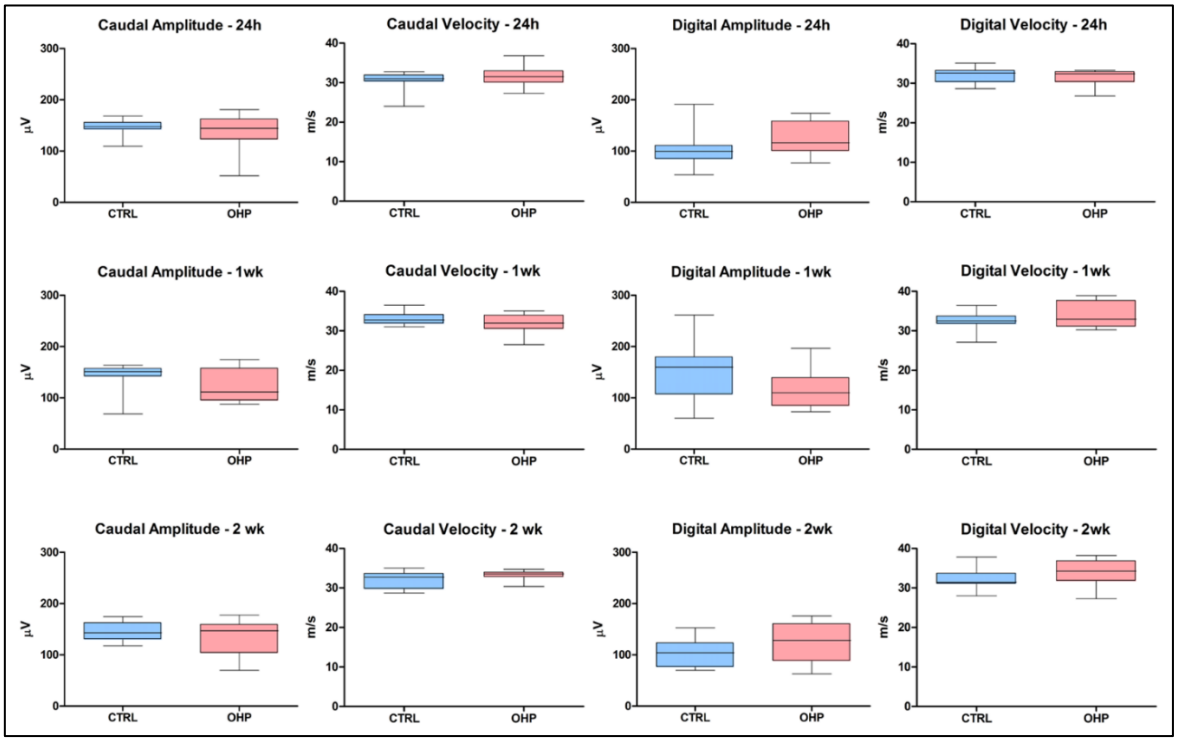

Figure 8. Assessment of NCV and SNAP of caudal and digital nerves.
There was no significant difference between OHP and CTRL groups in NCV and SNAP of caudal and digital nerves following treatment at each evaluation time point.
The values of amplitudes expressed in microvolts (µV) and the velocities expressed in meter per second (m/s) are shown as median (n=13 per group).

2.4 Morphological and morphometric analyses

Morphological and morphometric analyses of DRG, sciatic and caudal nerves were performed to evaluate the possible structural changes induced by OHP treatment. Data were obtained for the samples collected at 1 and 2 weeks from the 1st dose of OHP, while 24 hours from the 2nd OHP administration is considered a too early timing to observe structural alterations induced by OHP injections.

Moreover, the IENF density of hind paw skin was calculated to evaluate the effects of OHP on the peripheral unmyelinated fibers. This measurement was performed on biopsies collected at 1 week from the 1st OHP administration, which is considered the end of treatment time point.

2.4.1 DRG

Since DRG are the main target of platinum-based compound, the areas of soma, nucleus and nucleolus were measured.

Light microscopy analysis did not evidence apparent morphological changes between OHP-treated mice and relative CTRL group for both times of observation as shown in **Fig. 9**.

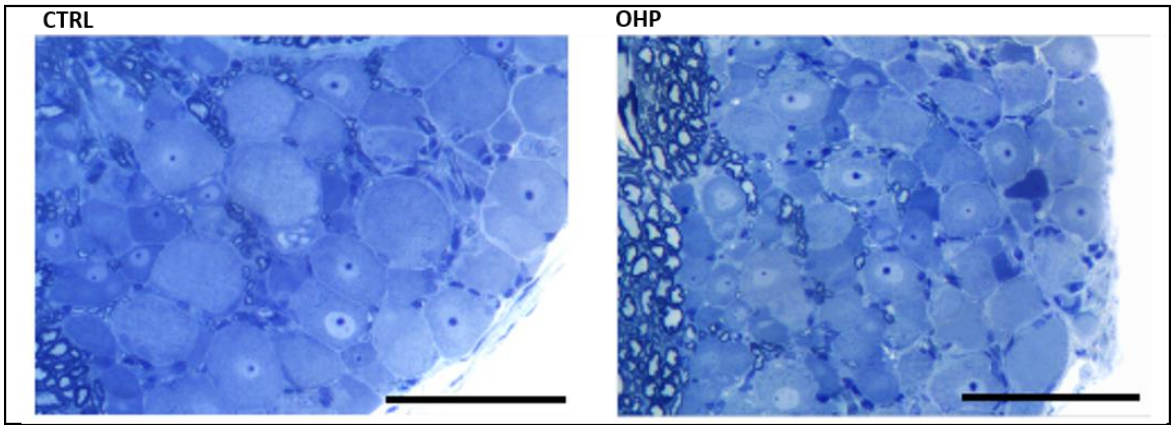

Figure 9. Assessment of morphology of DRG neurons.
No evident morphological changes between OHP and CTRL groups at both evaluation time points were observed in DRG.
Representative images of DRG collected at 1 week from the 1st OHP injection. 20x magnification. Scale bar 100 µm.

Regarding morphometry, at 1 week after the 1st OHP injection the mice treated with OHP showed a remarkable DRG neuronal atrophy with a significant decrease in the size of cell body ($p<0.001$), nucleus ($p<0.01$) and nucleolus ($p<0.0001$) compared to CTRL mice.

A significant reduction in somatic ($p<0.0001$) and nuclear ($p<0.001$) areas persisted at 2 weeks after the 1st OHP, while nucleolar area returned to normal value (**Fig. 10**).

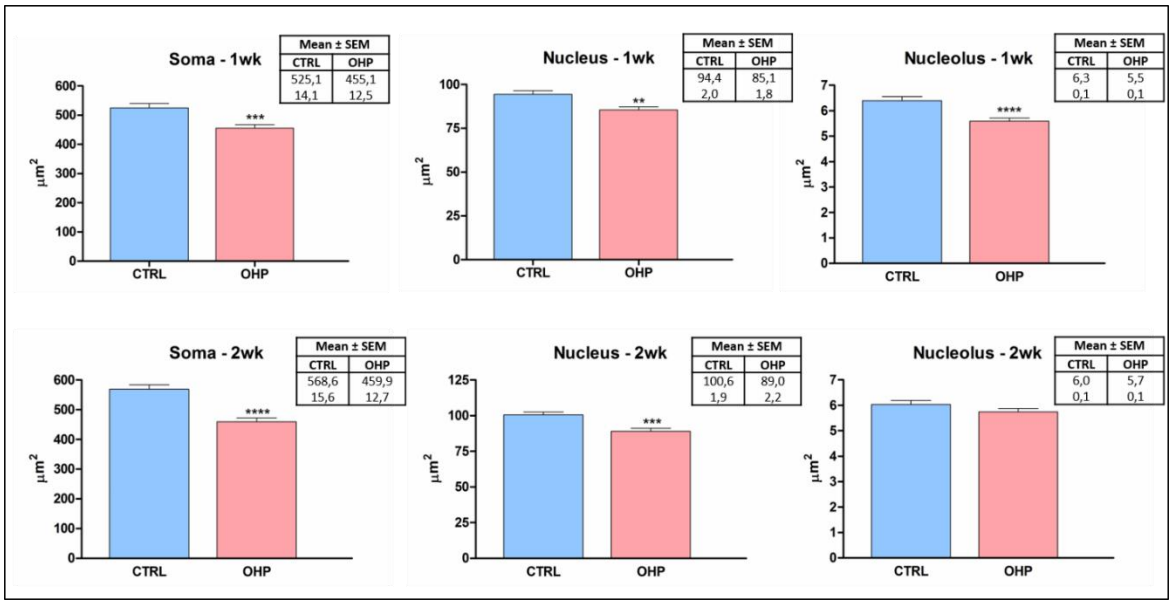

Figure 10. Assessment of morphometry of DRG neurons.
OHP treatment induced a significant decrease in the somatic, nuclear e nucleolar areas, except for nucleolar area at 2-week evaluation time point.
The neuronal sizes expressed in square micrometres (µm²) are shown as mean ± SEM (n=3 per group), **p<0.01, ***p<0.001, ****p<0.0001 vs CTRL, Unpaired t-test.

2.4.2 Peripheral nerves

To verify if OHP induced structural changes in peripheral nerves, morphological aspect, diameter and density of myelinated fibers of sciatic and caudal nerves were examined.

Light microscopy analysis did not reveal apparent morphological alterations of sciatic and caudal nerves in OHP-treated mice compared with CTRL group for both times of observation as shown in **Figs. 11-12**.

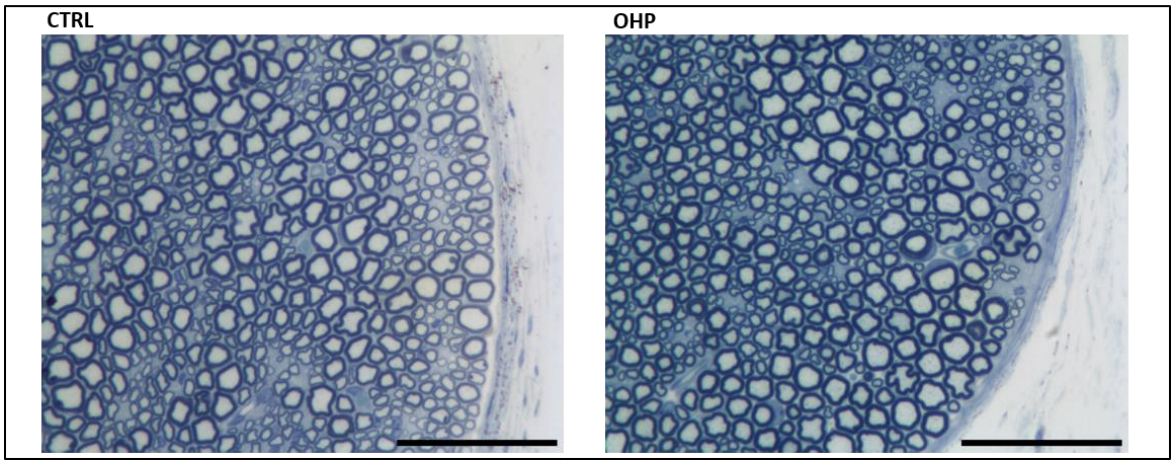

Figure 11. Assessment of morphology of sciatic nerves.
No evident morphological changes between OHP and CTRL groups at both evaluation time points were observed in sciatic nerves.
Representative images of sciatic nerves collected at 1 week from the 1st OHP injection. 40x magnification. Scale bar 50 µm.

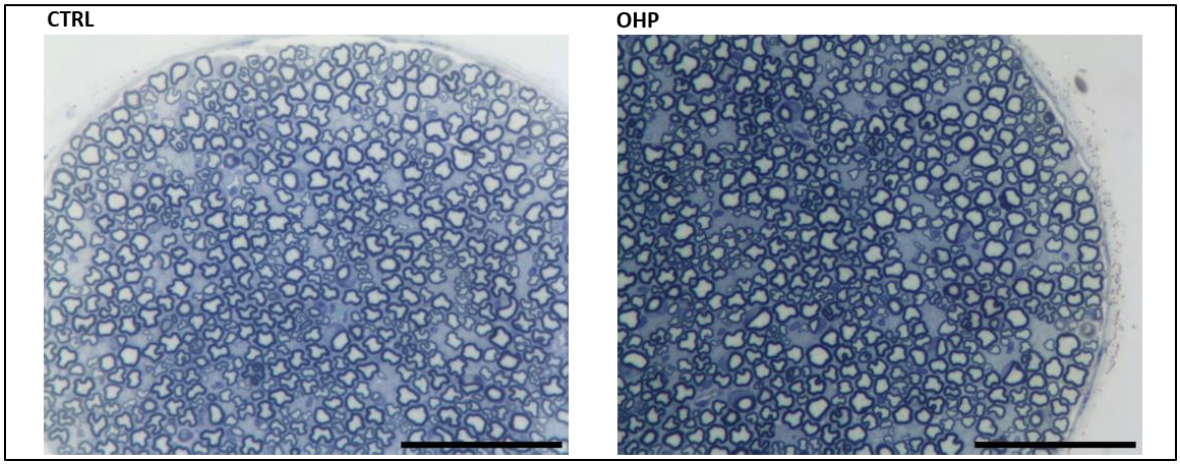

Figure 12. Assessment of morphology of caudal nerves.
No evident morphological changes between OHP and CTRL groups at both evaluation time points were observed in caudal nerves.
Representative images of sciatic nerves collected at 1 week from the 1st OHP injection. 40x magnification. Scale bar 50 µm.

Regarding morphometry, **Figs. 13-14** show that OHP treatment induced a significant reduction ($p<0.0001$) in the mean diameter of myelinated fibers in sciatic and caudal nerves only at 1 week from the 1st OHP administration. This decrease is consistent with the higher number of smaller myelinated fibers.

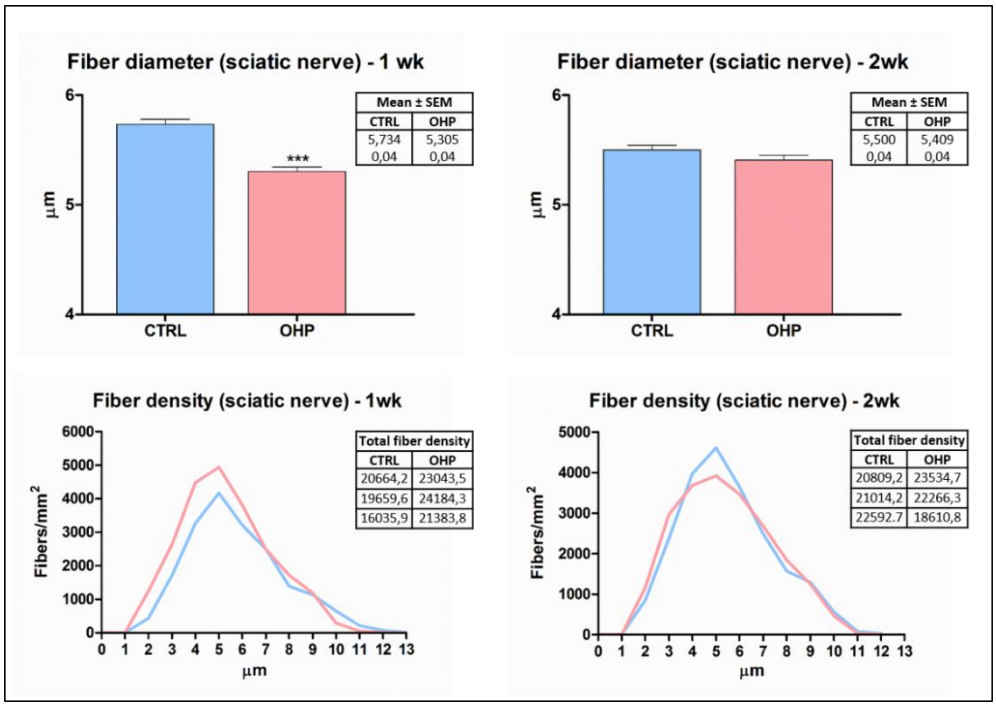

Figure 13. Assessment of myelinated fiber morphometry of sciatic nerve.
OHP treatment induced a significant decrease in mean fiber diameter in sciatic nerve at 1-week evaluation time point. The decrease in mean fiber diameter is consistent with the higher number of smaller myelinated fibers as shown in the curve (bottom left)
The fiber diameter (µm) is shown as mean ± SEM, ***p<0.0001 vs CTRL, Unpaired t-test. The fiber density is expressed as diameter distribution (fiber/mm^2) (n=3 per group).

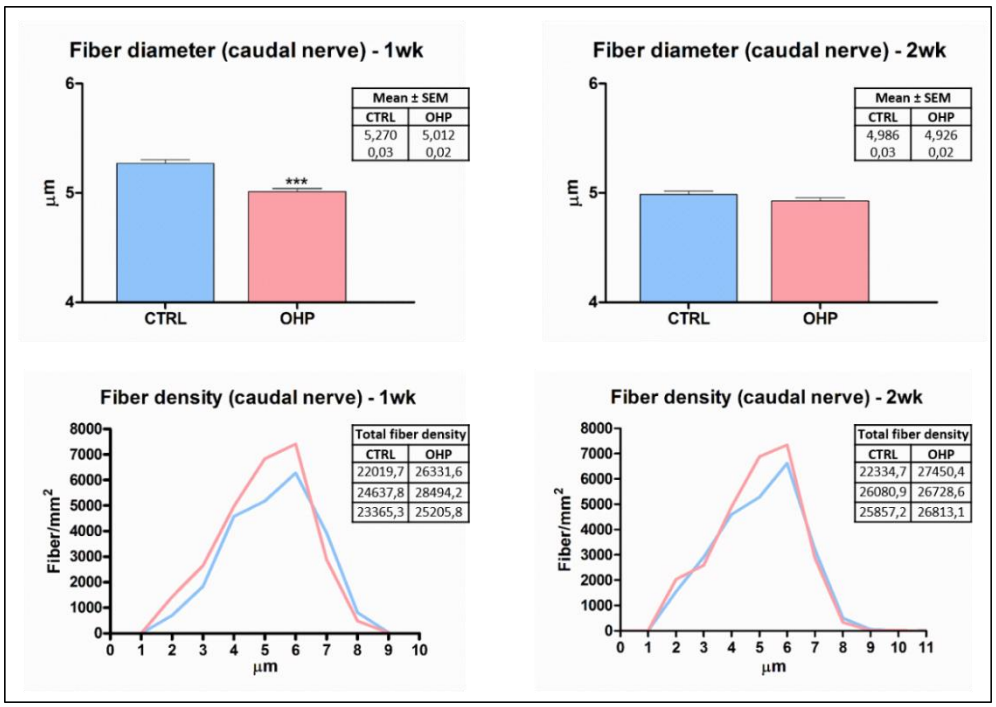

Figure 14. Assessment of myelinated fibers morphometry of caudal nerve.
OHP treatment induced a significant decrease in mean fiber diameter in caudal nerve at 1-week evaluation time point. The decrease in mean fiber diameter is consistent with the higher number of smaller myelinated fibers as shown in the curve (bottom left).
The fiber diameter (µm) is shown as mean ± SEM, ***p<0.0001 vs CTRL, Unpaired t-test. The fiber density is expressed as diameter distribution (fiber/mm^2) (n=3 per group).

2.4.3 IENF

To verify the possible damage of small unmyelinated C-fibers induced by OHP administration, hind paw skin biopsies were observed at light microscope and the density of PGP 9.5-positive IENF was calculated.

As shown in **Fig. 15**, IENF density did not change in OHP-treated mice compared to CTRL group at 1 week from the 1st dose of OHP.

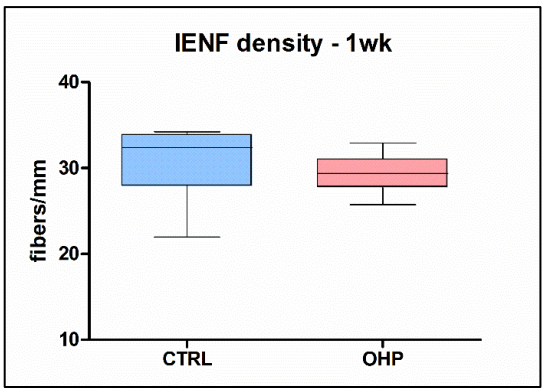

Figure 15. Assessment of IENF density.
OHP treatment did not induce a significant decrease in the IENF density at 1-week evaluation time point.
The IENF density expressed as number of IENF per millimeter (fiber/mm) is shown as median (n=3 per group).

At light microscopy a normal morphological appearance of IENF was observed both in OHP-treated and CTRL mice (**Fig. 16**).

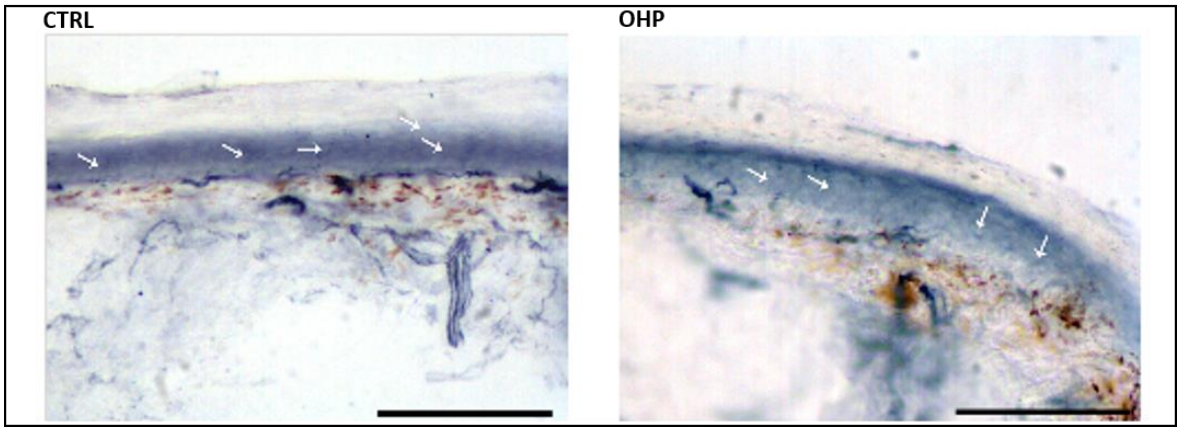

Figure 16. Hind paw skin biopsies.
The morphological appearance of IENF was the same between OHP and CTRL groups in hind paw skin biopsies. The IENF fibers are indicated with white arrows.
Representative images of skin biopsy section collected at 1 week from the 1st OHP injection. 20x magnification. Scale bar 100 µm.

B. OXIDATIVE STRESS EVALUATION

1. THIOBARBITURIC ACID REACTIVE SUBSTANCE ASSAY

Since the primary targets of free radical are cellular lipids, TBARS level was evaluated as standard marker for the lipid peroxidation. TBARS assay was performed to quantify the oxidative stress levels in DRG, sciatic and caudal nerves collected at 24 hours after the 2nd OHP injection, 1 and 2 weeks from the 1st injection of OHP.

TBARS levels did not increase significantly in DRG and peripheral nerves following treatment with OHP at each evaluation time point. Only a slightly increasing trend (p=0.08) was revealed in DRG of OHP-treated mice compared to CTRL at 24 hours from the two doses of OHP (**Fig. 17**).

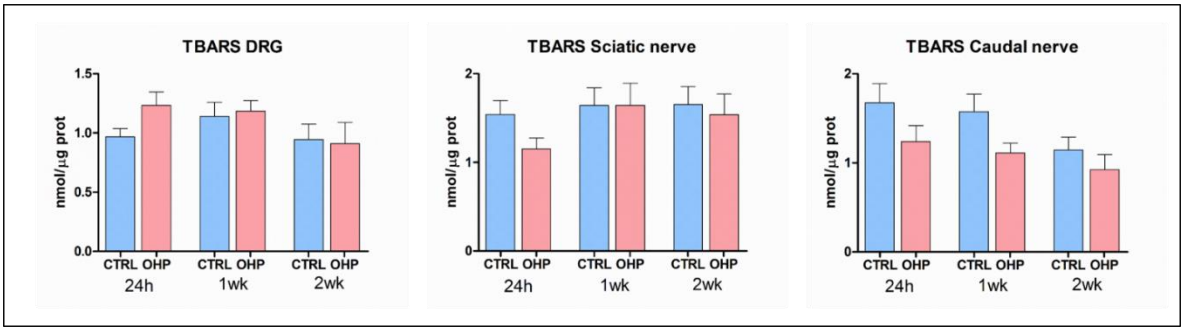

Figure 17. Assessment of oxidative stress level in DRG, sciatic and caudal nerves by TBARS assay.

OHP treatment did not induce significant changes in oxidative stress levels in the tissues analysed at each evaluation time point.

TBARS levels expressed as nanomoles of MDA per microgram of protein (nmol/µg) are shown as mean ± SEM (n=5 per group).

STUDY 2

A. *IN VIVO* STUDY AND OXALIPLATIN-INDUCED PERIPHERAL NEUROTOXICITY CHARACTERIZATION

1. CLINICAL MONITORING AND BODY WEIGHT

No mortality and deterioration in general health status were observed in mice treated with a single intraperitoneal injection of OHP 3 mg/kg and in vehicle-injected mice (CTRL). No significant changes in body weight were recorded during the period of observation as shown in **Fig. 18**.

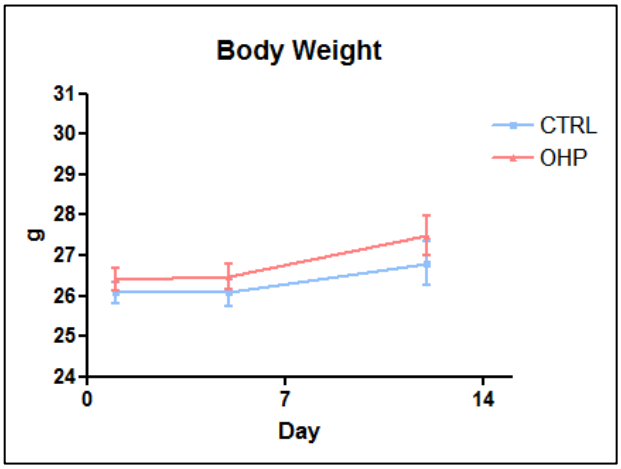

Figure 18. Body weight changes of mice treated with a single intraperitoneal injection of OHP 3 mg/kg compared to vehicle-injected mice (CTRL).
OHP injection did not cause any significant change in the body weight of mice.
Values of body weight expressed in grams (g) are shown as mean ± SEM.

2. ASSESSMENT OF OXALIPLATIN-INDUCED PERIPHERAL NEUROTOXICITY

Mechanical withdrawal threshold, cold sensitivity and neurophysiological analyses of nerves were assessed at 24 hours, 1 and 2 weeks from the 1st OHP administration.

Evaluation time points of morphological and morphometric analysis are reported in the specific paragraph.

2.1 Behavioral Testing - Dynamic Test

No significant changes in mechanical withdrawal threshold were observed neither at 24 hours nor at 1 and 2 weeks after the 1st OHP administration (**Fig. 19**).

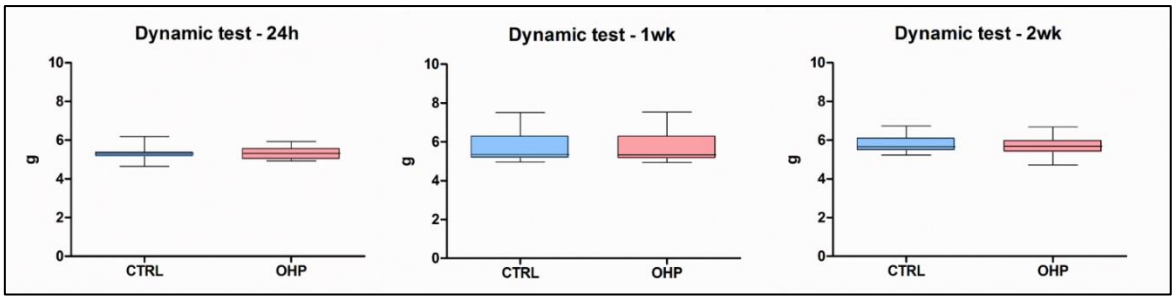

Figure 19. Assessment of mechanical withdrawal threshold.
A single intraperitoneal injection of OHP at the dose of 3 mg/kg did not induced changes in mechanical threshold in OHP-treated mice at the different time points.
The maximal pressure tolerated by the animals related to mechanical stimuli expressed in grams (g) is shown as median (n=13 per group).

2.2 Behavioural Testing - Cold Plate test

For the entire period of observation, no significant increase in the number of pain signs was observed in OHP-treated mice compared to CTRL group (**Fig. 20**).

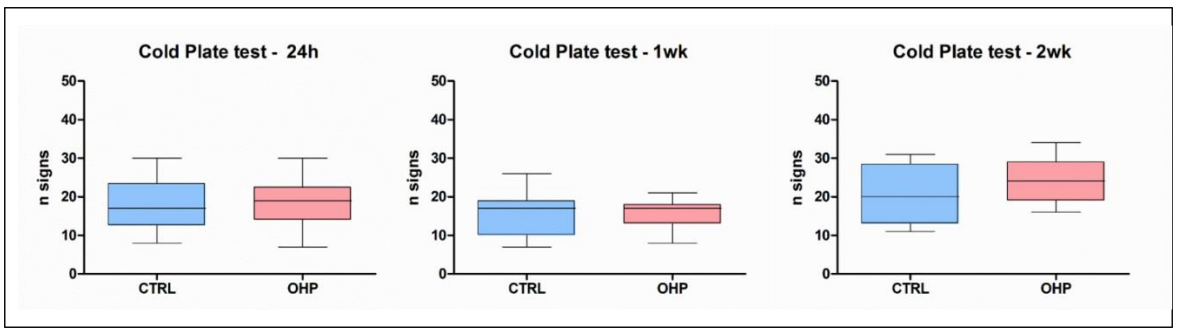

Figure 20. Assessment of cold nociceptive threshold.
A single intraperitoneal injection of OHP at the dose of 3 mg/kg did not induced cold hypo/hyperalgesia in OHP-treated mice at each evaluation time point.
The number of pain signs is shown as median (n=13 per group).

2.3 Neurophysiological examination

As shown in **Fig. 21**, no alterations in SNAP and NCV in caudal and digital nerves of OHP-treated mice were recorded at each evaluation time point.

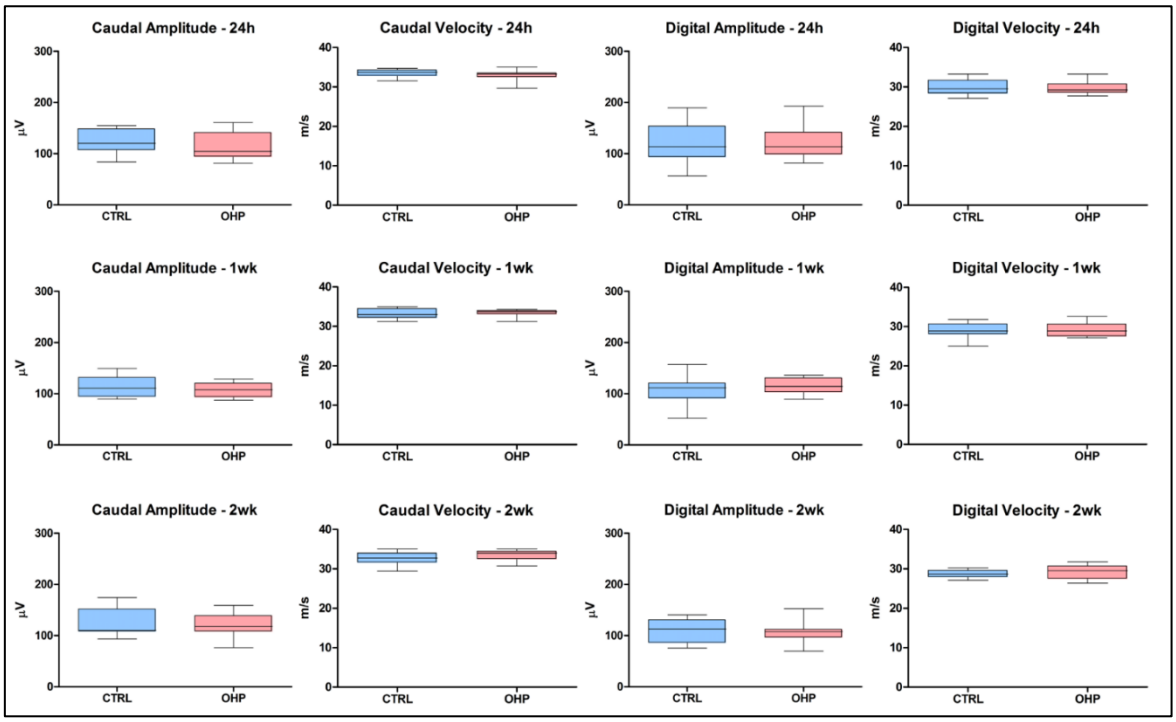

Figure 21. Assessment of NCV and SNAP of caudal and digital nerves.
A single dose of OHP 3 mg/kg injected intraperitoneally did not induced any alterations in SNAP and NCV of caudal and digital nerves at each evaluation time point.
The values of amplitudes expressed in microvolts (µV) and the velocities expressed in meter per second (m/s) are shown as median (n=13 per group).

2.4 Morphological and morphometric analyses

Morphological and morphometric results were obtained from DRG collected at 1 and 2 weeks after the OHP administration. Sciatic and caudal nerves and IENF from hind paw skin biopsies were analysed at 1-week time point, which is considered the end of treatment.

2.4.1 DRG

The single dose of OHP 3 mg/kg did not induce evident morphological alterations in DRG in both time points of observation.

Morphometric analysis, reported in **Fig. 22**, showed a significant ($p<0.0001$) decrease in nuclear area of OHP-treated mice DRG compared to CTRL group at 1 week from the injection of OHP. At 2 weeks of observation, the value of nuclear area of OHP-treated mice returned similar to CTRL group.

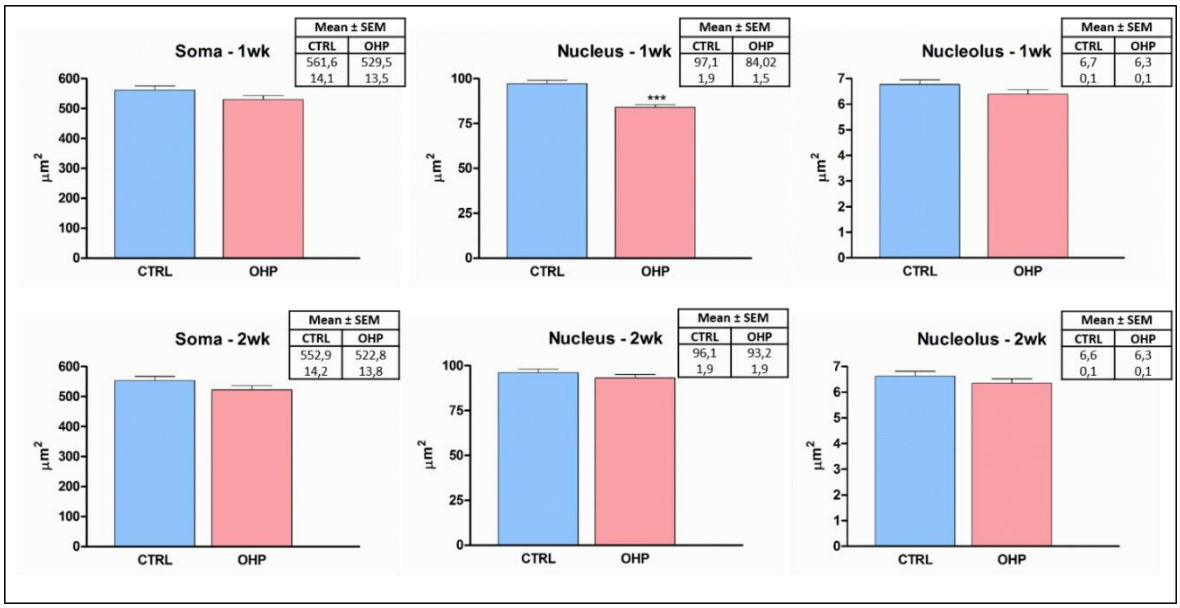

Figure 22. Assessment of neuronal morphometry of DRG.
A single dose of OHP 3 mg/kg injected intraperitoneally induced a significant reduction in nuclear area of OHP-treated mice at 1-week evaluation time point that return similar to CTRL group one week later.
The neuronal sizes expressed in square micrometres (µm²) are shown as mean ± SEM (n=3 per group), ***p<0.0001 vs CTRL, Unpaired t-test.

2.4.2 Peripheral nerves

Morphological and morphometric analyses were performed in OHP-treated mice compared to CTRL mice at 1 week from the OHP administration.

The morphological observation did not evidence in OHP-treated mice relevant structural changes in the two nerves examined in comparison with CTRL mice. Moreover, the mean diameter, distribution and density of myelinated fibers in sciatic and caudal nerves of OHP-treated mice were similar to CTRL group (**Figs. 23-24**).

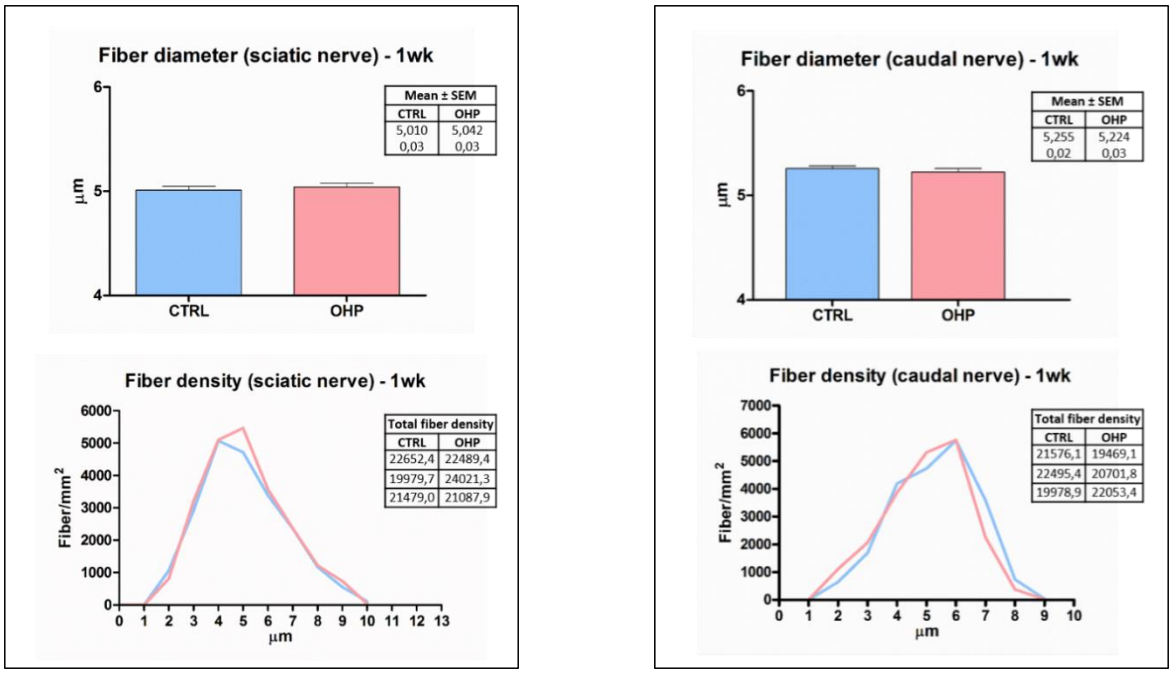

Figures 23-24. Assessment of myelinated fibers morphometry of sciatic and caudal nerves.
A single dose of 3 mg/kg injected intraperitoneally did not induced any significant change in mean fiber diameter, fiber density and distribution in sciatic and caudal nerves at 1-week evaluation time point.
The fiber diameter (µm) is shown as mean ± SEM. The fiber density is expressed as diameter distribution (fiber/mm^2) (n=3 per group).

2.4.3 IENF

The IENF density did not change in OHP-injected mice compared to CTRL group following a single OHP dose of 3 mg/kg (**Fig. 25**).

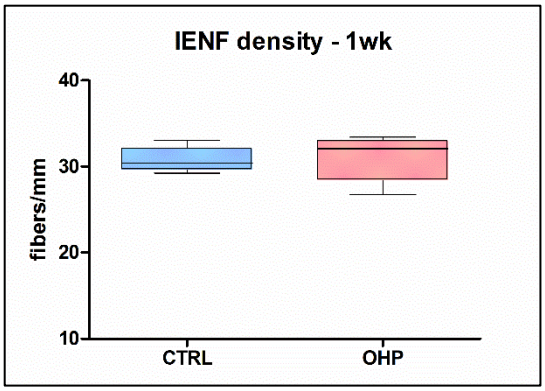

Figure 25. Assessment of IENF density.
A single dose of 3 mg/kg injected intraperitoneally did not induced a significant decrease in the IENF density at 1-week evaluation time point.
The IENF density expressed in number of IENF per millimeter (fiber/mm) is shown as median (n=3 per group).

At light microscopy a normal morphological appearance of IENF was observed both in OHP-treated and CTRL mice

B. OXIDATIVE STRESS EVALUATION

1. THIOBARBITURIC ACID REACTIVE SUBSTANCE ASSAY

TBARS assay was performed in DRG, sciatic and caudal nerves collected at 24 hours, 1 and 2 weeks from the injection of OHP.

TBARS levels did not increase significantly in DRG and in sciatic nerve following the OHP dose at the different evaluation time points. Due to technical problems TBARS levels in caudal nerves were not detectable (**Fig. 26**).

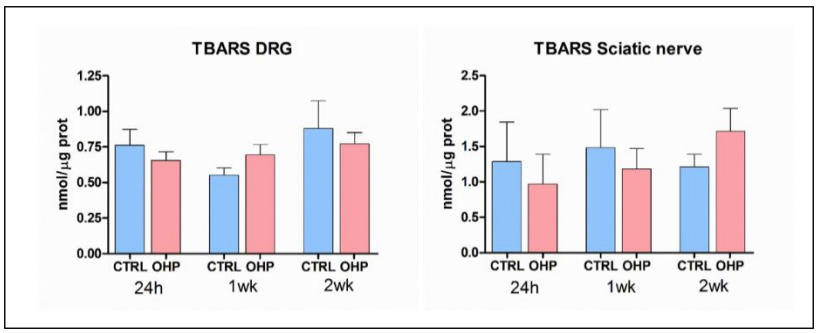

Figure 26. Assessment of oxidative stress level in DRG and sciatic nerve by TBARS assay.
OHP treatment did not induce significant changes in oxidative stress levels in DRG and sciatic nerve at each evaluation time point. In caudal nerve the data were not detectable.
TBARS levels expressed as nanomoles of MDA per microgram of protein (nmol/µg) are shown as mean ± SEM (n=5 per group).

STUDY 3

A. *IN VIVO* STUDY AND OXALIPLATIN-INDUCED PERIPHERAL NEUROTOXICITY CHARACTERIZATION

1. CLINICAL MONITORING AND BODY WEIGHT

There was no mortality observed during the study and there was no evidence of severe general toxicity. Mice treated with daily intraperitoneal injection of OHP 3 mg/kg for 5 days, followed by 5 days of rest, for two cycles, showed a significant decrease ($p<0.01$) in the body weight after the 3rd injection that remained significantly ($p<0.01$-0.0001) lower compared to vehicle-injected mice (CTRL) for the entire period of observation (**Fig. 27**).

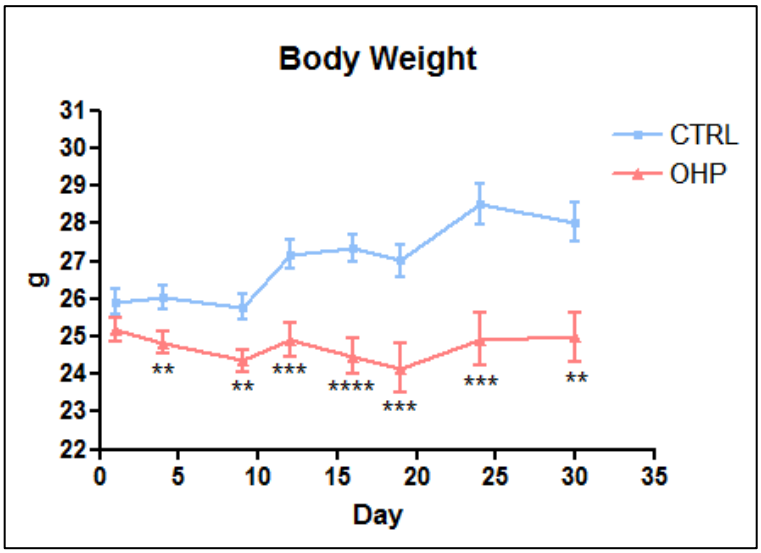

Figure 27. Body weight changes of mice treated with daily intraperitoneal injection of OHP 3 mg/kg for 5 days, followed by 5 days of rest, for two cycles compared to vehicle-injected mice (CTRL).
OHP treatment caused a significant body weight loss from the 3rd administration in mice.
Values of body weight expressed in grams (g) are shown as mean ± SEM, **p<0.01, ***p<0.001, ****p<0.0001 vs CTRL, Unpaired t-test.

2. ASSESSMENT OF OXALIPLATIN-INDUCED PERIPHERAL NEUROTOXICITY

In this study Dynamic test, Cold plate test and neurophysiological evaluations were conducted at 1, 2 and 4 weeks from the 1st dose of OHP. The 24-hour evaluation time point was not examined because it had already been investigated in the Study 2.

Evaluation time points of morphological and morphometric analysis are reported in the specific paragraph.

2.1 Behavioral Testing - Dynamic Test

The treatment schedule of this study did not significantly change the mechanical withdrawal threshold at the different time points (**Fig. 28**).

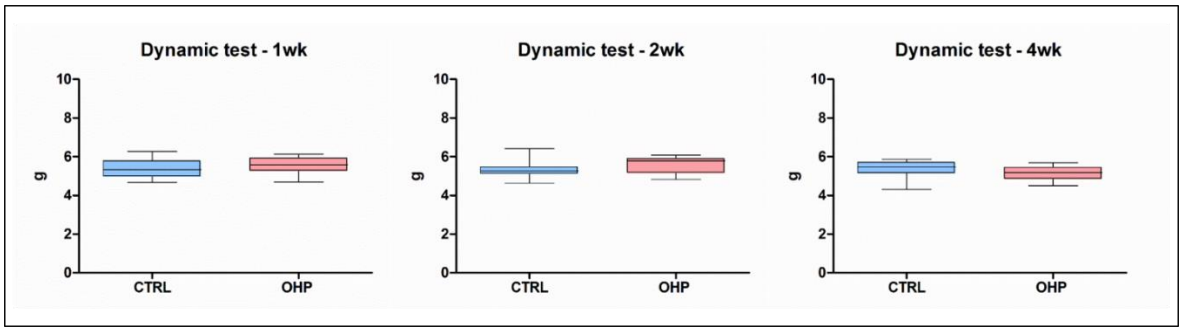

Figure 28. Assessment of mechanical withdrawal threshold.
There was no significant difference between OHP and CTRL groups with repeated administrations of OHP 3 mg/kg at the different evaluation time points.
The maximal pressure tolerated by the animals related to mechanical stimuli expressed in grams (g) is shown as median (n=13 per group).

2.2 Behavioral Testing - Cold Plate test

After the 1st cycle of OHP treatment (1-week time point) a slight but not significant increase in sensitivity to a cold stimulus was observed in OHP-treated mice compared to relative CTRL. Otherwise, after the 2nd cycle of OHP treatment the animals developed a significant ($p<0.05$) cold hypoalgesia that persisted after 2-weeks follow-up (2-week and 4-week time point, respectively), as shown in **Fig. 29**.

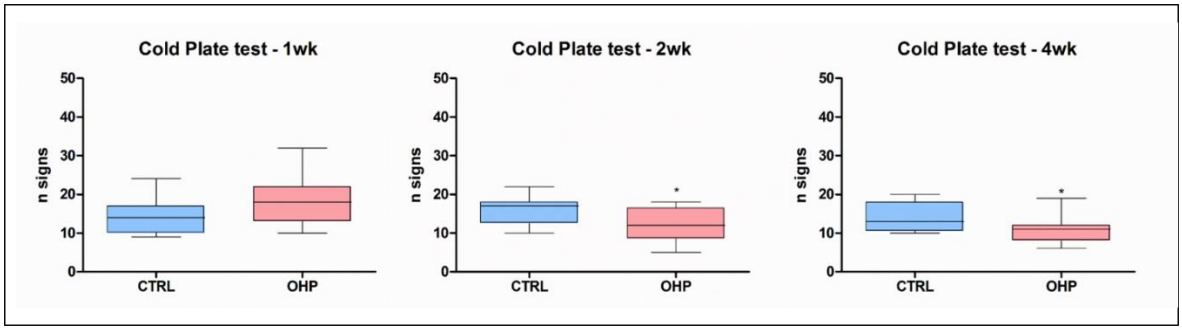

Figure 29. Assessment of cold nociceptive threshold.
The administration of OHP 3 mg/kg daily for five consecutive days for two cycles determined cold hypoalgesia, which persisted until 4 weeks from the start of treatment.
The number of pain signs is shown as median (n=13 per group), *$p<0.05$ vs CTRL, Mann-Whitney test.

2.3 Neurophysiological examination

The treatment schedule of this study did not induce any significant changes in SNAP and NCV in caudal and digital nerves at each evaluation time point (**Fig. 30**).

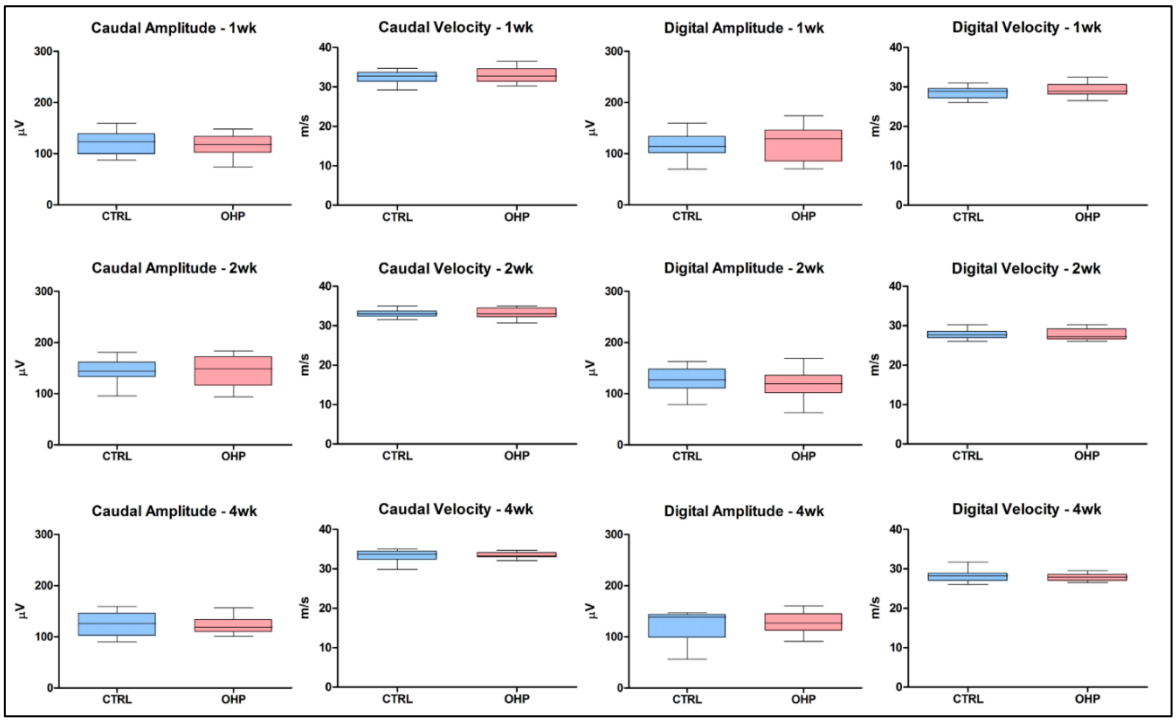

Figure 30. Assessment of NCV and SNAP of caudal and digital nerves.
Repeated intraperitoneal administrations of 3 mg/kg OHP did not induce any alterations in NCV and SNAP of caudal and digital nerves for the entire period of observation.
The values of amplitudes expressed in microvolts (µV) and the velocities expressed in meter per second (m/s) are shown as median (n=13 per group).

2.4 Morphological and morphometric analyses

At 1, 2 and 4 weeks from the start of OHP treatment morphological and morphometric analyses were performed on DRG neurons, while sciatic and caudal nerves were observed after the 1st and 2nd cycles of OHP treatment (1-week and 2-week time point, respectively). IENF density was calculated on skin biopsies collected at 2 weeks from the 1st dose of OHP, which correspond to the end of complete schedule treatment.

2.4.1 DRG

The morphology of DRG neurons did not show relevant change at each time point.

On the other hand, change in neuronal size was observed. In particular, a significant reduction ($p<0.0001$) in somatic and nucleolar areas of DRG neurons was evidenced after the 1st cycle of OHP treatment. At 2 and 4 weeks from the start of treatment DRG neurons

presented a severe atrophy in cell body ($p<0.05$, $p<0.0001$), nucleus ($p<0.05$, $p<0.01$) and nucleolus ($p<0.0001$) (**Fig. 31**).

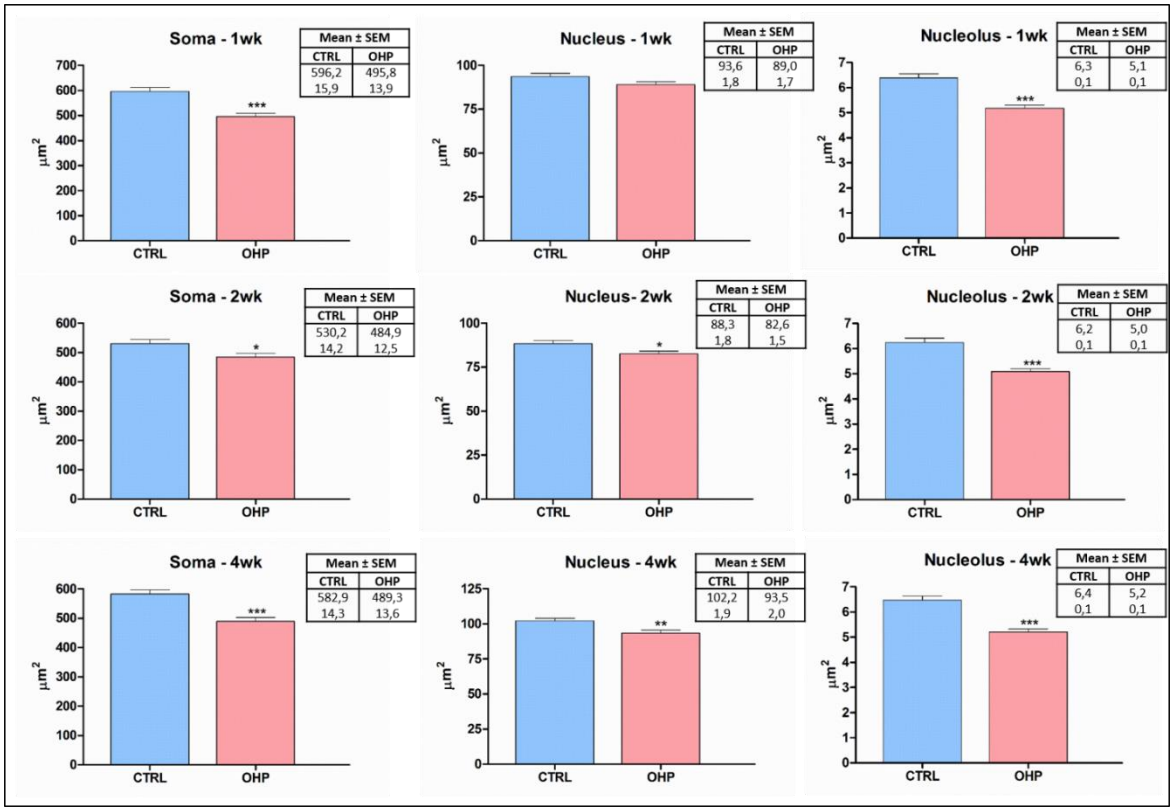

Figure 31. Assessment of morphometry of DRG neurons.
OHP treatment induced a significant decrease in somatic, nuclear and nucleolar areas, except for nuclear area at 1-week evaluation time point.
The neuronal sizes expressed in square micrometres (µm²) are shown as mean ± SEM (n=3 per group), *p<0.05, **p<0.01, ***p<0.0001 vs CTRL, Unpaired t-test.

2.4.2 Peripheral nerves

No apparent morphological alterations of sciatic and caudal nerves in OHP-treated mice and CTRL group were observed by light microscopy analysis for both observation time points. Morphometric analysis revealed no significant change in the mean diameter, density and distribution of myelinated fiber in sciatic nerve. On the other hand, the mean diameter of myelinated fiber in caudal nerve increase ($p<0.001$) in OHP-treated mice compared to CTRL at 1-week time point. This increase is unexpected and not strongly supported by the analysis of fiber size distribution (**Figs. 32-33**).

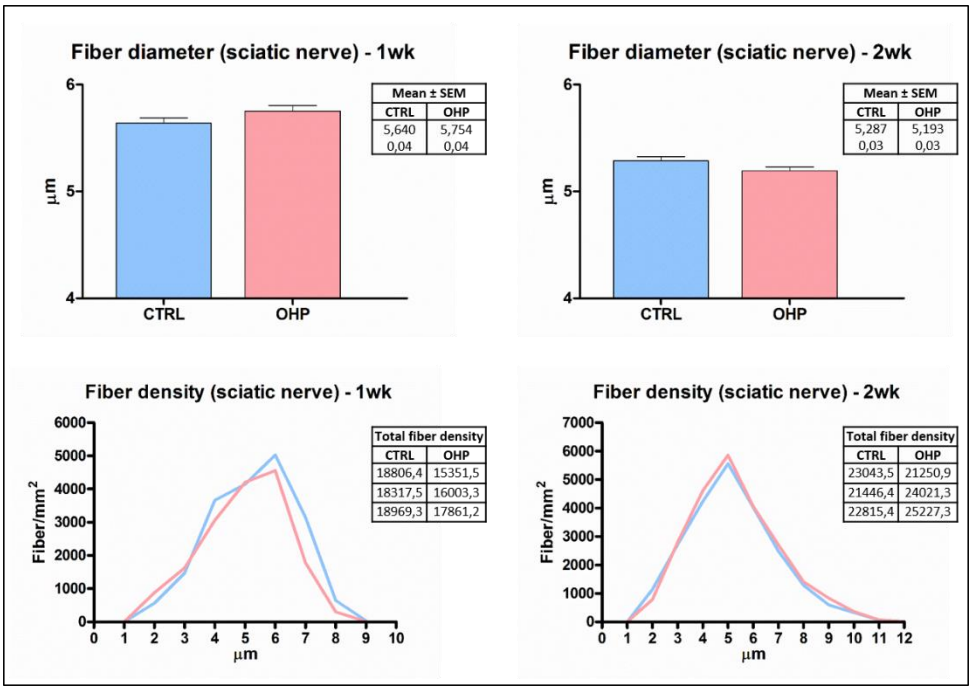

Figure 32. Assessment of myelinated fibers morphometry of sciatic nerve.
OHP treatment did not induce any change in mean fiber diameter, fiber density and distribution in sciatic nerve at 1- and 2-week evaluation time points.
The fiber diameter (µm) is shown as mean ± SEM. The fiber density is expressed as diameter distribution (fiber/mm^2) (n=3 per group).

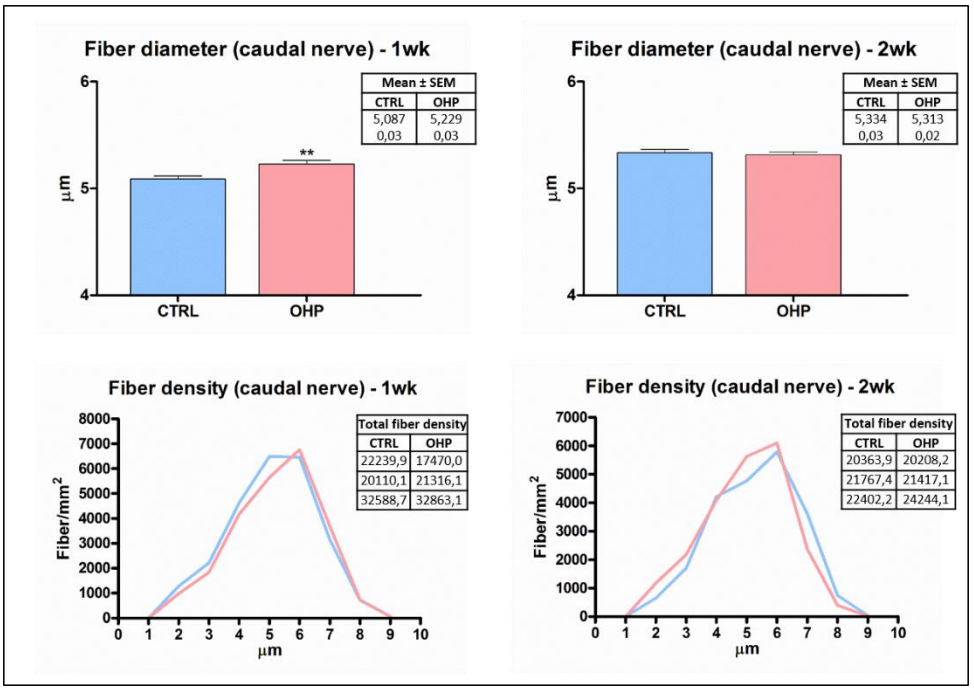

Figure 33. Assessment of myelinated fibers morphometry of caudal nerve.
OHP treatment induced an unexplained increase in mean fiber diameter in caudal nerve at 1-week evaluation time point. This statistical result is unexpected and not strongly supported by the analysis of fiber size distribution (bottom left).
The fiber diameter (µm) is shown as mean ± SEM, **p<0.001 vs CTRL, Unpaired t-test. The fiber density is expressed as diameters distribution (fiber/mm^2) (n=3 per group).

2.4.3 IENF

The IENF density did not change in OHP-injected mice compared to OHP-treated mice and CTRL group after the two cycles of OHP treatment (**Fig. 34**).

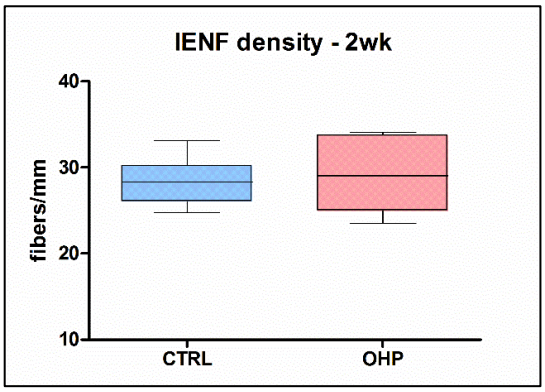

Figure 34. Assessment of IENF density.
OHP treatment did not induce significant changes in the IENF density at 2-week evaluation time point.
The IENF density expressed in number of IENF per millimeter (fiber/mm) are shown as median (n=3 per group).

At light microscopy a normal morphological appearance of IENF was observed both in OHP-treated and CTRL mice

B. OXIDATIVE STRESS EVALUATION

1. THIOBARBITURIC ACID REACTIVE SUBSTANCE ASSAY

TBARS assay was performed in DRG, sciatic and caudal nerves collected at 1, 2 and 4 weeks from 1st injection of OHP.

TBARS levels did not increase significantly in all samples analysed following the OHP treatment at the different evaluation time points, with the exception for sciatic nerves at 4 weeks ($p<0.001$). Moreover, an increase with a slight trend toward significance ($p=0.06$) was revealed in DRG collected from OHP-treated mice at 2-week evaluation time point (**Fig. 35**).

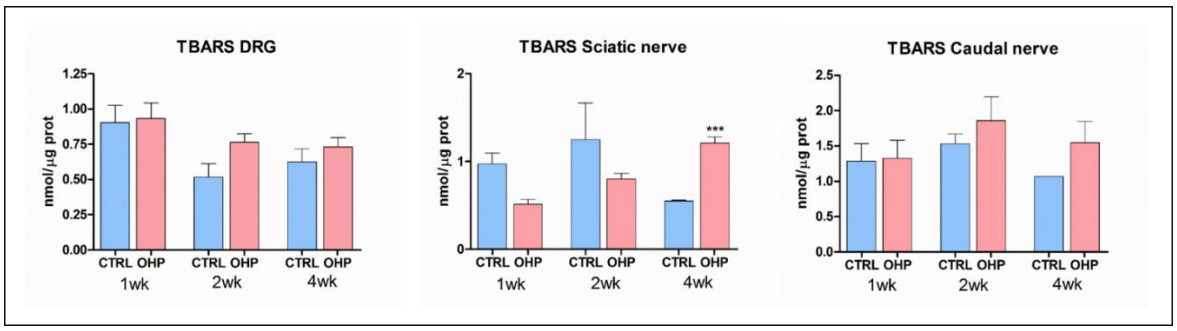

Figure 35. Assessment of oxidative stress level in DRG, sciatic and caudal nerves by TBARS assay.

OHP treatment did not induced significant changes in oxidative stress levels in the tissues analysed at each evaluation time point. Only an increase in TBARS level was observed in sciatic nerve at 2-week evaluation time point.

TBARS levels expressed as nanomoles of MDA per microgram of protein (nmol/µg) are shown as mean ± SEM (n=5 per group), ***$p<0.001$ vs CTRL, Unpaired t-test.

STUDY 4

A. *IN VIVO* STUDY AND OXALIPLATIN-INDUCED PERIPHERAL NEUROTOXICITY CHARACTERIZATION

1. CLINICAL MONITORING AND BODY WEIGHT

All mice treated intravenously with OHP 5 mg/kg twice a week for 4 weeks survived until the end of the study. No deterioration in general health status of the OHP-treated mice was observed, although approximately 20% of treated animals developed signs of piloerection and mild kyphosis and showed significant loss ($p<0.5$-0.01) of body weight from the last injection to the end of the study compared to vehicle-treated mice (CTRL) (**Fig. 36**).

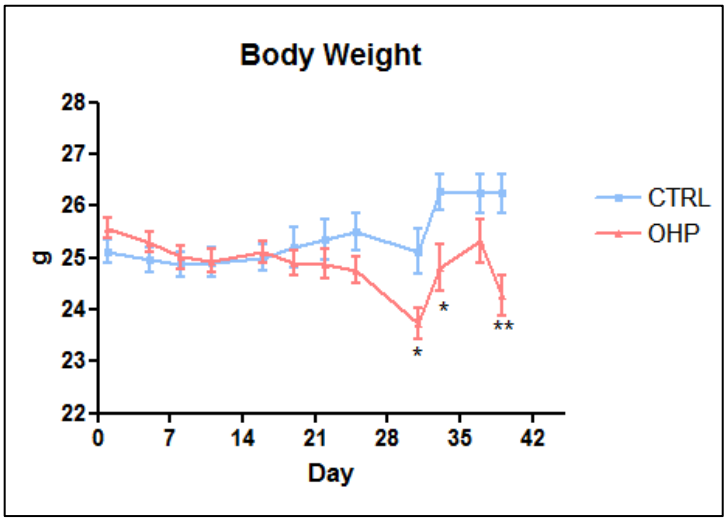

Figure 36. Body weight changes of mice treated intravenously with OHP 5 mg/kg twice a week for 4 weeks compared to vehicle-injected mice (CTRL).
OHP treatment caused a significant body weight loss in mice from the 8th administration. Values of body weight expressed in grams (g) are shown as mean ± SEM, *$p<0.05$, **$p<0.01$ vs CTRL, Unpaired t-test.

2. ASSESSMENT OF OXALIPLATIN-INDUCED PERIPHERAL NEUROTOXICITY

Regarding this study mechanical allodynia, cold sensitivity and neurophysiological alterations were verified at 24 hours, 1 week, 2 weeks (mid-treatment), 4 weeks (end of treatment) and 6 weeks (2-weeks follow-up) after the 1st dose of OHP.

Evaluation time points of morphological and morphometric analysis are reported in the specific paragraph.

2.1 Behavioral Testing - Dynamic Test

OHP-treated mice did not show any difference in mechanical withdrawal threshold until 2 weeks from the 1st OHP administration. Mechanical allodynia was observed in mice treated with OHP for 4 weeks ($p<0.001$) and persisted after 2-weeks follow-up with a lower significance level ($p<0.05$) compared to respective CTRL (**Fig. 37**).

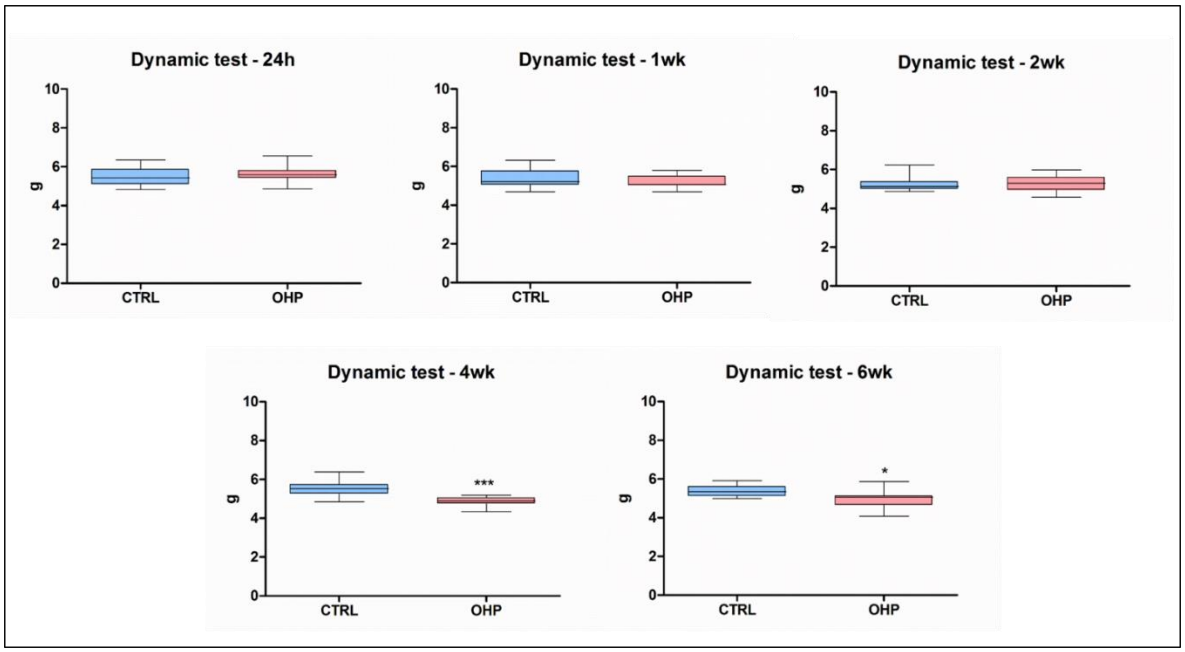

Figure 37. Assessment of mechanical withdrawal threshold.
OHP treatment induced mechanical allodynia in mice after 4 weeks and persisted after 2 weeks of follow-up.
The maximal pressure tolerated by the animals related to mechanical stimuli expressed in grams (g) is shown as median (n=13 per group), *p<0.05, ***p<0.001, vs CTRL, Mann-Whitney test.

2.2 Behavioral Testing - Cold Plate test

OHP-treated mice developed cold hyperalgesia at 24 hours from the 1st administration ($p<0.0001$, acute syndrome). This cold hypersensitivity recurred at 2 weeks ($p<0.001$) and also at 4 weeks ($p<0.05$) of OHP treatment (chronic syndrome) and resolved after 2-weeks follow-up (**Fig. 38**).

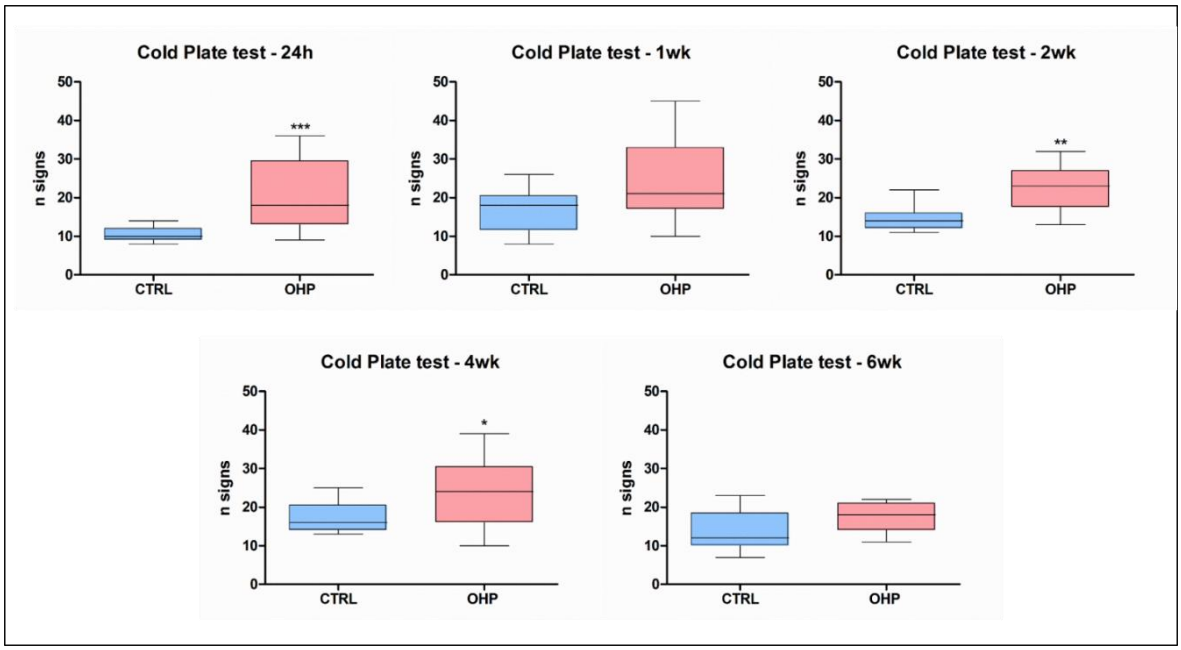

Figure 38. Assessment of cold nociceptive threshold.
A single intravenous injection of 5mg/kg OHP induced cold hyperalgesia in mice at 24-hour evaluation time point. A significant increase in the number of pain signs (hind paws lifts, flicking/licking and jumpings) was also observed in mice treated with OHP compared to CTRL group at mid and at the end of OHP treatment.
The number of pain signs is shown as median (n=13 per group), *p<0.05, **p<0.01, ***p<0.0001 vs CTRL, Mann-Whitney test.

2.3 Neurophysiological examination

Until the second week of OHP treatment no significant change in neurophysiological parameters were recorded in caudal and digital nerves of mice.

After 2 weeks of treatment a significant reduction ($p<0.01$) in SNAP was observed in caudal nerve of OHP-treated mice compared to CTRL group and at the end of the treatment a significant reduction ($p<0.001$) was detected also in the digital nerve. NCV in the two nerves examined of OHP-treated mice did not significantly differ from CTRL group at each evaluation time point (**Fig. 39**).

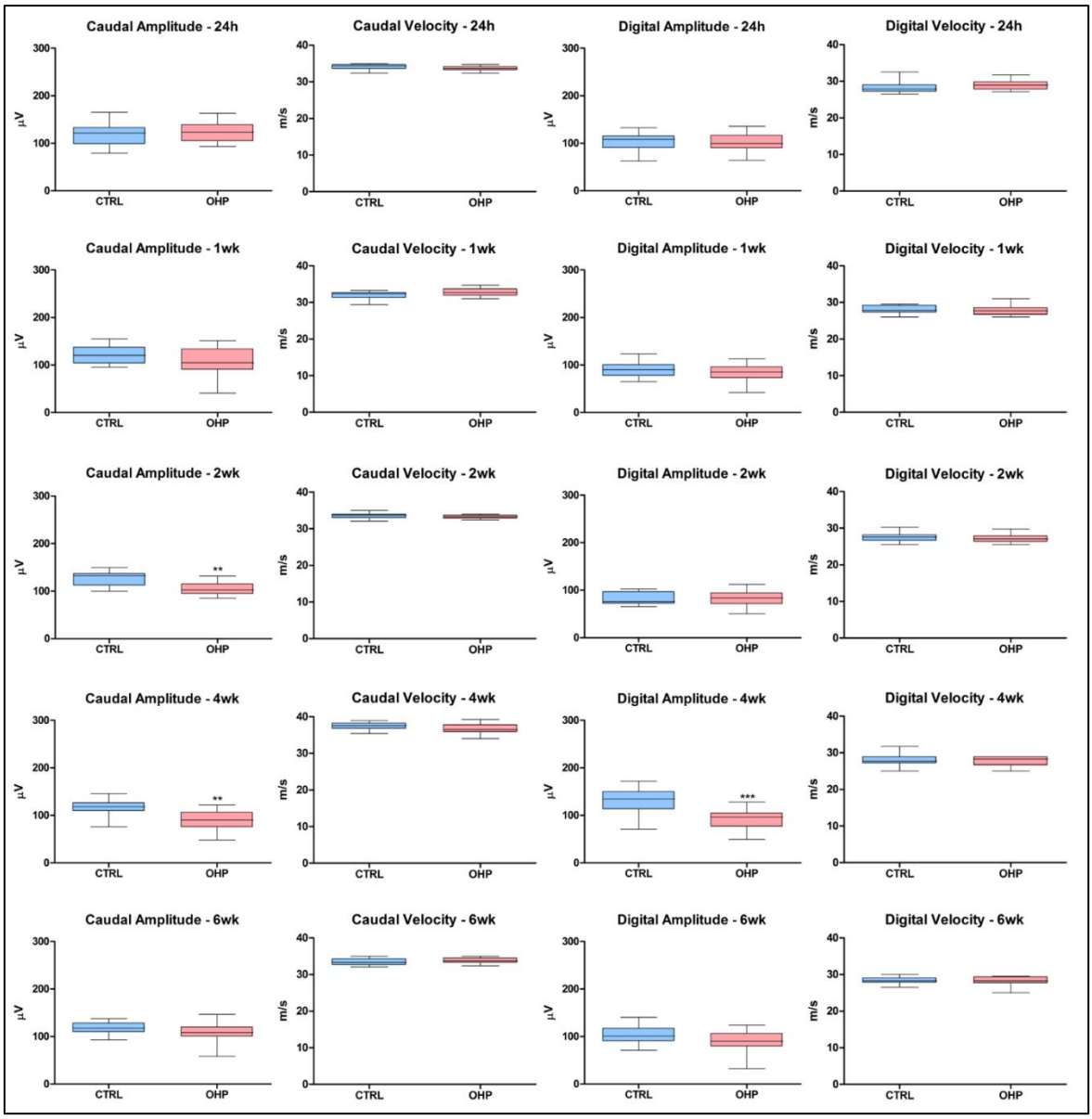

Figure 39. Assessment of NCV and SNAP of caudal and digital nerves.
OHP treatment induced a significant reduction only in caudal SNAP at mid-treatment and in the SNAP of both nerves at the end of treatment.
The values of amplitudes expressed in microvolts (µV) and the velocities expressed in meter per second (m/s) are shown as median (n=13 per group), **p<0.001, ***p<0.0001 vs CTRL, Mann-Whitney test.

2.4 Morphological and morphometric analyses

At each time of observation, except for 24-hour time point, L4-L5 DRG were collected to perform morphological and morphometric analyses of DRG neurons. Sciatic and caudal nerves were observed at 2, 4 and 6 weeks from the 1st OHP administration while IENF density was calculated on skin biopsies collected at the end of the treatment and follow-up.

2.4.1 DRG

After 1, 2 and 6 weeks of OHP treatment no evident alterations in morphology were observed in DRG neurons. On the other hand, at the end of treatment (4-week time point) DRG neurons of OHP-treated mice showed a remarkable amount of multiple nucleoli, eccentric nuclei and vacuolation (**Fig. 40**).

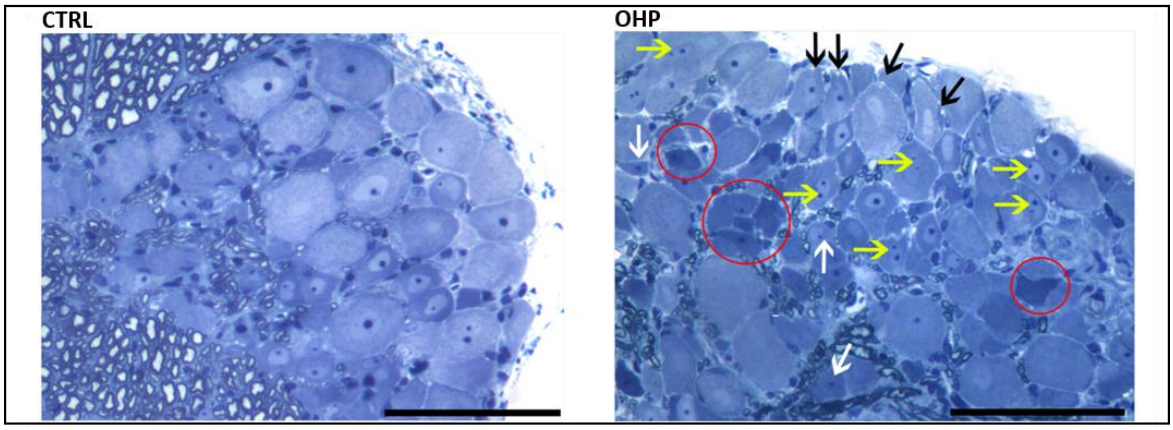

Figure 40. Assessment of morphology of DRG neurons.
At the end of treatment, OHP induced degenerated neurons (red circles), multi-nucleolated neurons (yellow arrows), eccentric nuclei (white arrows) and vacuolation (black arrows). Representative images of DRG neurons collected from CTRL and OHP-treated mice at 4 weeks from the 1st OHP injection. 20x magnification. Scale bar 100 µm.

Regarding morphometric analysis, as shown in **Fig. 41**, OHP treatment induced alterations in neuronal size after 2 and 4 weeks.

In particular, somatic and nuclear areas showed a significant increase ($p<0.01$) at mid-treatment, wheras a significant reduction in the area of the same neuronal structures ($p<0.05$ and $p<0.0001$ respectively) was detected at the end of treatment in DRG of OHP-treated mice compared to CTRL. After 2 weeks of follow-up the neuronal size in DRG of the animals injected with OHP returned comparable to CTRL mice.

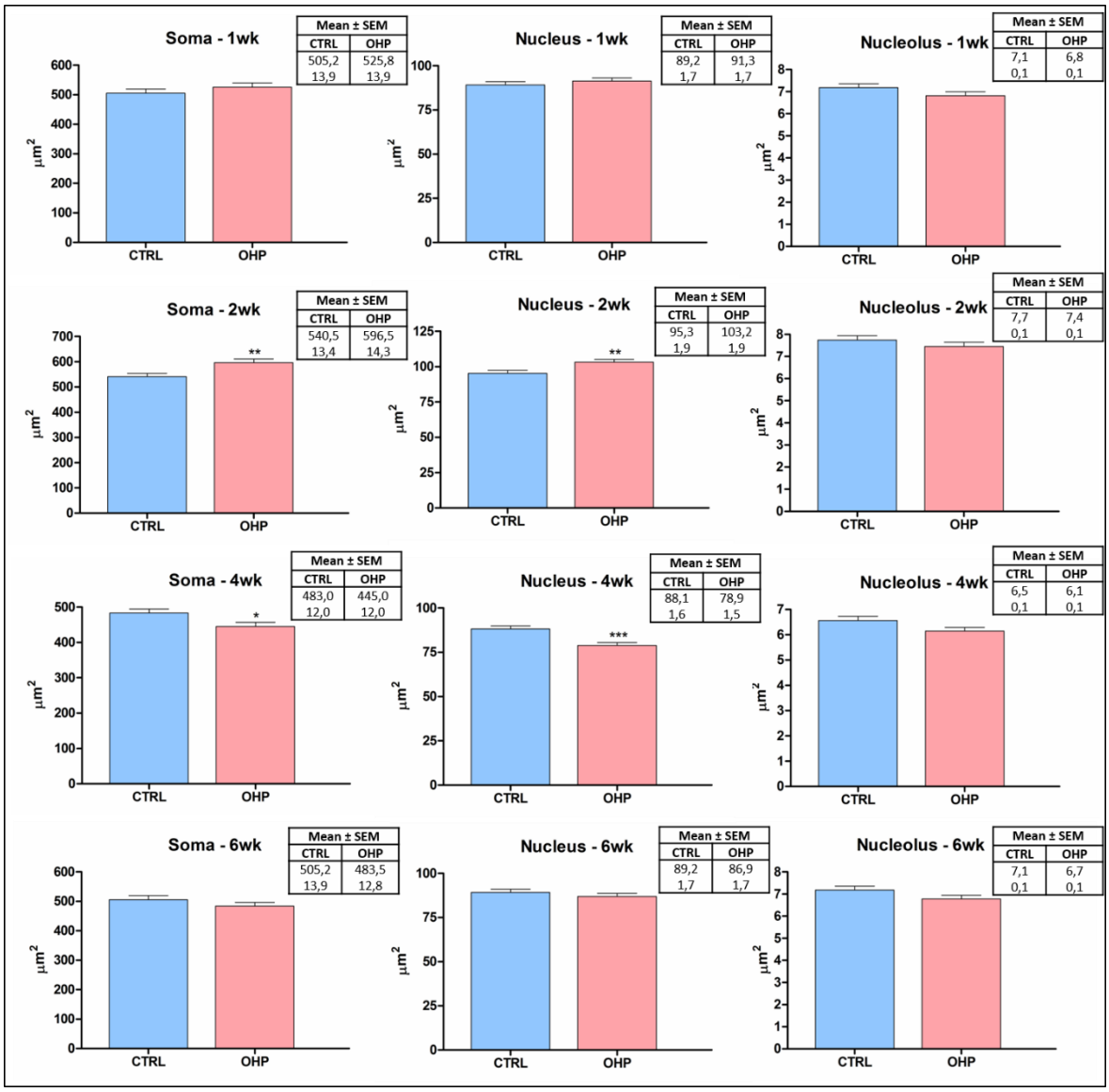

Figure 41. Assessment of morphometry of DRG neurons.
OHP treatment induced significant alterations in somatic and nuclear areas: an increase at 2-week time point and a decrease at 4-week time point were observed in OHP-treated mice.
The neuronal sizes expressed in square micrometres (µm²) are shown as mean ± SEM (n=3 per group), *p<0.05, **p<0.001, ***p<0.0001 vs CTRL, Unpaired t-test.

2.4.2 Peripheral nerves

The morphological observation did not evidence in OHP-treated mice relevant structural changes in the two nerves examined, in comparison with CTRL mice.

Morphometric analysis, showed in **Figs. 42-43**, demonstrated a significant decrease ($p<0.0001$, $p<0.01$) in the mean diameter of myelinated fibers in sciatic nerve of OHP-treated mice at 4- and 6- weeks evaluation time points. The fiber density distribution shows a shift to the left in sciatic nerves of OHP-treated mice compared to CTRL group at each time point, slightly less evident at 2 weeks, indicating a trend in losing fibers with larger

diameter. A significant decrease ($p<0.0001$) in the mean diameter of myelinated fibers was also observed in caudal nerve at 4 weeks from the 1st OHP administration. This decrease is consistent with the higher number of smaller myelinated fibers.

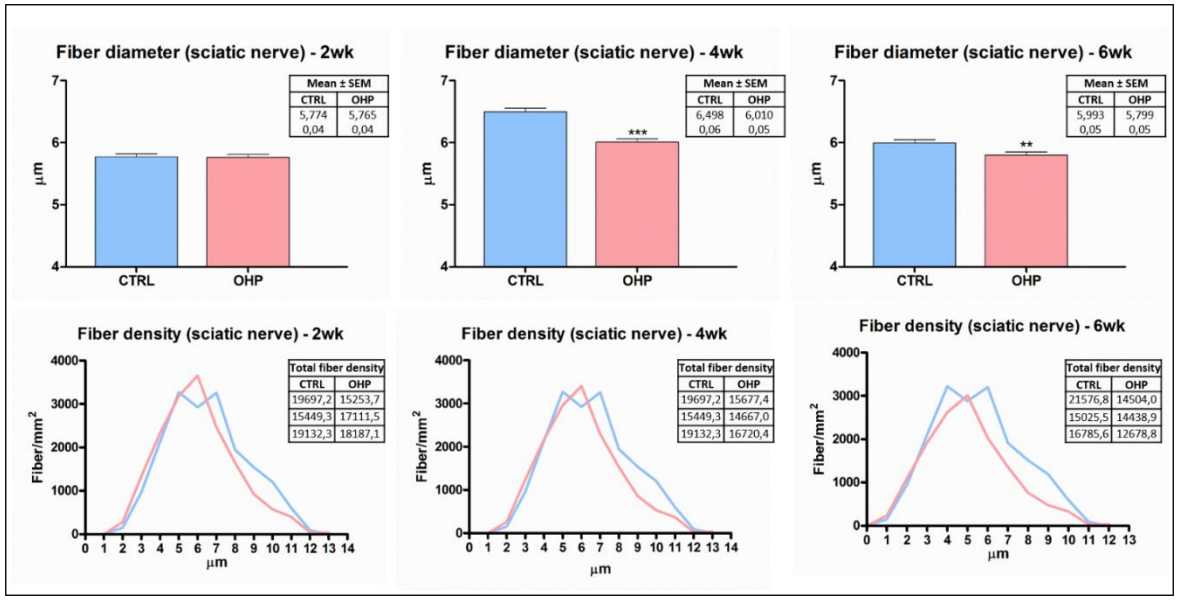

Figure 42. Assessment of myelinated fiber morphometry of sciatic nerve.
OHP treatment induced significant decrease in mean fiber diameter in sciatic nerves at 4- and 6-week evaluation time points. The fiber density distribution shows a shift to the left in sciatic nerve of OHP-treated mice compared to CTRL at each time point, slightly less evident at 2 weeks.
The fiber diameter (µm) is shown as mean ± SEM, ***$p<0.0001$, **$p<0.01$ vs CTRL, Unpaired t-test. The fiber density is expressed as diameter distribution (fiber/mm^2) (n=3 per group).

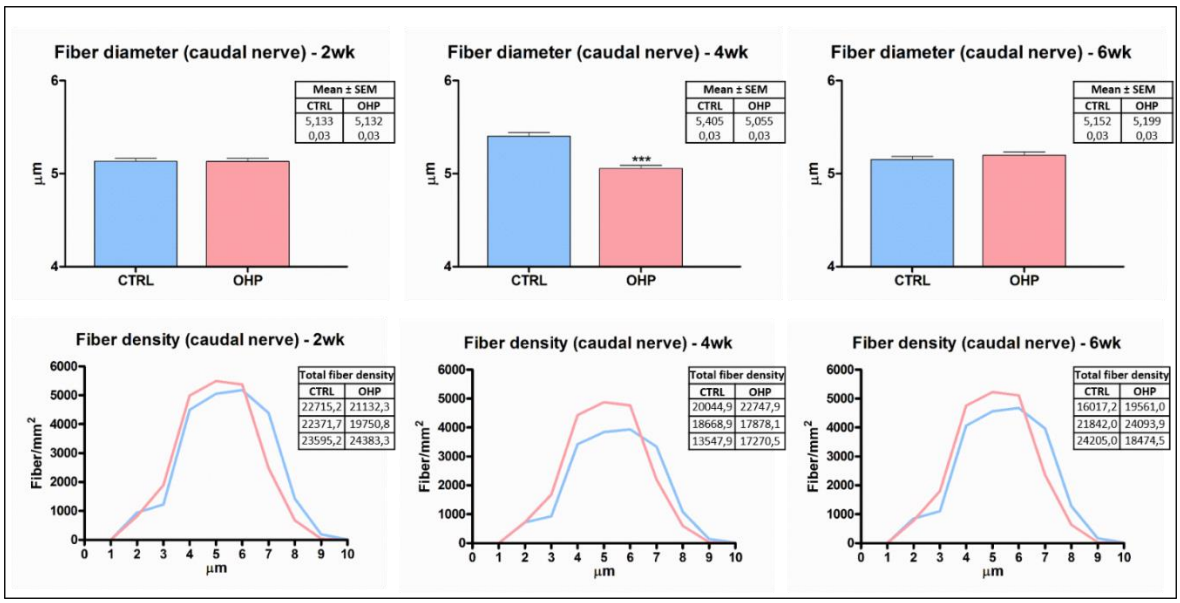

Figure 43. Assessment of myelinated fiber morphometry of caudal nerve.
OHP treatment induced significant decrease in mean fiber diameter in caudal nerve at 4-week evaluation time point. The decrease in mean fiber diameter is consistent with the higher number of smaller myelinated fibers as shown in the curve (bottom centre).
The fiber diameter (µm) is shown as mean ± SEM, ***$p<0.0001$ vs CTRL, Unpaired t-test. The fiber density is expressed as diameters distribution (fiber/mm^2) (n=3 per group).

2.4.3 IENF

At the end of OHP treatment a significant reduction ($p<0.0001$) in IENF density was observed at light microscopy analysis in hind paw skin biopsies of OHP-treated mice compared to CTRL group. This reduction persisted significant after 2 weeks of follow-up period (**Figs. 44-45**).

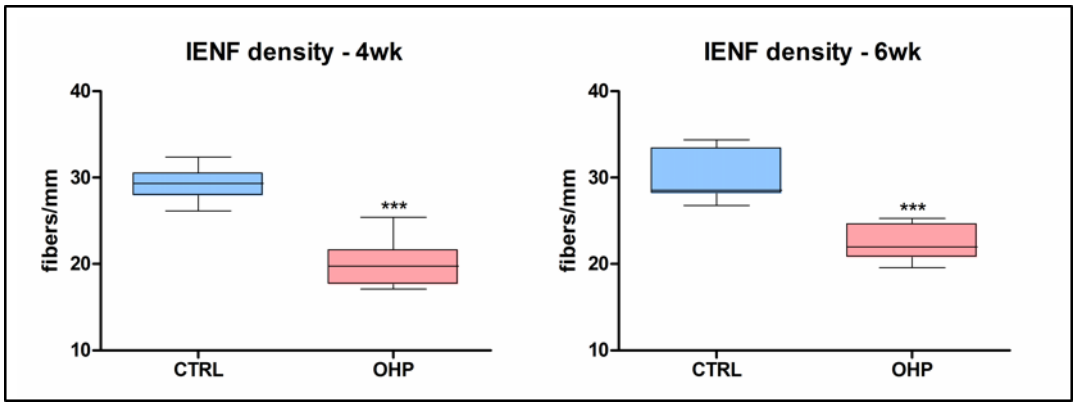

Figure 44. Assessment of IENF density.
OHP treatment induced a significant decrease in the IENF density at end of treatment, which remained after 2 weeks of follow-up.
The IENF density expressed in number of IENF per millimeter (fiber/mm) is shown as median (n=3 per group), ***$p<0.0001$ vs CTRL, Mann-Whitney test.

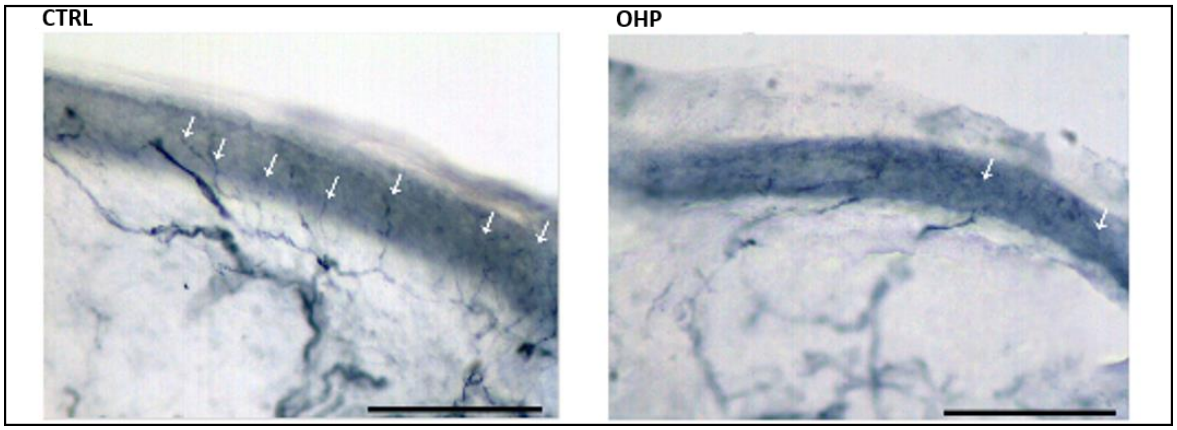

Figure 45. Hind paw skin biopsies.
The density of IENF appeared reduced in the hind paw skin biopsies collected from OHP-treated mice compared to CTRL group at 4- and 6-week evaluation time points. The IENF are indicated with white arrows.
Representative images of skin biopsy sections collected from CTRL and OHP-treated mice at 4 week from the 1st OHP injection. 20x magnification. Scale bar 100 µm.

B. OXIDATIVE STRESS EVALUATION

1. THIOBARBITURIC ACID REACTIVE SUBSTANCE ASSAY

TBARS assay was performed in DRG, sciatic and caudal nerves collected at 24 hours, 1, 2, 4 and 6 weeks after the 1st dose of OHP.

TBARS levels did not increase significantly in all samples analysed following the OHP treatment at the different evaluation time points, with exception for the mid-treatment time point that showed a significance ($p<0.05$) in sciatic nerves of OHP-treated mice compared to CTRL mice (**Fig. 46**).

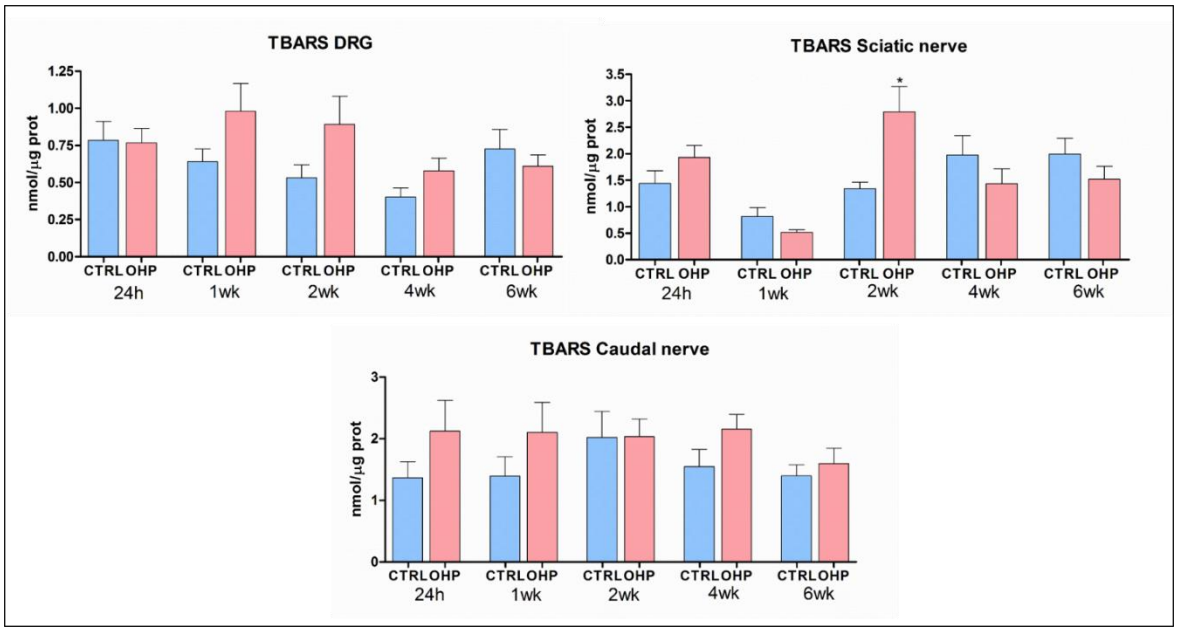

Figure 46. Assessment of oxidative stress level in DRG, sciatic and caudal nerves by TBARS assay.

OHP treatment induced a significant increase in oxidative stress levels in sciatic nerves at mid-treatment time point.

TBARS levels expressed as nanomoles of MDA per microgram of protein (nmol/µg) are shown as mean ± SEM (n=5 per group), *$p<0.05$ vs CTRL, Unpaired t-test.

2. WESTERN BLOT ANALYSIS

Since mitochondria are the site of oxidative phosphorylation (OXPHOS/respiratory chain Complex I-IV) and DRG neurons are the main target of OHP damage, protein expression of respiratory chain complexes was evaluated in DRG collected at 24 hours, 1, 2, 4 and 6 weeks after the 1st dose of OHP.

Moreover, since mitochondria fusion may be activated in response to mitochondrial damage, the protein expression of DRP1 was evaluated in both total (DRP1t) and phosphorylated (DRP1p) forms.

These analyses were performed exclusively for the *Study 4*, in which OHP treatment is prolonged and several time points were investigated.

As reported in **Fig. 47**, quantitative Western blot showed a significant increase ($p<0.05$) in respiratory chain Complex I expression level in DRG of mice treated with OHP for 4 weeks. At the other evaluation time points and in the other type of respiratory chain complexes, OHP did not induce a significant change in protein expression. Only an increase with a slight trend toward significance ($p=0.08$) was observed in respiratory chain Complex IV expression level in DRG harvested after 2 weeks of OHP treatment.

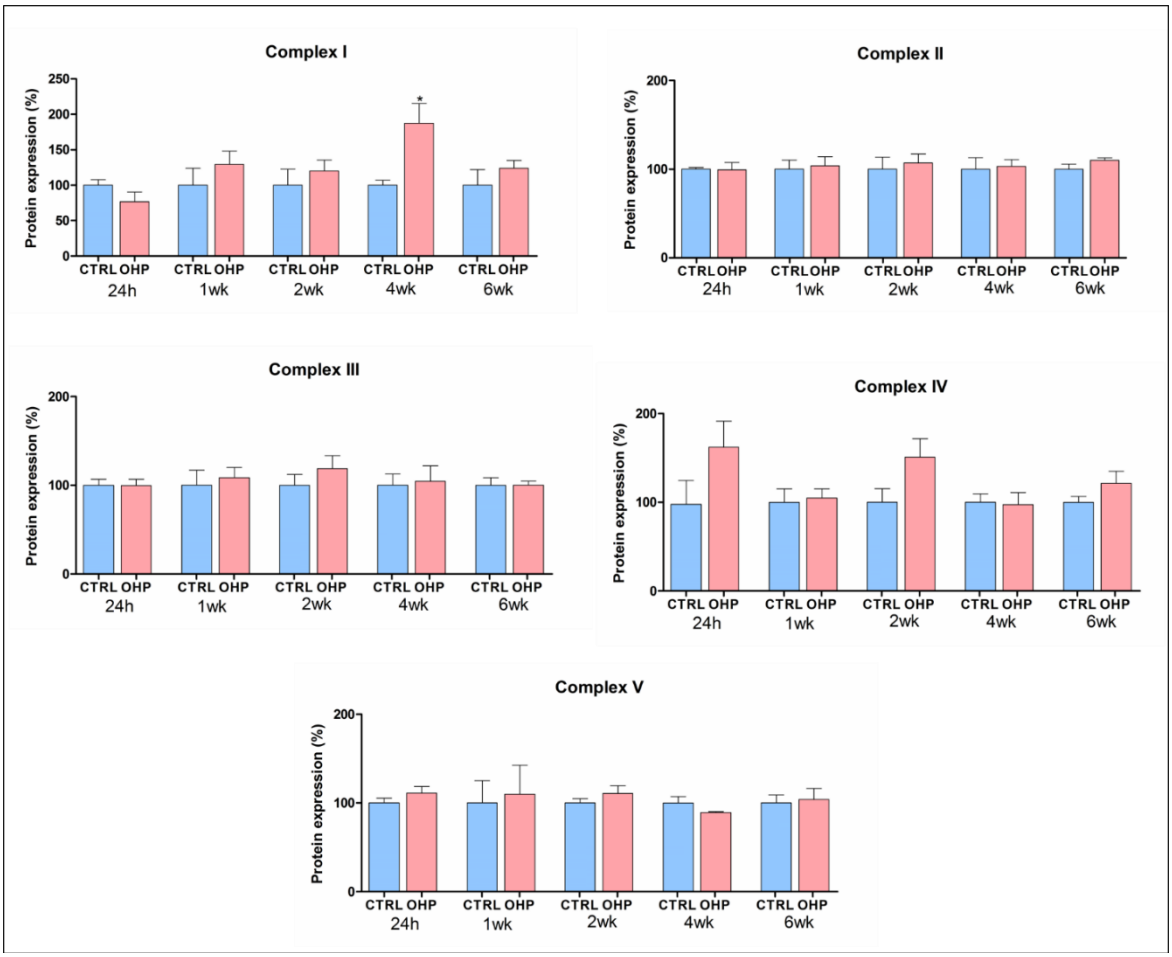

Figure 47. Assessment of protein expression of OXPHOS in DRG by Western blot analysis.
OHP treatment induced a significant increase only in respiratory chain Complex I in DRG at the end of treatment.
The housekeeping protein was β-actin. Protein level expressed in % vs CTRL is shown as mean ± SEM (n=5 per group), *$p<0.05$ vs CTRL, Unpaired t-test.

To verify if OHP treatment could interfere with the mitochondrial fission, the phosphorylation level of DRP1 at serine 616 was quantified and normalized on total DRP1 level.

The protein expression of DRP1t did not change significantly in DRG of OHP-treated mice compared to CTRL at the different time points (data not shown).

As shown in **Fig. 48**, the ratio between the phosphorylated and total form of DRP1 did not change significantly in DRG following the OHP treatment at the different evaluation time points. Only a decrease with a strong tendency towards statistical significance (p=0.051) was revealed in DRG harvested after 2 weeks of OHP treatment.

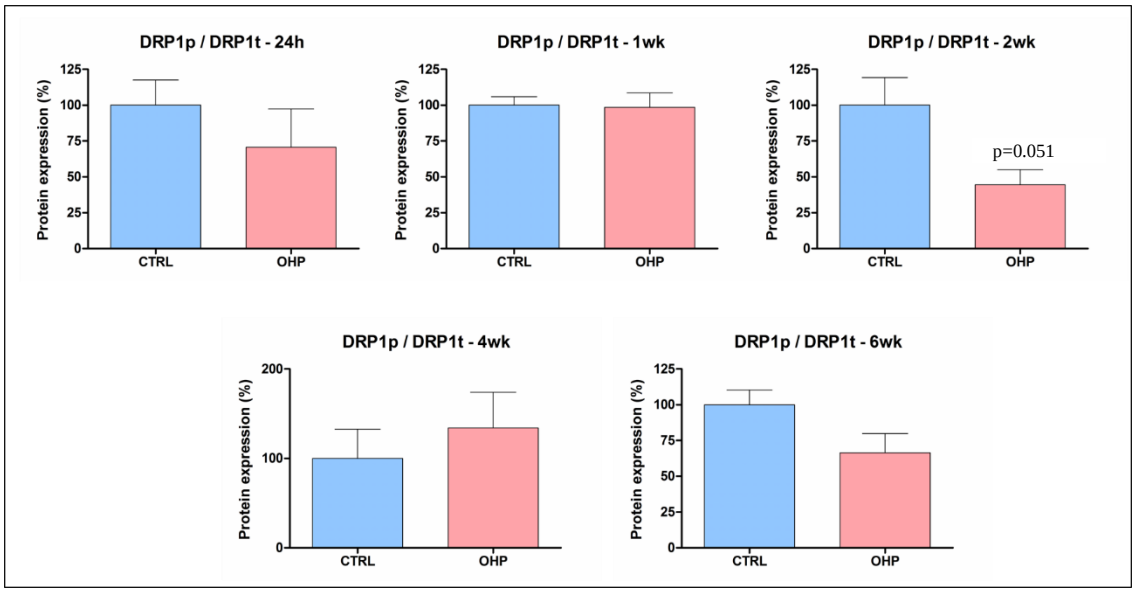

Figure 48. Assessment of protein expression of DRP1p in DRG by Western blot analysis.
OHP treatment did not induce any significant changes in the ratio of DRP1p/DRPt in DRG at each time point. Only a decrease with a strong tendency towards statistical significance (p=0.051) was observed at 2-week time point (Unpaired t-test).
Protein expressions expressed in % vs CTRL are shown as mean ± SEM (n=5 per group).

DISCUSSION AND CONCLUSIONS

OHP is a platinum-based anticancer drug commonly used in the treatment of digestive tract tumors and in combination with folinic acid (Leucovorin) and 5-FU (FOLFOX regimen) as first-line metastatic colorectal cancer therapy. Despite its antineoplastic efficacy, its clinical use is associated with severe side effects; among them OIPN is the most frequent dose-limiting toxicity. This adverse effect can reduce the quality of life of cancer patients and lead to dose reduction or discontinuation of the anticancer treatment. OHP is responsible for two distinct forms of peripheral neurotoxicity. Acute neurotoxicity is a distinctive side effect of OHP, occurs in up to 90% of patients shortly after OHP administration and consists of reversible cold-induced dysesthesias and paresthesias in distal extremities and/or perioral and pharyngolaryngeal regions. Approximately 70% of patients treated with OHP also develop a chronic cumulative sensory neuropathy with a typical stocking-and-glove distribution, characterized by dysesthesias, paresthesias and sensory impairment, sometimes associated with neuropathic pain. The chronic form of neuropathy usually occurs when the cumulative dose exceeds 780-850 mg/m^2 and can persist for months and progress after treatment cessation ("coasting" phenomenon) (Griffith et al., 2017; Kanat et al., 2017).

Currently there is no effective preventive and/or therapeutic strategies for OIPN. For this reason, the investigation and identification of mechanisms underlying the OIPN pathogenesis is mandatory in order to develop new treatment strategies.

The accumulation of platinum in DRG is considered a key step in the onset of platinum-based drugs neurotoxicity but the molecular mechanisms involved are still largely unknown. For this reason, it is important to establish a good animal model of OIPN to investigate the possible mechanisms underlying this pathology.

Over the last years *in vitro* studies and *in vivo* models of OIPN have been developed. The OIPN mice models reported in literature have been obtained using different OHP doses and treatment schedules. In many of these models only the neuropathic pain, among the clinical features of OIPN, was evaluated by means of behavioural tests. However, in order to reproduce the OIPN features faithfully, neurophysiological and histopathological analyses should also be performed. Moreover, since OHP induces two different syndromes of peripheral neurotoxicity as described above, the "acute" OIPN mice models should be distinguished from the "chronic" ones.

In this work we reproduced OIPN mice models using four different OHP treatment schedules (**Tabs. 3-6**). Three of them are reported in literature (*Studies 1-3*): two short-term OHP treatment characterized by high or low cumulative doses (20 and 3 mg/kg, respectively) and a longer schedule with a cumulative dose of 30 mg/kg. The last one is a long-term schedule, previously established and usually used in our laboratory, with cumulative dose of OHP 40 mg/kg (*Study 4*). In order to monitor the development of OIPN, for each study the peripheral neurotoxicity was assessed at different time points through a multimodal approach.

As shown in **Tabs. 3-6**, we evaluated the general toxicity (body weight monitoring), mechanical and cold nociceptive thresholds (Dynamic Aesthesiometer test and Cold Plate test, cut-off force 15g and plate set at +4°C, respectively) and neurophysiological function (NCV and SNAP recordings of caudal and digital nerves). Moreover, *ex vivo* analyses such as the evaluation of DRG, sciatic and caudal nerves morphology and morphometry as well as IENF density were performed.

Since in clinical practice the onset of acute OIPN occurs during or within 1-2 days after OHP infusion, the first evaluation time point we considered was within few hours from OHP injection. At this time point (24 hours) behavioural tests and neurophysiological analyses were performed, while at the subsequent time points morphological and morphometric analyses were also executed (**Tabs. 3-6**).

As far as behavioural tests are concerned, the development of severe cold hypersensitivity at 24 hours was observed in mice treated with OHP only in *Study 4*. In *Study 1* cold hyperalgesia developed in OHP group at later times, in *Study 2* no change in thermal sensitivity was observed in OHP-treated mice compared to CTRL group, while in *Study 3* we observed cold hyposensitivity at the last two time points, which can be considered a characteristic of the chronic form of OIPN. Mechanical threshold was also evaluated to determine the presence of allodynia or hypoesthesia. Only in *Study 4* a severe mechanical allodynia was detected at the end of OHP treatment which persisted until 2 weeks of follow-up with low severity. Neurophysiological analysis was performed in order to evaluate the large myelinated fibers function. Significant reduction in SNAP both in caudal and digital nerves was observed at the end of OHP treatment only in *Study 4*. The complete recovery detected after only 2 weeks of follow-up could indicate that our mouse model requires an increase in dose-intensity of OHP treatment to mimic the “coasting” phenomena observed in patients. In fact, in patients treated with OHP alterations in neurophysiology persist for months or even years after discontinuation of therapy (Briani et al, 2014).

Morphological and morphometric studies evaluated DRG, sciatic and caudal nerves and IENF density. Due to the lack of an efficient blood-brain and blood-nerve barrier, DRG are the most vulnerable sites to neurotoxic damage due to the accumulation of platinum (Kanat et al., 2017). We observed alterations in the size of DRG neurons after almost all OHP treatment schedule used, confirming that DRG is the primary target of platinum toxicity. Except for *Study 2*, morphometric analysis of L4-L5 DRG revealed a consistent size reduction of DRG sensory neurons following OHP treatment, according to previous studies (Jamieson et al., 2003; McKeage et al., 2011; Renn et al., 2011). Otherwise, for the first time, a transient increase in somatic and nuclear size (swelling) was observed in an animal model of OIPN: it was detected at mid-treatment in *Study 4*. In previous works, nucleolar enlargement in DRG collected from rats with PTX-induced sensory neuropathy and DRG hypertrophy in association with sciatic nerve crush injuries and in cases of polyradiculoneuropathy have been observed (Jamieson et al., 2003; Dietemann et al., 2012). Moreover, a recent clinical study described cases of DRG hypertrophy observed with magnetic resonances imaging in patients treated with OHP (Apostolidis et al. 2017).

In *Study 4*, nerve morphometry showed a significant reduction in the mean fiber diameter in sciatic and caudal nerves collected from OHP-treated mice after 4 weeks of treatment. This impairment persisted in sciatic nerve after 2 weeks of follow-up while resolved more distally (in caudal nerve). The reduction in the mean fiber diameter in sciatic and caudal nerves was also observed in *Study 1*, but only at 1 week from the first OHP administration, although not associated with alterations in neurophysiological recordings, probably due to the administration of two high dose of OHP in quick succession. No morphometric changes in both nerves were observed in *Study 2*. In *Study 3* a significant increase in the mean fiber diameter of caudal nerve was evidenced at 1 week in OHP-treated mice: this unexpected increase resulted to be statistically significant, although not strongly supported by the analysis of fiber size distribution.

Since standard neurophysiological techniques and nerve morphometry assess myelinated fibers, we thought it appropriate to assess the IENF density in the hind paw of mice in order to evaluate also the alteration in the small unmyelinated fibers. A severe reduction in IENF density was observed at the end of OHP treatment only in *Study 4* and persisted until 2 weeks of follow-up. This result was very interesting because it is known that small fiber dysfunction is associated with thermo-algesic sensory impairment (Santiago et al., 2000). In fact, in *Study*

4 we observed that the IENF reduction was accompanied by cold hyperalgesia at the end of the OHP treatment. All these results are summarized in **Tabs. 3-6**.

These results, obtained with our multimodal approach, allowed to demonstrate that 1) a single administration of OHP 3 mg/kg used in *Study 2* was not enough to induce any aspect of OIPN; 2) two doses of OHP 10 mg/kg in two alternate days (*Study 1*) and repeated administrations of OHP 3 mg/kg (*Study 3*) were able to induce alterations mainly in cold sensitivity, DRG morphometry and, only in *Study 1*, also in nerve morphometry; 3) the OHP schedule usually used in our laboratory (*Study 4*) induced both the acute and chronic forms of OIPN, showing alterations in almost all the parameters examined.

Some observations must be done about the three studies from the literature taken into consideration. The OHP schedules used in all these studies were aimed to induce neuropathic pain, either to study mechanisms underlying this symptom (Nassini et al., 2011; Jang et al., 2015) or to assess a mouse model of painful peripheral neuropathy (Ta et al., 2009). Moreover, two models evaluate OHP treatment of very brief duration, one a single low-dose administration and the other two high-dose administration every other day; in the third study OHP administration was prolonged for 15 days, with the schedule already described. In all studies OHP was intraperitoneally administered.

Thus, since the three published schedules we reproduced were only focused on the study of neuropathic pain induced by OHP, no other features were investigated in the original articles. Instead, we applied the same multimodal approach used for OHP model in our laboratory (*Study 4*) to the three schedules (*Studies 1-3*), in order to better analyse the different results. In this way, more parameters were examined in comparison with the original works and the results obtained have been reported (**Tabs. 3-6**).

It must be noted that the results obtained in the present study are not in agreement with the published results. Certainly, the different methods used to detect the OIPN onset might largely explain these discrepancies. For example, in order to evaluate mechanical threshold Von Frey filaments are used rather than Dynamic aesthesiometer test. Moreover, Cold plate test (and the different temperature used), Tail immersion or Acetone test are different methods to evaluate cold sensitivity (**Tabs. 3-6**). On the other hand, some of the results reported in the original articles are quite surprising, for instance the persistence of significant allodynia until 20 days after a single OHP 3 mg/kg injection in the *Study 2* (Nassini et al. 2011).

Furthermore, more generally, the difference among animal models could be due to several reasons. Beyond the dose, duration of treatment and the type of behavioural tests used, the route of drug administration and the animal strain employed could influence the results. For instance, in the three studies taken into consideration the route of drug administration (intraperitoneal) is different from the one employed in the *Study 4* (intravenous). Indeed, in our laboratory intravenous route of administration is the choice for all the drugs (except CDDP) used in CIPN animal models, the same route utilized in humans for these anticancer drugs. Moreover, it should be also pointed out that in the *Studies 1-3* a mouse strain (C57BL/6) different from the one of *Study 4* (BALB/c) has been employed. Our workgroup recently demonstrated that different mice strains, exposed to the same OHP treatment, show some variations in neurotoxicity development (Marmiroli et al., 2017).

A good disease animal model should at least represent the features of human disease faithfully, show little variability between workgroups and be easy to reproduce. Regarding OIPN, the dose and duration of treatment, the route of administration of the drug and the method of evaluation of pathology onset are key factors in order to establish a good animal model. Moreover, a good model of OIPN should be able to induce both acute and chronic form of this disease.

The mouse model used in our laboratory (*Study 4*) is characterized by 1) long-term treatment, 2) route of drug administration and cumulative dose comparable to the ones used for humans and 3) evaluation of acute and chronic neurotoxicity together with neuropathic pain using a multimodal approach.

As a matter of fact, it must be said that the three models from the literature do not allow the study of both acute and chronic forms of the disease, which can be studied only with appropriate OHP doses and treatment duration; they may possibly be suitable for the study of the mechanisms underlying the pathogenesis of neuropathic pain.

The second aim of this work was to investigate whether mitochondrial dysfunction and oxidative stress can be mechanisms underlying OIPN onset. This hypothesis rise from the evidence that mitochondrial dysfunction and increased levels of ROS have been shown to be involved in several neurological disorders such as Alzheimer, Parkinson and Huntington disease, multiple sclerosis, CMT hereditary polyneuropathy and amyotrophic lateral sclerosis (Palau et al., 2009; Hameren et al., 2018). Moreover, some evidence supports the hypothesis that mitochondrial damage may play an important role in platinum-induced

peripheral neurotoxicity and in other CIPN (Carozzi et al., 2010; Canta et al., 2015; Waseem et al., 2018). Thus, oxidative stress following OHP treatment was assessed in all the four studies in DRG, sciatic and caudal nerves by evaluation of lipid peroxidation, since cellular membrane lipids represent most often substrates of oxidative damage. In general, we did not find an evident increase in lipid peroxidation associated with OHP administration in DRG and caudal nerves, whereas a significant increase was observed at 2 and 4 weeks in sciatic nerves in *Study 4* and *Study 3*, respectively. These results may suggest that oxidative stress is induced only by repeated OHP administrations, in particular after a cumulative dose at about 20 mg/kg when OHP is administered intravenously whereas at about 30 mg/kg when administered intraperitoneally. The return to normal values observed at 4-week time point in *Study 4*, could indicate that some detoxification systems occurred. In fact, it is known that the concentration of ROS is controlled by internal defence mechanisms such as antioxidants (polyphenols, ascorbic acid and glutathione) or enzymes involved in oxygen radical scavenging (superoxide dismutase, catalase, glutathione peroxidase) (Ighodaro et al., 2018). In the future, it will be very interesting to further investigate this hypothesis.

Some evidence suggests that the involvement of mitochondria in the pathogenesis of neurological disease is usually associated with defects of the mitochondrial ETC and oxidative phosphorylation (Palau et al., 2009). For this reason, we also analysed mitochondrial function and biogenesis by evaluation of protein expression levels of ETC complexes and DRP1, a protein involved in mitochondrial fission pathway. These analyses were performed in DRG of OHP-treated and CTRL mice of *Study 4* as DRG neurons are the main target of OHP damage. These further evaluations were executed only in samples collected in *Study 4* since OHP was chronically administered and several time points were considered. We found an interesting increase in mitochondrial protein content of Complex I at the end of OHP treatment, maybe as a result of protective mechanism against stress condition induced by this compound in mitochondria. Complex I is the largest respiratory complex of the mitochondrial ETC, contributing to the proton-motive force required for mitochondrial ATP synthesis for about 40%. A previous study reported deficit in Complex I-mediated respiration in sciatic nerves collected from rats with OIPN (Zheng et al., 2011). Moreover, there is also evidence suggesting that mutations in genes encoding Complex I subunits are potential risk factors for the onset of neurodegenerative diseases and diabetic neuropathy (Elango et al., 2013; Rodenburg, 2016; Urra et al., 2017). It is possible to state

that also in our study Complex 1 showed some changes due to OHP treatment, even if the real significance of its temporary increased level is not clear.

Regarding mitochondrial dynamics, levels of total DRP1 protein were similar between OHP-treated and control mice. On the other hand, a decrease ($p=0.051$) in phosphoryled form of DRP1 at Ser616 (activated form) was observed after 2 weeks of OHP treatment, indicating that a cumulative dose of OHP 20 mg/kg could induce a reduction in mitochondrial fission. It is important to note that altered mitochondrial fission and fusion can result in mitochondrial dysfunction, as observed in several cardiac, renal and pulmonary diseases, in diabetes, cancer, as well as in neurodegenerative disorders such as Azheimer and Parkinson disease. In fact an imbalance of protein activity involved in mitochondrial dynamics may lead to dysfunction and cell death (Fields et al., 2016; Breitzig et al., 2018; Oliver and Raddy, 2019). Increased levels of the fission protein DRP1 and mitochondrial fragmentation have been reported after exposure of cultured neurons to oxidative stress and in association with several neurological disease. In particular, numerous studies reported that levels of DRP1 were increased in neurons derived from autoptic brain of patients with Alzheimer disease and in brain tissues collected from transgenic Alzheimer mice, causing excessive fragmentation of mitochondria that leads to mitochondrial dysfuction and neuronal damage (Chen et al., 2015; Manczak et al., 2019; Oliver and Raddy, 2019). However, a recent study reported a time course of mitochondrial fission and fusion after cardiac arrest in rats showing a remarkable reduction in DRP1 protein and mRNA levels at 4 hours after the restoration of spontaneous circulation, which then increased at 12 and 24 hours. These results suggest that cerebral mitochondrial fission decreased at the early stage and increased at the later time after ischemic injury induced by cardiac arrest (Li et al., 2017). Despite the different kind of disorders, this trend is similar to our observations; in fact at 2 weeks from the first OHP administration we observed a reduction in fission processes which instead shows a tendency to increase at 4 weeks.

Even if the results discussed above did not give a strong evidence of mitochondrial dysfunction and oxidative stress involvement in OIPN onset, their role cannot be excluded in the pathogenesis of OIPN. For this reason, further investigations such as measurement of mitochondrial respiration and ATP production are needed, possibly with examination of a greater number of DRG and peripheral nerves samples.

In conclusion:

1) Reliable OIPN animal model should be able to evaluate acute and chronic neurotoxicity. Biological mechanism underlying acute peripheral neurotoxicity could be studied in models of acute OIPN, whereas the chronic form, which is the most relevant in clinical practice, cannot be fully reproduced with single OHP administration or short-term OHP schedule;
2) it should be useful to standardize the animal model as well as the investigation methods in order to obtain more consistent results among different workgroups;
3) mitochondrial dysfunction and oxidative stress may be factors contributing to the onset of OIPN but further investigations are required.

Study 1 **(OHP 10 mg/kg, day1 and day3, i.p., C57BL/6)**		
	Jiang et al., 2016	**Our laboratory**
Body weight (gr)	//	decrease after the 1st administration
Mechanical nociceptive threshold (gr)	Von frey filaments **d0** basal **d3** ** **d6** *** **d9** *** **d12** *** **d15** *** allodynia	Dynamic Aesthesiometer test **24h** ns **1wk** ns **2wk** ns
Cold nociceptive threshold (sec/n signs)	Tail immersion +4°C (sec) **d0** basal **d3** ** **d6** *** **d9** *** **d12** *** **d15** *** hyperalgesia	Cold Plate test +4°C (n signs) **24h** ns **1wk** ** hyperalgesia **2wk** *
Neurophysiology **- caudal SNAP** (μV) **- caudal NCV** (m/sec) **- digital SNAP** (μV) **- digital NCV** (m/sec)	//	**24h** **1wk** **2wk** ns ns ns ns ns ns ns ns ns ns ns ns
DRG morphometry (μm^2) **- soma** **- nucleus** **- nucleolus**	//	**1wk** **2wk** *** **** ** *** atrophy **** ns
Nerves morphometry **- sciatic nerve** **- caudal nerve** (fiber diameter and density)	//	**1wk** **2wk** *** diameter reduction ns *** ns
IENF density ($IENF/mm^2$)	//	**1wk** ns

Table 3. Results of OIPN assessment of *Study 1* obtained with authors study approach and our multimodal approach.

Study 2 **(OHP 3 mg/kg, single i.p., C57BL/6)**		
	Nassini et al., 2011	**Our laboratory**
Body weight (gr)	//	ns
Mechanical nociceptive threshold (gr)	Von frey filaments **d0** basal **d1** ns **d3** * **d6** * **d10** * **d15** * **d20** * allodynia **d30** ns	Dynamic Aesthesiometer test **24h** ns **1wk** ns **2wk** ns
Cold nociceptive threshold (sec/n signs)	Acetone evaporation test (sec) **d0** basal **d1** ns **d3** * **d6** * **d10** * allodynia **d15** ns **d20** ns **d30** ns	Cold Plate test +4°C (n signs) **24h** ns **1wk** ns **2wk** ns
Neurophysiology **- caudal SNAP** (μV) **- caudal NCV** (m/sec) **- digital SNAP** (μV) **- digital NCV** (m/sec)	//	**24h** **1wk** **2wk** ns ns ns ns ns ns ns ns ns ns ns ns
DRG morphometry (μm^2) **- soma** **- nucleus** **- nucleolus**	//	**1wk** **2wk** ns ns *** atrophy ns ns ns
Nerves morphometry **- sciatic nerve** **- caudal nerve** (fiber diameter and density)	//	**1wk** **2wk** ns ns ns ns
IENF density (IENF/mm^2)	//	**1wk** ns

Table 4. Results of OIPN assessment of *Study 2* obtained with authors study approach and our multimodal approach.

Study 3 **(OHP 3 mg/Kg, q1dx5, 2 cycles with 5 days rest, i.p., C57/BL6)**		
	Ta et al., 2009	**Our laboratory**
Body weight (gr)	ns	decrease after the 3rd administration
Mechanical nociceptive threshold (gr)	Von frey filaments **d0** basal **1wk** ns **3wk** *** allodynia **6wk** ns **8wk** ns	Dynamic Aesthesiometer test **1wk** ns **2wk** ns **4wk** ns
Cold nociceptive threshold (sec/n signs)	Cold plate test -4°C (sec) **d0** basal **1wk** * ⎫ **3wk** *** ⎬ hyperalgesia **6wk** * ⎭ **8wk** ns	Cold plate test +4°C (n signs) **1wk** ns **2wk** * ⎫ hypoalgesia **4wk** * ⎭
Neurophysiology **- caudal SNAP** (μV) **- caudal NCV** (m/sec) **- digital SNAP** (μV) **- digital NCV** (m/sec)	//	**1wk 2wk 4wk** ns ns ns ns ns ns ns ns ns ns ns ns
DRG morphometry (μm^2) **- soma** **- nucleus** **- nucleolus**	//	**1wk 2wk 4wk** *** * *** ⎫ ns * *** ⎬ atrophy *** ** *** ⎭
Nerves morphometry **- sciatic nerve** **- caudal nerve** (fiber diameter and density)	//	**1wk** **2wk** ns ns ** diameter increase ns
IENF density (IENF/mm^2)	//	**2wk** ns

Table 5. Results of OIPN assessment of *Study 3* obtained with authors study approach and our multimodal approach.

Study 4 **(OHP 5mg/Kg, 2qwx4, i.v., BALB/c)**	
	Our laboratory
Body weight (gr)	decrease after the last administration
Mechanical nociceptive threshold (gr)	Dynamic Aesthesiometer test **24h** ns **1wk** ns **2wk** ns **4wk** ***] allodynia **6wk** *
Cold nociceptive threshold (n signs)	Cold plate test +4°C **24h** ***] **1wk** ns] hyperalgesia **2wk** **] **4wk** *] **6wk** ns
Neurophysiology **- caudal SNAP** (µV) **- caudal NCV** (m/sec) **- digital SNAP** (µV) **- digital NCV** (m/sec)	**24h** **1wk** **2wk** **4wk** **6wk** ns ns ** **] ns ns ns ns ns] reduction ns ns ns ns ***] ns ns ns ns ns ns
DRG morphometry (µm²) **- soma** **- nucleus** **- nucleolus**	**1wk** **2wk** **4wk** **6wk** ns **] swelling *] atrophy ns ns ** *** ns ns ns ns ns
Nerves morphometry **- sciatic nerve** **- caudal nerve** (fiber diameter and density)	**2wk** **4wk** **6wk** ns *** **] diameter ns *** ns] reductionn
IENF density (IENF/mm²)	**4wk** **6wk** *** *** reduction

Table 6. Results of OIPN assessment of *Study 4* obtained with authors study approach and our multimodal approach.

ABBREVIATIONS

5-FU	Fluorouracil
ATP	Adenosine triphosphate
BER	Base excision repair
BTZ	Bortezomib
CDDP	Cisplatin
CIPN	Chemotherapy-induced peripheral neurotoxicity
CMAP	Compound muscle action potential
CMT	Charcot-Marie-Tooth
CRB	Carboplatin
CTR	Copper transporter
CTRL	Control
DACH	Diaminocyclohexane
DIPN	Drug-induced peripheral neurotoxicity
DRG	Dorsal root ganglia
DRP	Dynamin-related protein
ETC	Electron transport chain
FDA	Food and Drug Administration
FIS	Fission protein
GDP	Guanosine 5'-phosphate
HIV	Human immunodeficiency virus
IENF	Intraepidermal nerve fibers
IL	Interleukin
MFN	Mitofusin
NCV	Nerve conduction velocity
NER	Nucleotide excision repair
OCT	Organic cation transporter
OHP	Oxaliplatin
OIPN	Oxaliplatin-induced peripheral neurotoxicity
OPA	Optic atrophy
PNS	Peripheral nervous system
PTX	Paclitaxel
RNS/ROS	Reactive nitrogen species / Reactive oxygen species
SEM	Standard error of the mean
TBARS	Thiobarbituric acid reactive substances
TLR	Toll-like receptor
TNF	Tumor necrosis factor
TRP	Transient receptor potential ion channel
VCR	Vincristine

REFERENCES

Akude, E., Zherebitskaya, E., Chowdhury, S. K. R., Smith, D. R., Dobrowsky, R. T., & Fernyhough, P. (2011). Diminished superoxide generation is associated with respiratory chain dysfunction and changes in the mitochondrial proteome of sensory neurons from diabetic rats. *Diabetes*, *60*(1), 288–297. https://doi.org/10.2337/db10-0818

Alcindor, T., & Beauger, N. (2011). *Oxaliplatin: a review in the era of molecularly targeted therapy* (Vol. 18). https://doi.org/10.3747/co.v18i1.708

Aoki, M., Kurauchi, Y., Mori, A., Nakahara, T., Sakamoto, K., & Ishii, K. (2014). Comparison of the effects of single doses of elcatonin and pregabalin on oxaliplatin-induced cold and mechanical allodynia in rats. *Biological and Pharmaceutical Bulletin*, *37*(2), 322–326. https://doi.org/10.1248/bpb.b13-00735

Apostolidis, L., Schwarz, D., Xia, A., Weiler, M., Heckel, A., Godel, T., … Bäumer, P. (2017). Dorsal root ganglia hypertrophy as in vivo correlate of oxaliplatin-induced polyneuropathy. *Plos One*, *12*(8). https://doi.org/10.1371/journal.pone.0183845

Arango, D., Wilson, A. J., Shi, Q., Corner, G. A., Arañes, M. J., Nicholas, C., … Augenlicht, L. H. (2004). Molecular mechanisms of action and prediction of response to oxaliplatin in colorectal cancer cells. *British Journal of Cancer*, *91*(11), 1931–1946. https://doi.org/10.1038/sj.bjc.6602215

Areti, A., Yerra, V. G., Naidu, V. G. M., & Kumar, A. (2014). Oxidative stress and nerve damage: Role in chemotherapy induced peripheral neuropathy. *Redox Biology*. Elsevier B.V. https://doi.org/10.1016/j.redox.2014.01.006

Argyriou, A. A., Kyritsis, A. P., Makatsoris, T., & Kalofonos, H. P. (2014). Cancer Management and Research Dovepress Chemotherapy-induced peripheral neuropathy in adults: a comprehensive update of the literature. *Cancer Management and Research*, 6–135. https://doi.org/10.2147/CMAR.S44261

Baloh, R. H., Schmidt, R. E., Pestronk, A., & Milbrandt, J. (2007). Neurobiology of Disease Altered Axonal Mitochondrial Transport in the Pathogenesis of Charcot-Marie-Tooth Disease from Mitofusin 2 Mutations. *Journal of Neuroscience*. https://doi.org/10.1523/JNEUROSCI.4798-06.2007

Banki, K., Hutter, E., Gonchoroff, N. J., & Perl, A. (1998). Molecular ordering in HIV-induced apoptosis: Oxidative stress, activation of caspases, and cell survival are regulated by transaldolase. *Journal of Biological Chemistry*, *273*(19), 11944–11953. https://doi.org/10.1074/jbc.273.19.11944

Barrière, D. A., Rieusset, J., Chanteranne, D., Busserolles, J., Chauvin, M.-A., Chapuis, L., … Morio, B. (2012). Paclitaxel therapy potentiates cold hyperalgesia in streptozotocin-induced diabetic rats through enhanced mitochondrial reactive oxygen species production and TRPA1 sensitization. *Pain*, *153*(3), 553–61. https://doi.org/10.1016/j.pain.2011.11.019

Bennett, G. J., Doyle, T., & Salvemini, D. (2014). Mitotoxicity in distal symmetrical sensory peripheral neuropathies. *Nature Reviews Neurology*. https://doi.org/10.1038/nrneurol.2014.77

Bobylev, I., Joshi, A. R., Barham, M., Ritter, C., Neiss, W. F., Höke, A., & Lehmann, H. C. (2015). Paclitaxel inhibits mRNA transport in axons. *Neurobiology of Disease*, *82*, 321–331. https://doi.org/10.1016/j.nbd.2015.07.006

Boyette-Davis, J. A., Hou, S., Abdi, S., & Dougherty, P. M. (2018). An updated understanding of the mechanisms involved in chemotherapy-induced neuropathy. *Pain Management*, *8*(5), 363–375. https://doi.org/10.2217/pmt-2018-0020

Breitzig, M. T., Alleyn, M. D., Lockey, R. F., & Kolliputi, N. (2018). A mitochondrial delicacy: dynamin-related protein 1 and mitochondrial dynamics. *American Journal of Physiology. Cell Physiology*, *315*(1), C80–C90. https://doi.org/10.1152/ajpcell.00042.2018

Breitzig, M. T., Alleyn, M. D., Lockey, R. F., & Kolliputi, N. (2018). A mitochondrial delicacy: dynamin-related protein 1 and mitochondrial dynamics. *American Journal of Physiology. Cell Physiology*, *315*(1), C80–C90. https://doi.org/10.1152/ajpcell.00042.2018

Briani, C., Argyriou, A. A., Izquierdo, C., Velasco, R., Campagnolo, M., Alberti, P., … Kalofonos, H. P. (2014). Long-term course of oxaliplatin-induced polyneuropathy: a prospective 2-year follow-up study. *Journal of the Peripheral Nervous System*, *19*(4), 299–306. https://doi.org/10.1111/jns.12097

Canta, A., Pozzi, E., & Carozzi, V. A. (2015). Mitochondrial Dysfunction in Chemotherapy-Induced Peripheral Neuropathy (CIPN). *Toxics*, *3*, 198–223. https://doi.org/10.3390/toxics3020198

Carozzi, V. A., Marmiroli, P., & Cavaletti, G. (2010). The role of oxidative stress and anti-oxidant treatment in platinum-induced peripheral neurotoxicity. *Current Cancer Drug Targets*, *10*(7), 670–82. http://www.ncbi.nlm.nih.gov/pubmed/20578989

Carozzi, V. A., Canta, A., & Chiorazzi, A. (2015). Chemotherapy-induced peripheral neuropathy: What do we know about mechanisms? *Neuroscience Letters*. Elsevier Ireland Ltd. https://doi.org/10.1016/j.neulet.2014.10.014

Cavaletti, G., Tredici, G., Petruccioli, M. ., Dondè, E., Tredici, P., Marmiroli, P., … Griffon Etienne, G. (2001). Effects of different schedules of oxaliplatin treatment on the peripheral nervous system of the rat. *European Journal of Cancer*, *37*(18), 2457–2463. https://doi.org/10.1016/S0959-8049(01)00300-8

Cavaletti, G., & Marmiroli, P. (2015). Chemotherapy-induced peripheral neurotoxicity. *Current Opinion in Neurology*, *28*(5), 500–507. https://doi.org/10.1097/WCO.0000000000000234

Chahbouni, M., Del Señor López, M., Molina-Carballo, A., De Haro, T., Muñoz-Hoyos, A., Fernández-Ortiz, M., … Acuña-Castroviejo, D. (2017). Melatonin Treatment Reduces Oxidative Damage and Normalizes Plasma Pro-Inflammatory Cytokines in Patients Suffering from Charcot-Marie-Tooth Neuropathy: A Pilot Study in Three Children. *Molecules.* https://doi.org/10.3390/molecules22101728

Chen, S. Der, Lin, T. K., Yang, D. I., Lee, S. Y., Shaw, F. Z., Liou, C. W., & Chuang, Y. C. (2015). Roles of PTEN-induced putative kinase 1 and dynamin-related protein 1 in transient global ischemia-induced hippocampal neuronal injury. *Biochemical and Biophysical Research Communications*, *460*(2), 397–403. https://doi.org/10.1016/j.bbrc.2015.03.045

Choi, S., Chae, H. K., Heo, H., Hahm, D.-H., Kim, W., & Kim, S. K. (2019). Analgesic Effect of Melittin on Oxaliplatin-Induced Peripheral Neuropathy in Rats. *Toxins*, *11*(7), 396. https://doi.org/10.3390/toxins11070396

Conklin, K. A. (2004). Chemotherapy-associated oxidative stress: Impact on chemotherapeutic effectiveness. *Integrative Cancer Therapies*. https://doi.org/10.1177/1534735404270335

Coriat, R., Alexandre, J., Nicco, C., Quinquis, L., Benoit, E., Chéreau, C., … Batteux, F. (2014). Treatment of oxaliplatin-induced peripheral neuropathy by intravenous mangafodipir. *The Journal of Clinical Investigation*, *124*(1), 262–72. https://doi.org/10.1172/JCI68730

Dalakas, M. C., Semino-Mora, C., & Leon-Monzon, M. (2001). Mitochondrial alterations with mitochondrial DNA depletion in the nerves of AIDS patients with peripheral neuropathy induced by 2′3′-dideoxycytidine (DDC). *Laboratory Investigation*, *81*(11), 1537–1544. https://doi.org/10.1038/labinvest.3780367

Di Cesare Mannelli, L., Zanardelli, M., Failli, P., & Ghelardini, C. (2012). Oxaliplatin-induced neuropathy: oxidative stress as pathological mechanism. Protective effect of silibinin. *The Journal of Pain : Official Journal of the American Pain Society*, *13*(3), 276–84. https://doi.org/10.1016/j.jpain.2011.11.009

Dietemann, J. L., Bogorin, A., Abu Eid, M., Sanda, R., Mourao Soares, I., Draghici, S., … Koob, M. (2012). Tips and traps in neurological imaging: Imaging the perimedullary spaces. *Diagnostic and Interventional Imaging*, *93*(12), 985–992. https://doi.org/10.1016/j.diii.2012.08.005

Elango, S., Venugopal, S., Thangaraj, K., & Viswanadha, V. P. (2014). Novel mutations in ATPase 8, ND1 and ND5 genes associated with peripheral neuropathy of diabetes. *Diabetes Research and Clinical Practice*, *103*(3). https://doi.org/10.1016/j.diabres.2013.12.015

Fernyhough, P., Chowdhury, S. K. R., & Schmidt, R. E. *Mitochondrial stress and the pathogenesis of diabetic neuropathy Clinical impact of diabetic neuropathy*. http://www.diabetes.org

Fields, J. A., Serger, E., Campos, S., Divakaruni, A. S., Kim, C., Smith, K., … Masliah, E. (2016). HIV alters neuronal mitochondrial fission/fusion in the brain during HIV-associated neurocognitive disorders. *Neurobiology of Disease*, *86*, 154–169. https://doi.org/10.1016/j.nbd.2015.11.015

Flatters, S. J. L., & Bennett, G. J. (2006). Studies of peripheral sensory nerves in paclitaxel-induced painful peripheral neuropathy: evidence for mitochondrial dysfunction. *Pain*, *122*(3), 245–57. https://doi.org/10.1016/j.pain.2006.01.037

Fong, C. W. (2016). Platinum anti-cancer drugs: Free radical mechanism of Pt-DNA adduct formation and anti-neoplastic effect. *Free Radical Biology & Medicine*, *95*, 216–29. https://doi.org/10.1016/j.freeradbiomed.2016.03.006

Gamelin, E., Gamelin, L., Bossi, L., & Quasthoff, S. (2002). Clinical Aspects and Molecular Basis of Oxaliplatin Neurotoxicity: Current Management and Development of Preventive Measures. *Seminars in Oncology*. https://doi.org/10.1053/sonc.2002.35525

Gourdier, I., Crabbe, L., Andreau, K., Pau, B., & Kroemer, G. (2004). Oxaliplatin-induced mitochondrial apoptotic response of colon carcinoma cells does not require nuclear DNA. *Oncogene*, *23*(45), 7449–7457. https://doi.org/10.1038/sj.onc.1208047

Graham, J., Mushin, M., & Kirkpatrick, P. (2004). Oxaliplatin. *Nature Reviews. Drug Discovery*, *3*(1), 11–2. https://doi.org/10.1038/nrd1287

Griffith, K. A., Zhu, S., Johantgen, M., Kessler, M. D., Renn, C., Beutler, A. S., … Dorsey, S. G. (2017). Oxaliplatin-Induced Peripheral Neuropathy and Identification of Unique Severity Groups in Colorectal Cancer. *Journal of Pain and Symptom Management*, *54*(5), 701–706.e1. https://doi.org/10.1016/j.jpainsymman.2017.07.033

Grisold, W., Cavaletti, G., & Windebank, A. J. (2012). Peripheral neuropathies from chemotherapeutics and targeted agents: diagnosis, treatment, and prevention. *Neuro-Oncology*, *14*, 45–54. https://doi.org/10.1093/neuonc/nos203

Ha, H., & Endou, H. (1992). Lipid peroxidation in isolated rat nephron segments. *The American Journal of Physiology*, *263*(2 Pt 2), F201-7. https://doi.org/10.1152/ajprenal.1992.263.2.F201

Hameren, G. van, Campbell, G., Deck, M., Berthelot, J., Chrast, R., & Tricaud, N. (2018). CMT disease 2A and demyelination decouple ATP and ROS production by axonal mitochondria. *bioRxiv*, 462523. https://doi.org/10.1101/462523

Hu, C., Huang, Y., & Li, L. (2017). Drp1-dependent mitochondrial fission plays critical roles in physiological and pathological progresses in mammals. *International Journal of Molecular Sciences*. MDPI AG. https://doi.org/10.3390/ijms18010144

Ighodaro, O. M., & Akinloye, O. A. (2018). First line defence antioxidants-superoxide dismutase (SOD), catalase (CAT) and glutathione peroxidase (GPX): Their fundamental role in the entire antioxidant defence grid. *Alexandria Journal of Medicine*, *54*(4), 287–293. https://doi.org/10.1016/j.ajme.2017.09.001

Ivanov, A. V., Valuev-Elliston, V. T., Ivanova, O. N., Kochetkov, S. N., Starodubova, E. S., Bartosch, B., & Isaguliants, M. G. (2016). Oxidative Stress during HIV Infection: Mechanisms and Consequences. *Oxidative Medicine and Cellular Longevity*. https://doi.org/10.1155/2016/8910396

Jamieson, S. M. F., Liu, J., Hsu, T., Baguley, B. C., & McKeage, M. J. (2003). Paclitaxel induces nucleolar enlargement in dorsal root ganglion neurons in vivo reducing oxaliplatin toxicity. *British Journal of Cancer*, *88*(12), 1942–1947. https://doi.org/10.1038/sj.bjc.6601012

Jiang, S.-P., Zhang, Z.-D., Kang, L.-M., Wang, Q.-H., Zhang, L., & Chen, H.-P. (2016). Celecoxib reverts oxaliplatin-induced neuropathic pain through inhibiting PI3K/Akt2 pathway in the mouse dorsal root ganglion. *Experimental Neurology*, *275 Pt 1*, 11–6. https://doi.org/10.1016/j.expneurol.2015.11.001

Joseph, E. K., Levine, J. D., & Joseph, E. K. (2009). Comparison of Oxaliplatin-and Cisplatin-induced Painful Peripheral Neuropathy in the Rat. *J Pain*, *10*(5), 534–541. https://doi.org/10.1016/j.jpain.2008.12.003

Kanat, O., Ertas, H., & Caner, B. (2017). Platinum-induced neurotoxicity: A review of possible mechanisms. *World J Clin Oncol*, *8*(4), 329–335. https://doi.org/10.5306/wjco.v8.i4.329

Kawashiri, T., Egashira, N., Watanabe, H., Ikegami, Y., Hirakawa, S., Mihara, Y., … Oishi, R. (2011). Prevention of oxaliplatin-induced mechanical allodynia and neurodegeneration by neurotropin in the rat model. *European Journal of Pain*, *15*(4), 344–50. https://doi.org/10.1016/j.ejpain.2010.08.006

Kelley, M. R., Jiang, Y., Guo, C., Reed, A., Meng, H., Vasko, M. R., & Kirchmair, R. (2014). Role of the DNA Base Excision Repair Protein, APE1 in Cisplatin, Oxaliplatin, or Carboplatin Induced Sensory Neuropathy. *Plos One*. https://doi.org/10.1371/journal.pone.0106485

Kim, W., Kim, M. J., Go, D., Min, B. Il, Na, H. S., & Kim, S. K. (2016). Combined effects of bee venom acupuncture and morphine on Oxaliplatin-induced neuropathic pain in mice. *Toxins*, 8(2). https://doi.org/10.3390/toxins8020033

Kim, P. G., Bridgham, K., Chen, E. C., Vidula, M. K., Pozdnyakova, O., Brunner, A. M., & Fathi, A. T. (2018). Incident adverse events following therapy for acute promyelocytic leukemia. *Leukemia Research Reports*, *9*, 79–83. https://doi.org/10.1016/j.lrr.2018.05.001

Lee, C. S., Ryan, E. J., & Doherty, G. A. (2014 a). Gastro-intestinal toxicity of chemotherapeutics in colorectal cancer: The role of inflammation. *World J Gastroenterol*, *20*(14), 3751–3761. https://doi.org/10.3748/wjg.v20.i14.3751

Lee, J. H., Li, D. X., Yoon, H., Go, D., Quan, F. S., Min, B. Il, & Kim, S. K. (2014 b). Serotonergic mechanism of the relieving effect of bee venom acupuncture on oxaliplatin-induced neuropathic cold allodynia in rats. *BMC Complementary and Alternative Medicine*, 14(1). https://doi.org/10.1186/1472-6882-14-471

Li, Y., Tang, Q., Wang, P., Qin, J., Wu, H., Lin, J., & Huang, Z. (2017). Dynamic Changes of Mitochondrial Fusion and Fission in Brain Injury after Cardiac Arrest in Rats. *BioMed Research International*, *2017*. https://doi.org/10.1155/2017/1948070

Lim, T. K. Y., Rone, M. B., Lee, S., Antel, J. P., & Zhang, J. (2015). Mitochondrial and bioenergetic dysfunction in trauma-induced painful peripheral neuropathy. *Molecular Pain*, *11*, 58. https://doi.org/10.1186/s12990-015-0057-7

Ling, B., Coudoré-Civiale, M. A., Balayssac, D., Eschalier, A., Coudoré, F., & Authier, N. (2007 a). Behavioral and immunohistological assessment of painful neuropathy induced by a single oxaliplatin injection in the rat. *Toxicology*, *234*(3), 176–184. https://doi.org/10.1016/j.tox.2007.02.013

Ling, B., Authier, N., Balayssac, D., Eschalier, A., & Coudore, F. (2007 b). Behavioral and pharmacological description of oxaliplatin-induced painful neuropathy in rat. *Pain*, *128*(3), 225–234. https://doi.org/10.1016/j.pain.2006.09.016

Makker, P. G. S., Duffy, S. S., Lees, J. G., Perera, C. J., Tonkin, R. S., Butovsky, O., … Moalem-Taylor, G. (2017). Characterisation of Immune and Neuroinflammatory Changes Associated with Chemotherapy-Induced Peripheral Neuropathy. *Plos One*. https://doi.org/10.1371/journal.pone.0170814

Malacrida, A., Meregalli, C., Rodriguez-Menendez, V., & Nicolini, G. (2019). Chemotherapy-induced peripheral neuropathy and changes in cytoskeleton. *International Journal of Molecular Sciences*. MDPI AG. https://doi.org/10.3390/ijms20092287

Manczak, M., Kandimalla, R., Yin, X., & Hemachandra Reddy, P. (2019). Mitochondrial division inhibitor 1 reduces dynamin-related protein 1 and mitochondrial fission activity. *Human Molecular Genetics*, *28*(2), 177–199. https://doi.org/10.1093/hmg/ddy335

Marmiroli, P., Scuteri, A., Cornblath, D. R., & Cavaletti, G. (2017). Pain in chemotherapy-induced peripheral neurotoxicity. *Journal of the Peripheral Nervous System*, *22*(3), 156–161. https://doi.org/10.1111/jns.12226

McKeage, MJ, & al. (2001). Nucleolar damage correlates with neurotoxicity induced by different platinum drugs. *British Journal of Cancer*. https://doi.org/10.1054/bjoc.2001.2024

Mcwhinney, S. R., Goldberg, R. M., & Mcleod, H. L. (2009). Platinum Neurotoxicity Pharmacogenetics. *Molecular Cancer Therapeutics*, *8*(1), 10–16. https://doi.org/10.1158/1535-7163.MCT-08-0840

Mehmood, R. K. (2014). Review of cisplatin and oxaliplatin in current immunogenic and monoclonal antibodies perspective. *Oncology Reviews*. Page Press Publications. https://doi.org/10.4081/oncol.2014.256

Nassini, R., Gees, M., Harrison, S., De Siena, G., Materazzi, S., Moretto, N., … Geppetti, P. (2011). Oxaliplatin elicits mechanical and cold allodynia in rodents via TRPA1 receptor stimulation. *Pain*, *152*(7), 1621–31. https://doi.org/10.1016/j.pain.2011.02.051

Niemann, A., Huber, N., Wagner, K. M., Somandin, C., Horn, M., Dé Ric Lebrun-Julien, F., … Suter, U. (2014). The Gdap1 knockout mouse mechanistically links redox control to Charcot-Marie-Tooth disease. *A Journal Of Neurology*. https://doi.org/10.1093/brain/awt371

Norcini, M., Vivoli, E., Galeotti, N., Bianchi, E., Bartolini, A., & Ghelardini, C. (2009). Supraspinal role of protein kinase C in oxaliplatin-induced neuropathy in rat. *Pain*, *146*(1–2), 141–147. https://doi.org/10.1016/j.pain.2009.07.017

Oliver, D., & Reddy, P. H. (2019). Dynamics of Dynamin-Related Protein 1 in Alzheimer's Disease and Other Neurodegenerative Diseases. *Cells*, *8*(9). https://doi.org/10.3390/cells8090961

Oun, R., Moussa, Y. E., & Wheate, N. J. (2018). The side effects of platinum-based chemotherapy drugs: A review for chemists. *Dalton Transactions*. Royal Society of Chemistry. https://doi.org/10.1039/c8dt00838h

Palau, F., Estela, A., Pla-Martín, D., & Sánchez-Piris, M. (2009). The role of mitochondrial network dynamics in the pathogenesis of charcot-marie-tooth disease. In *Advances in Experimental Medicine and Biology* (Vol. 652, pp. 129–137). https://doi.org/10.1007/978-90-481-2813-6_9

Park, S. B., Lin, C. S.-Y., Krishnan, A. V, Goldstein, D., Friedlander, M. L., & Kiernan, M. C. (2011). Dose Effects of Oxaliplatin on Persistent and Transient Na + Conductances and the Development of Neurotoxicity. *Plos One*. https://doi.org/10.1371/journal.pone.0018469

Pesaresi, M., Giatti, S., Spezzano, R., Romano, S., Diviccaro, S., Borsello, T., … Melcangi, R. C. (2018). Axonal transport in a peripheral diabetic neuropathy model: sex-dimorphic features. *Biology of Sex Differences*, *9*(1), 6. https://doi.org/10.1186/s13293-018-0164-z

Podratz, J. L., Knight, A. M., Ta, L. E., Staff, N. P., Gass, J. M., Genelin, K., … Windebank, A. J. (2010). Cisplatin induced Mitochondrial DNA Damage In Dorsal Root Ganglion Neurons. *Neurobiology of Disease*. https://doi.org/10.1016/j.nbd.2010.11.017

Qi, X., Qvit, N., Su, Y.-C., & Mochly-Rosen, D. (2013). A novel Drp1 inhibitor diminishes aberrant mitochondrial fission and neurotoxicity. *Journal of Cell Science*, *126*(Pt 3), 789–802. https://doi.org/10.1242/jcs.114439

Rajapakse, G., & Dunuweera, S. P. (2017). To cite this article: Rajapakse Mudiyanselage Gamini Rajapakse, Shashiprabha Punyakantha Dunuweera. Discovery, Chemistry, Anticancer Action and Targeting of Cisplatin. *International Journal of Clinical Oncology and Cancer Research*, *2*(3), 65–74. https://doi.org/10.11648/j.ijcocr.20170203.13

Renn, C. L., Carozzi, V. A., Rhee, P., Gallop, D., Dorsey, S. G., & Cavaletti, G. (2011). Multimodal assessment of painful peripheral neuropathy induced by chronic oxaliplatin-based chemotherapy in mice. *Molecular Pain*, *7*. https://doi.org/10.1186/1744-8069-7-29

Rodenburg, R. J. (2016). Mitochondrial complex I-linked disease. *Biochimica et Biophysica Acta - Bioenergetics*, *1857*(7), 938–945. https://doi.org/10.1016/j.bbabio.2016.02.012

Rosenberg, B., Van Camp, L., & Krigas, T. (1965). Inhibition of cell division in Escherichia coli by electrolysis products from a platinum electrode [17]. *Nature*. https://doi.org/10.1038/205698a0

Rosenberg, B., VanCamp, L., Trosko, J. E., & Mansour, V. H. (1969). Platinum compounds: A new class of potent antitumour agents [24]. *Nature*. https://doi.org/10.1038/222385a0

Roy Chowdhury, S. K., Zherebitskaya, E., Smith, D. R., Akude, E., Chattopadhyay, S., Jolivalt, C. G., … Fernyhough, P. (2010). Mitochondrial respiratory chain dysfunction in dorsal root ganglia of streptozotocin-induced diabetic rats and its correction by insulin treatment. *Diabetes*, *59*(4), 1082–1091. https://doi.org/10.2337/db09-1299

Santiago, S., Ferrer, T., & Espinosa, M. L. (2000). Neurophysiological studies of thin myelinated (A delta) and unmyelinated (C) fibers: Application to peripheral neuropathies. *Neurophysiologie Clinique*, *30*(1), 27–42. https://doi.org/10.1016/S0987-7053(00)88865-6

Schmoll, H.-J., & Jim Cassidy. (2001). Integrating Oxaliplatin into the Management of Colorectal Cancer. *The Oncologist*, *6*(90004), 24–28. https://doi.org/10.1634/theoncologist.6-suppl_4-24

Siau, C., Xiao, W., & Bennett, G. J. (2006). Paclitaxel- and vincristine-evoked painful peripheral neuropathies: loss of epidermal innervation and activation of Langerhans cells. *Experimental Neurology*, *201*(2), 507–14. https://doi.org/10.1016/j.expneurol.2006.05.007

Smith, G. M., & Gallo, G. (2018). The role of mitochondria in axon development and regeneration. *Developmental Neurobiology*, *78*(3), 221–237. https://doi.org/10.1002/dneu.22546

Sorensen, J. C., Petersen, A. C., Timpani, C. A., Campelj, D. G., Cook, J., Trewin, A. J., … Rybalka, E. (2017). BGP-15 protects against oxaliplatin-induced skeletal myopathy and mitochondrial reactive oxygen species production in mice. *Frontiers in Pharmacology*, *8*(APR). https://doi.org/10.3389/fphar.2017.00137

Ta, L. E., Espeset, L., Podratz, J., & Windebank, A. J. (2006). Neurotoxicity of oxaliplatin and cisplatin for dorsal root ganglion neurons correlates with platinum-DNA binding. *NeuroToxicology*, *27*(6), 992–1002. https://doi.org/10.1016/j.neuro.2006.04.010

Ta, L. E., Low, P. A., & Windebank, A. J. (2009). Mice with cisplatin and oxaliplatin-induced painful neuropathy develop distinct early responses to thermal stimuli. *Molecular Pain*, 5(1), 9. https://doi.org/10.1186/1744-8069-5-9

Tilokani, L., Nagashima, S., Paupe, V., & Prudent, J. (2018). Mitochondrial dynamics: overview of molecular mechanisms. *Essays in Biochemistry*, *62*, 341–360. https://doi.org/10.1042/EBC20170104

Toyama, S., Shimoyama, N., Ishida, Y., Koyasu, T., Szeto, H. H., & Shimoyama, M. (2014). Characterization of acute and chronic neuropathies induced by oxaliplatin in mice and differential effects of a novel mitochondria-targeted antioxidant on the neuropathies. *Anesthesiology*, *120*(2), 459–73. https://doi.org/10.1097/01.anes.0000435634.34709.65

Urra, F. A., Muñoz, F., Lovy, A., & Cárdenas, C. (2017). The mitochondrial Complex(I)ty of cancer. *Frontiers in Oncology*. Frontiers Media S.A. https://doi.org/10.3389/fonc.2017.00118

Velasco, R., & Bruna, J. (2010). Chemotherapy-induced peripheral neuropathy: An unresolved issue. *Neurología*, *25*(2), 116–131. https://doi.org/10.1016/s2173-5808(10)70022-5

Velasco, R., Navarro, X., Gil-Gil, M., Herrando-Grabulosa, M., Calls, A., & Bruna, J. (2017). Neuropathic Pain and Nerve Growth Factor in Chemotherapy-Induced Peripheral Neuropathy: Prospective Clinical-Pathological Study. *Journal of Pain and Symptom Management*. https://doi.org/10.1016/j.jpainsymman.2017.04.021

Vilholm, O. J., Christensen, A. A., Zedan, A. H., & Itani, M. (2014). Drug-Induced Peripheral Neuropathy. *Basic & Clinical Pharmacology & Toxicology*, *115*(2), 185–192. https://doi.org/10.1111/bcpt.12261

Wanchu, A., Rana, S. V., Pallikkuth, S., & Sachdeva, R. K. (2009). Short communication: Oxidative stress in HIV-infected individuals: A cross-sectional study. *AIDS Research and Human Retroviruses*, *25*(12), 1307–1311. https://doi.org/10.1089/aid.2009.0062

Waseem, M., Kaushik, P., Tabassum, H., & Parvez, S. (2018). Role of Mitochondrial Mechanism in Chemotherapy-Induced Peripheral Neuropathy. *Current Drug Metabolism*, *19*(1), 47–54. https://doi.org/10.2174/1389200219666171207121313

Xiao, W. H., Zheng, H., & Bennett, G. J. (2012). Characterization of oxaliplatin-induced chronic painful peripheral neuropathy in the rat and comparison with the neuropathy induced by paclitaxel. *Neuroscience*, *203*, 194–206. https://doi.org/10.1016/j.neuroscience.2011.12.023

Yamamoto, K., Tsuboi, M., Kambe, T., Abe, K., Nakatani, Y., Kawakami, K., … Taguchi, K. (2016). Oxaliplatin administration increases expression of the voltage-dependent calcium channel α2δ-1 subunit in the rat spinal cord. *Journal of Pharmacological Sciences*, *130*(2), 117–122. https://doi.org/10.1016/j.jphs.2016.01.006

Zajaczkowska, R, Kocot-K, Epska, M., Leppert, W., Wrzosek, A., Mika, J., & Wordliczek, J. (2019). Molecular Sciences Mechanisms of Chemotherapy-Induced Peripheral Neuropathy. *International Journal of Molecular Sciences.* https://doi.org/10.3390/ijms20061451

Zhao, R.-Z., Jiang, S., Zhang, L., & Yu, Z.-B. (2019). Mitochondrial electron transport chain, ROS generation and uncoupling (Review). *International Journal of Molecular Medicine*, *44*(1), 3–15. https://doi.org/10.3892/ijmm.2019.4188

Zheng, H., Xiao, W. H., & Bennett, G. J. (2011). Functional deficits in peripheral nerve mitochondria in rats with paclitaxel- and oxaliplatin-evoked painful peripheral neuropathy. *Experimental Neurology*, *232*(2), 154–61. https://doi.org/10.1016/j.expneurol.2011.08.016

Zheng, H., Xiao, W. H., & Bennett, G. J. (2012). Mitotoxicity and bortezomib-induced chronic painful peripheral neuropathy. *Experimental Neurology*, *238*(2), 225–234. https://doi.org/10.1016/j.expneurol.2012.08.023